72-19,997

NELSON, Stuart Owen, 1927-
  FREQUENCY DEPENDENCE OF THE DIELECTRIC
  PROPERTIES OF WHEAT AND THE RICE WEEVIL.

  Iowa State University, Ph.D., 1972
  Engineering, agricultural

University Microfilms, A XEROX Company, Ann Arbor, Michigan

Frequency dependence of the dielectric properties

of wheat and the rice weevil

by

Stuart Owen Nelson

A Dissertation Submitted to the

Graduate Faculty in Partial Fulfillment of

The Requirements for the Degree of

DOCTOR OF PHILOSOPHY

Major Subject: Agricultural Engineering

Approved:

In Charge of Major Work

For the Major Department

For the Graduate College

Iowa State University
Ames, Iowa

1972

PLEASE NOTE:

Some pages may have

indistinct print.

Filmed as received.

University Microfilms, A Xerox Education Company

TABLE OF CONTENTS

TABLE OF CONTENTS (continued)

TABLE OF CONTENTS (continued)

TABLE OF CONTENTS (continued)

LIST OF SYMBOLS AND ABBREVIATIONS

(Symbol identification unless otherwise specified)

a waveguide dimension, rectangular: $a > b$; cylindrical: a = diameter; coaxial: $a < b$

    constant coefficient

    subscript denoting air measurement

a-c   alternating-current

b waveguide dimension

bu   bushel

$\vec{B}$ complex vector magnetic flux density

B susceptance

c velocity of electromagnetic wave propagation in free space

c   specific heat

C capacitance

C   constant (magnitude of complex number)

cm   centimeter

c.v.   coefficient of variation

CW   continuous-wave

d sample length in waveguide

d-c   direct-current

$\vec{D}$ complex vector electric flux density

D   dielectric dissipation factor (loss tangent)

dB   decibel

dBm   decibels referenced to 1-mW power level

e base of natural or Naperian logarithms

$\vec{E}$ complex vector electric field intensity

E electric field intensity

f frequency

FM   frequency modulation

g   gram

G conductance

GHz   gigahertz (10^9 hertz)

h sample height

$\vec{H}$ complex vector magnetic field intensity

H magnetic field intensity

hr   hour

Hz   hertz (cycles/second)

I electric current

IF   intermediate-frequency

j $\sqrt{-1}$, denotes imaginary component of complex quantities

$\vec{J}$ complex vector electric current density

kHz   kilohertz (10^3 hertz)

kV   kilovolt

lb.   pound

ln   natural logarithm

log   common logarithm (base ten)

L inductance

m   meter

m integer

mg   milligram

mks	meter-kilogram-second units system
ml	milliliter (10^{-3} liter)
mm	millimeter
mmho	millimho
MHz	megahertz (10^6 hertz)
ms	millisecond
mW	milliwatt
n	integer
nH	nanohenry (10^{-9} henry)
nmho	nanomho
P	power density
P	$(\lambda_o/\lambda_c)^2$ in computer program
P_r	power ratio
pF	picofarad (10^{-12} farad)
pps	pulses per second
Q	electric charge density
R	resistance
R	waveguide reference dimension (distance from short circuit to slotted-section scale zero)
R_p	power dissipation ratio
RF	radiofrequency
rms	root-mean-square
s	subscript denoting sample measurement
S	$\lambda_o/2\pi d$ in computer program
t	time
T	temperature

T	constant (magnitude of complex number)
tan δ	dielectric loss tangent
TE	transverse electric mode
TEM	transverse electric and magnetic mode
v	volume or volume fraction
V	voltage
VSWR	voltage standing-wave ratio
w	subscript denoting conductor walls
w	width of slot in slotted section
x	independent variable
	coordinate of orthogonal coordinate system
X	independent variable in computer program
y	dependent variable
	coordinate of orthogonal coordinate system
Y	admittance
z	coordinate of orthogonal coordinate system parallel to direction of propagation
Z	impedance
Δ	change in value of variable it precedes
α	attenuation constant for wave propagation
	Cole-Cole relaxation-time distribution parameter
β	phase constant for wave propagation
	Cole-Davidson relaxation-time distribution parameter
γ	complex propagation constant
Γ	complex reflection coefficient
δ	loss angle

ε complex permittivity (complex capacitivity or complex dielectric constant)

ε_o permittivity of free space (8.85419×10^{-12} farad/m)

ε' dielectric constant (real part of ε)

ε'' dielectric loss factor (imaginary part of ε)

ε_r complex relative permittivity

ε_r' relative dielectric constant

ε_r'' relative dielectric loss factor

ζ angle associated with exponential notation for complex number

θ angle, radians

λ wavelength

λ_c cutoff wavelength

λ_g guide wavelength (phase wavelength in waveguide)

λ_o free-space wavelength

μ complex permeability

μ_o permeability of free space ($4\pi \times 10^{-7}$ henry/m)

μH microhenry (10^{-6} henry)

μmho   micromho

μV microvolt

π ratio of circumference of a circle to its diameter (3.141592654)

ρ specific gravity or density in g/ml

σ a-c conductivity

σ_c complex conductivity associated with conduction current

τ relaxation time

        root of Bessel function for zero value

        angle associated with exponential notation for complex number

ϕ phase angle, degrees

ω angular frequency $(2\pi f)$

$^{\circ}$ C   degrees Celcius

$^{\circ}$ F   degrees Fahrenheit

%   percent

I. INTRODUCTION

A. General Background

By world standards, the United States has been quite successful in
controlling insect pests. Good insect control programs contributed ma-
terially to the agricultural revolution which has resulted in an abun-
dance of food at reasonable cost in the United States. Still, there is
need for improvement, for insects consume substantial portions of our
food supplies and limit our food production to considerably lower levels
than would be possible were it unnecessary for man to compete with the
insects for his food.

The remarkable success of chemical insecticides has been the major
factor in development of effective insect control programs over the last
few decades. Our farm production and economy are dependent upon pesti-
cides in order to provide the quantity of food needed and the quality of
food products which the consuming public now demands. Most well-informed
people realize, in spite of the alarm concerning pesticide residues, that
chemical insecticides are essential to American agriculture and will be
for some time in the future. On the other hand, the threat of pesticide
residues to human and animal health is real. Substantial efforts are be-
ing devoted to study of a wide variety of methods which may be helpful in
minimizing the environmental hazards associated with the use of chemical
insecticides.

Such studies include ways of minimizing required pesticide quanti-
ties through improved methods of application and distribution as well as

appropriate timing of applications and limiting them to the minimum level needed to keep economic insect populations under control. Among biological control possibilities are the breeding of insect-resistant strains and lines, uses of insect parasites and predators, and the use of natural or synthetic attractants and repellents. Chemical sterilants and synthetic nutrients which produce physiological deficiencies in insects are also under consideration. "Physical methods" is another classification used, in contrast to chemical methods, in discussion of new insect control methods. Some improved cultural practices in farm production operations offer physical means of more effective insect control. Considerable interest has developed in the possible uses of different kinds of radiation as new insect control techniques. Extensive reviews of insect control possibilities using sonic and electromagnetic radiation have been prepared (Nelson and Seubert, 1966; Nelson, 1966; Nelson, 1967).

Certain ranges in all regions of the electromagnetic spectrum have been studied for possible insect control implications. At the high-energy end of the spectrum, ionizing gamma radiation has been studied extensively to determine its lethal and sterilizing influence on many species of insects. Gamma rays from cobalt 60 were used to sterilize artificially reared screw-worm pupae which were air-dropped over large areas of the southern and southwestern regions of the United States and in Mexico in the classic and well-publicized screw-worm eradication program. The "sterile-male" principle was highly effective in this application and is still in use to prevent reinvasion of the United States by screw-worm populations which still exist outside of the country's

boundaries. Ultraviolet and visible electromagnetic energy have been studied principally for use in attracting nocturnal insect species, and, while control programs based on the principle of trapping such insects have not been too successful generally, there is still interest in such possibilities. Infrared radiation has been used in experimental work to control certain stored-grain insect species through radiant heating. There has also been speculation that insects may utilize infrared radiation in their communication processes, and, while responses to infrared radiation have been demonstrated for a few species, the validity of such theories is still open to question. Portions of the radiofrequency spectrum have been explored as to their potential for insect control through dielectric heating. Since this is the area into which the subject for this dissertation falls, findings relating to insect control with radio-frequency energy will be treated in more detail subsequently (Sec. I, B).

Though economic losses to insects in the United States are substantial, the ravages resulting from insect activity in some of the less well developed countries of the world are much greater. Unfortunately, food supplies in many of these countries are in short supply, and effective insect control measures are badly needed. It is, therefore, important to explore the various possible means for achieving control of many economic insect species in considerable detail in order to provide the necessary understanding on which intelligent decisions can be based with regard to the potential of any particular method.

B. Radiofrequency Insect Control Studies

A thorough review of the literature from a few years prior to 1930 through 1966 pertaining to effects of high-frequency electric fields on insects has been published (Nelson, 1967). Therefore, a summary of the principal findings should suffice, and only a few references pertinent to the work at hand and some more recent reports will be cited here.

While many researchers have looked for some "specific effect" of the electromagnetic fields on insects, no clear-cut evidence of anything other than thermal effects has been obtained. A few observations do not appear to be completely and satisfactorily explained on the basis of heating effects alone (Nelson, 1967; Kadoum, 1969; Carpenter and Livstone, 1971), but nonthermal effects of radiofrequency (RF) electric fields useful for insect control have not yet been substantiated. Further research is needed to establish the facts and to substantiate any suspected effects not attributable to dielectric heating, particularly as related to the lethal action of RF fields on insects.

1. Entomological factors

The influences of a number of entomological and physical factors have been determined, especially for stored-grain insect species. For the rice weevil, *Sitophilus oryzae* (L.), the granary weevil, *Sitophilus granarius* (L.), and the lesser grain borer, *Rhyzopertha dominica* (F.), the adult stage is more susceptible to control by RF fields than are the immature stages when exposed in infested wheat. The difference in larval and adult susceptibility varies among species, however, and larvae of the

cadelle, *Tenebroides mauritanicus* (L.), are more susceptible than the adult. Differences within developmental stages have also been noted. Younger rice weevil adults appeared a bit more resistant to RF treatment than older adults of the same species. The age of yellow mealworm, *Tenebrio molitor* (L.), larvae, at time of sublethal exposure, influences the degree of resulting morphological abnormality which is observed in adults developing from these larvae (Kadoum *et al.*, 1967; Rai *et al.*, 1971). Rai (1970) also found that 1-day-old eggs of *T. molitor* (L.) were more susceptible than 3-day-old eggs. Differences in required exposures for control of adults of different species have also been noted, and the order of susceptibility has been established for several stored-grain species (Nelson and Kantack, 1966).

Reproductive studies with insects have shown that sublethal RF exposures reduce progeny significantly or completely, depending upon severity of exposure, but that sterilization of the type obtainable with ionizing radiations does not result following treatment with RF fields. Observations by Rai (1970) indicate that lowered reproductive capacity results from probable heat damage to sperm cells and ovarian tissues.

Physical factors which have received some attention include the nature of the host material, i.e., its degree of homogeneity, moisture content, temperature and dielectric properties, the frequency of the applied electric field, the electric field intensity, and the type of modulation employed. Discussion of these factors is deferred (Sec. I, B, 3) until a basis is provided for theoretical interpretation of the influence of these various factors.

2. Theoretical basis for radiofrequency insect control

Basic to any discussion of the interaction of electromagnetic waves and matter are Maxwell's equations

$$\nabla \times \vec{E} = -j\omega\vec{B} \qquad \nabla \cdot \vec{B} = 0$$
$$\nabla \times \vec{H} = j\omega\vec{D} + \vec{J} \qquad \nabla \cdot \vec{D} = Q \qquad \text{[1-1]}$$

and the associated constitutive relationships

$$\vec{D} = \varepsilon\vec{E}$$
$$\vec{B} = \mu\vec{H} \qquad \text{[1-2]}$$
$$\vec{J} = \sigma_c\vec{E}$$

where $\vec{E}$, $\vec{H}$, $\vec{D}$, $\vec{B}$, and $\vec{J}$ are complex vector quantities of rms value and $e^{j\omega t}$ dependence, i.e., time-harmonic functions (sinusoidally varying with time), since $e^{j\omega t} = \cos \omega t + j \sin \omega t$. $\vec{E}$ represents the electric field intensity, $\vec{H}$ the magnetic field intensity, $\vec{D}$ the electric flux density (or dielectric displacement), $\vec{B}$ the magnetic flux density (or magnetic induction), $\vec{J}$ the electric current density, and Q is the electric charge density, a scalar quantity. ε, μ, and σ_c represent the complex a-c constitutive parameters of the material, respectively the permittivity or capacitivity, the permeability, and the conductivity associated with conduction current. Employing the rationalized mks system for units (meter, kilogram, second), where the coulomb is also a basic unit for charge, the free-space constants μ_o and ε_o have respective values of $4\pi \times 10^{-7}$ henry/m (by international agreement) and 8.85419×10^{-12} farad/m, as a consequence of the requirement that $c = 1/\sqrt{\mu_o\varepsilon_o}$ (the velocity of propagation for electromagnetic waves in free space) in order to satisfy Maxwell's equations, Eqs. 1-1, using the accepted value for c of

2.997925 x 10^8 m/sec. Conductivity of free space is zero.

For most materials other than ferromagnetic substances, μ has essentially the value of μ_o, and this holds true for the biological materials of interest in this study. The complex permittivity is conveniently expressed as

$$\varepsilon = \varepsilon' - j\varepsilon'' = |\varepsilon|e^{-j\delta} \qquad [1-3]$$

Note that this is equivalent to specifying a phase difference of angle δ between the field intensity $\vec{E}$ and the flux density or displacement $\vec{D}$ in the material, since $\vec{E} = \vec{E}_o e^{j\omega t}$, and

$$\vec{D} = \varepsilon\vec{E} = |\varepsilon|e^{-j\delta}\vec{E}_o e^{j\omega t} = |\varepsilon|\vec{E}_o e^{j(\omega t - \delta)} = \vec{D}_o e^{j(\omega t - \delta)}, \text{ where } \vec{E}_o \text{ and } \vec{D}_o$$

denote peak values. The real part of the complex permittivity, ε', is simply the permittivity, often called the dielectric constant, and also capacitivity. ε'' is the dielectric loss factor, and the angle δ is the dielectric loss angle. The value

$$\tan \delta = \varepsilon''/\varepsilon' \qquad [1-4]$$

is referred to as the loss tangent or dissipation factor of the material.

In most practical work it is the dielectric properties of materials relative to the dielectric properties of vacuum or free space which are of interest. Therefore, the relative complex permittivity, relative permittivity, relative loss factor, and loss tangent (Eq. 1-4) are related as follows:

$$\varepsilon_r = \frac{\varepsilon}{\varepsilon_o} = \frac{\varepsilon'}{\varepsilon_o} - j\frac{\varepsilon''}{\varepsilon_o} = \varepsilon_r' - j\varepsilon_r'' = \varepsilon_r' \, (1 - j\tan \delta) \qquad [1-5]$$

$$\tan \delta = \varepsilon_r''/\varepsilon_r' \qquad [1-6]$$

The complex conductivity σ_c may be written $\sigma_c = \sigma_c' + j\sigma_c''$. Using

this expression and substitutions of Eqs. 1-3 and 1-2 in Eq. 1-1, we may write

$$\nabla \times \vec{H} = j\omega(\varepsilon' - j\varepsilon'')\vec{E} + (\sigma_c' + j\sigma_c'')\vec{E} = [j\omega(\varepsilon' + \sigma_c'') + \omega\varepsilon'' + \sigma_c']\vec{E} \quad [1\text{-}7]$$

The term $j\omega\varepsilon\vec{E} = j\omega(\varepsilon' - j\varepsilon'')\vec{E}$ represents the displacement current, while $\sigma_c\vec{E}$ represents the conduction current. Normally σ_c'' is negligible. The currents of Eq. 1-7 may also be considered as shown in the right-hand member where $(\omega\varepsilon'' + \sigma_c')\vec{E}$ represents a dissipative current in phase with $\vec{E}$ and $j\omega(\varepsilon' + \sigma_c'')\vec{E}$ represents a reactive current out of phase with $\vec{E}$. In free space, where there are no free electrons, $\sigma_c = 0$, and there is no conduction current. There is, however, a free-space displacement current $j\omega\varepsilon_0\vec{E}$. In materials there is a polarization current because of the motion of bound charges, $j\omega(\varepsilon - \varepsilon_0)\vec{E}$, and this represents the difference between the displacement current in the material and the free-space displacement current.

In measuring dielectric properties one detects only the components of current in phase, dissipative, and out of phase, reactive, with respect to $\vec{E}$. According to Harrington (1961, Sec. 1-9), the distinction between the current components due to σ_c and ε is primarily philosophical. In conductors, where current results from the movement of free electrons, the effect is attributed to σ_c and the total current is $(\sigma_c + j\omega\varepsilon_0)\vec{E}$. In dielectrics, where bound charges predominate, the current is normally considered to be $j\omega\varepsilon\vec{E}$. Bussey and Dalke (1967) also comment on the inability to distinguish between currents attributable to conductivity and permittivity except in the extreme cases of pure conductors and pure insulators. Efforts to separate losses associated with ε''

and those associated with σ_c have been successful for some pure compounds

and known mixtures of such materials when data are available over a wide

frequency range (Davies, 1969). Generally, however, in work with dielec-

trics, the dissipative current is attributed to the dielectric loss, and

the influence of the σ_c' component is lumped in with the ε'' component so

that the total loss current is considered to be $\omega\varepsilon''\vec{E}$. This convention

will be followed in this study. One can then calculate an a-c conduc-

tivity for the material equivalent to $\omega\varepsilon''$ when ε'' has been determined

$$\sigma = \omega\varepsilon'' = \omega\varepsilon_o\varepsilon_r'' \qquad [1\text{-}8]$$

The relationships of Eqs. 1-5, 1-6, and 1-8 may also be derived from

equivalent-circuit concepts, where a dielectric material is represented

for a given frequency by a parallel-equivalent capacitance and resistance

(von Hippel, 1954a; Nelson, 1965).

Since the total dissipative current is encompassed by the term

$\omega\varepsilon_o\varepsilon_r''E$, the power dissipation in the material per unit volume will be

$$P = \omega\varepsilon_o\varepsilon_r''E^2 = 55.6325 \ f \ E^2 \ \varepsilon_r'' \ \times 10^{-12} \ \text{watts/m}^3 \qquad [1\text{-}9]$$

where E is expressed in rms volts/m and f is in hertz. The heating which

results from the absorption of energy from a radiofrequency field by ma-

terial in the field is generally termed dielectric heating. The result-

ing temperature rise in the material depends upon its specific heat and

density as well as the power dissipation. Neglecting any changes in

state, such as vaporization of moisture, and radiant, convective, or con-

ductive heat losses, the rate of temperature increase in degrees C per

second would be

$$dT/dt = 0.239 \ P/c\rho = 0.133 \ f \ E^2 \ \epsilon_r''/c\rho \qquad [1\text{-}10]$$

where P is in watts/cm^3, f is in MHz, E is in kilovolts/cm (kV/cm), and c and ρ represent specific heat and specific gravity, respectively.

3. <u>Physical factors</u>

   a. <u>Differential heating</u>   Turning attention now to the question of controlling insects in infested material, examination of Eqs. 1-9 and 1-10 reveals the possibility for controlling insects through selective dielectric heating if their dielectric properties are sufficiently different from those of the host material. Dielectric heating can raise the temperature of the insects to a lethal level, but if, at the same time, it produces heat damage in the host material, it is impractical. Also, absorption of energy by the host material may make such applications economically impractical. In a detailed and excellent review and analysis of the question of insect control using high-frequency electric fields, Thomas (1952) concluded that differential heating explained the lethal action of high-frequency electric fields in controlling insects in infested products without damaging the products. He also showed that differential heating could be expected, in some situations, on the basis of a theoretical analysis with some knowledge of the dielectric properties of the two materials. A simplified analysis based on Eq. 1-10 and the case for a sphere embedded in an infinite medium was reported using measured values for the dielectric properties of rice weevils, confused flour beetles, *Tribolium confusum* Jacquelin duVal, wheat, and wheat shorts (Nelson and Whitney, 1960). It was noted that the dielectric

properties not only influence power absorption through the presence of ε_r'' in Eq. 1-9, but also through the influence of ε_r and principally ε_r' on the value of E in the respective materials. For a sphere embedded in an infinite medium

$$E_1 = E_2 \left(1 - \frac{\varepsilon_{r1} - \varepsilon_{r2}}{2\varepsilon_{r2} + \varepsilon_{r1}}\right) = E_2 \left(\frac{3\varepsilon_{r2}}{2\varepsilon_{r2} + \varepsilon_{r1}}\right) \qquad [1\text{-}11]$$

where the subscript 1 refers to the sphere and 2 to the medium in which it is embedded. Dielectric properties of bulk wheat and of insects in bulk were measured at 40 MHz and about 80° F. Values of ε_r for the insects and the wheat were assigned, respectively, to the sphere and the infinite medium as represented in Eq. 1-11. With resulting estimates for relative field intensities, measured values for ε_r'', and estimates for c and ρ, consideration of Eq. 1-10 indicated a heating rate for the rice weevils in wheat about 1.8 times greater than that of the wheat. For the confused flour beetle treated in wheat, the differential heating factor was 1.6 and for the same insects treated in wheat shorts, this factor was 0.9.

These differential heating factors bore the proper relationship to each other to explain results of experiments in which infested wheat and wheat shorts were exposed to high-intensity 40-MHz electric fields. As judged from resulting temperatures in the wheat and wheat shorts for complete mortality of the insects, the rice weevils were the most suscep-tible. Confused flour beetles in wheat required higher temperatures in the wheat for comparable mortality and even higher temperatures in the wheat shorts, where the theoretical analysis indicated that selective

heating of the insects was unlikely.

Additional experiments (Nelson and Whitney, 1960) with rice weevils and wheat, in which infested samples were conditioned at different temperatures prior to RF exposure and a linear heating model used in an effort to derive an empirical differential heating factor, gave results in reasonable agreement with the theoretical prediction. The experimental results indicated a temperature dependence for the differential heating factor which could be expected but was not taken into account in the simple model.

b. <u>Effects of host material</u>   Because the field intensity to which the insects are subjected depends upon geometrical or spatial factors as well as the dielectric properties of the insects and host material, it appears that the particle size and shape of granular host material might influence lethal exposure levels. Experiments with granary weevils, *Sitophilus granarius* (L.), in wheat and corn of the same moisture content revealed that the insects suffered lower mortalities in wheat than in corn at mortality levels below about 80 percent (Nelson and Kantack, 1966). For higher mortalities there was little difference. Rice weevil adults exposed to RF fields in different-sized glass beads survived better in smaller-sized glass particles (Nelson *et al.*, 1966).

Mortalities of rice weevil adults treated in wheat of 11.4- and 12.8-percent moisture were reported to be indistinguishable (Whitney *et al.*, 1961), but more recent work indicates that, within the moisture range from 12 to 16 percent, RF treatment may be slightly more effective as the moisture content of the wheat increases (Nelson and Kantack,

1966). Moisture content of the host medium after treatment has a definite effect on insect survival. Mortalities of insects transferred to higher moisture wheat following exposure to RF electric fields were lower than those of insects transferred to wheat of lower moisture contents which were still high enough to maintain normal insect activity (Nelson *et al.*, 1966). Because insects treated at lethal exposures lose moisture amounting to a few percent of their weight, it seems reasonable that those subjected to sublethal exposures should survive better in media of higher moisture content, for they should then be able to regain the lost moisture more rapidly.

c. Influence of field intensity   Because field intensity, E in Eq. 1-10, is an important factor influencing the heating rate, its effects have received some attention. Effects of field intensity and frequency on insect mortality are difficult to distinguish because both influence the heating rate. The three factors--frequency, field intensity, and heating rate--must, therefore, be considered in relation to one another. A number of experiments at 10 and 39 MHz, involving exposure times ranging from a few seconds to a minute or more, with different combinations of field intensities and heating rates, indicated that there are subtle frequency effects which depend upon the species and developmental stages of the insects (Nelson *et al.*, 1966). In comparing 10- and 39-MHz treatments with similar heating rates, the 10-MHz treatment was consistently better for some species and stages, whereas the 39-MHz treatment was consistently better for others. For still others, the two frequencies produced similar mortalities.

High field intensities were found much more efficient than low intensities in killing adult rice weevils in wheat at both 10 and 39 MHz, but with immature stages of the same species, high or low intensities produced the same results (Nelson and Whitney, 1960; Whitney *et al.*, 1961). Generally, differences in insect mortality attributable to field intensity diminished at intensities greater than 1.2 kV/cm. For a given frequency, an increase in field intensity increases the heating rate. The more rapid elevation of temperature accompanying high-field-intensity treatments appears to offer a logical explanation for the greater efficiency of high-intensity treatments which should produce a higher degree of thermal shock in biological organisms. Heating rate alone, however, does not appear to determine the efficiency of treatment at different frequencies (Nelson *et al.*, 1966).

d. **Pulse modulation**   Possible advantages in controlling insects by use of pulse-modulated RF electric fields were suggested by Thomas (1952), though no theoretical basis for any particular optimism was evident. Experiments with pulse-modulated 39-MHz fields ranging from 5 to 40 milliseconds (ms) in pulse width and from 10 to 40 pulses per second (pps) in pulse repetition rate did not show any major improvement in efficiency for control of adult rice weevils and confused flour beetles in wheat (Nelson *et al.*, 1966). Some improvement in treatment efficiency was noted for controlling lesser grain borer adults using 10-ms pulses at a repetition rate of 10 pps and field intensity of 3.5 kV/cm, compared to unmodulated treatment at 1.4 kV/cm. Much higher field intensities can be used with pulse modulation, even with these relatively long pulse

durations. For clean wheat of 13- to 14-percent moisture, field intensities for unmodulated RF treatment at a frequency of 40 MHz are limited to about 1.6 kV/cm because of the tendency for arcing to occur in the grain which chars the kernels. The maximum permissible intensities increase with decreasing grain moisture content. The length of exposure also influences arcing, and moisture escaping from the grain kernels during dielectric heating increases the tendency for arcing. The maximum field intensity which may be employed with pulse modulation appears to increase as the pulse width and pulse repetition frequency are decreased.

    e. <u>Influence of frequency</u>   Most studies on stored-grain insect control with RF electric fields have been conducted in the frequency range from 1 to 50 MHz. Often the choice of frequency has been dictated by the operating frequency of commercially available power oscillators designed for other dielectric heating applications. Based on electrical theory, however, and also from experimental results, the frequency for insect control by differential heating does not appear critical as long as it exceeds a certain "transitional frequency" which, according to Thomas (1952), lies in the frequency range between about 1 and 200 MHz for most biological materials. Early implications that certain frequencies were more effective for heating insect tissues than plant tissues were based on faulty assumptions, as explained by Thomas (1952). Also, the idea that certain selective frequencies might exist for certain insects has not been borne out by either theory or experiment.

    Studies with confused flour beetles in flour and granary weevils in wheat which were exposed to 2,450-MHz microwave energy in a microwave

oven indicated that no differential heating was obtained. Temperatures in excess of 180° F (82° C) and 170° F (77° C), respectively, were required for control of immature stages (Baker *et al.*, 1956). Corresponding control of granary weevils, rice weevils, and lesser grain borers in wheat at 40 MHz was achieved at grain temperatures near 140° F (60° C) (Whitney *et al.*, 1961). Complete control of the confused flour beetle was reported by Hamid and Boulanger (1969) using 2,450-MHz energy to expose insects in grain passing through a waveguide section; however, it was not stated whether the tests included the more resistant immature forms. Also, the insects were subjected to higher temperatures by leaving them in the hot grain for at least 30 minutes, so these tests would not provide convincing evidence of any differential heating results. A microwave grain-treating system operating at 2,450-MHz and a 13-MHz dielectric heating system were compared by Boulanger *et al.* (1969), but, unfortunately, a clear comparison of the relative effectiveness of the two different frequencies for controlling stored-grain insects was not set forth in their report. On the basis of available data, therefore, it does not appear that the 2,450-MHz frequency offers any differential heating advantage compared to the region around 40 MHz where substantial evidence for differential heating has been obtained.

In order to properly assess the degree of differential heating to be expected at different frequencies in the RF spectrum, data are needed on the respective dielectric properties of insects and grain at several different frequencies. If there is significant variation of the dielectric properties with frequency for either insects or grain, it is obvious

from examination of Eqs. 1-9 and 1-11 that we would wish to choose for further study frequency ranges with the highest insect-to-grain dielectric loss-factor ratio and lowest insect-to-grain dielectric-constant ratio. Data have been presented for the relative dielectric constant and loss factor of rice weevil adults and hard red winter wheat for the 1- to 50-MHz range (Nelson *et al.*, 1966). The dielectric constant for wheat at 13-percent moisture decreases slightly between 1 and 50 MHz, but the dielectric constant of bulk rice weevils changes substantially from 11.6 to 5.9 between the same two frequencies. The loss factor for wheat increased from about 0.25 at 1 MHz to about 0.5 at 50 MHz, while the loss factor for the weevils increased to about 2.4 in the 2- to 4-MHz region, then dropped slightly and increased again to about 2.3 at 50 MHz. It would, therefore, appear that 50 MHz might be as good a choice as any in this frequency range, but the relative importance of the dielectric-constant ratio and the loss-factor ratio has not been carefully evaluated.

C. Statement of the Problem

In view of all available information on the use of radiofrequency electric fields for possible control of stored-grain insects, the most important question has to do with means for improving the efficiency of the method. Accumulated evidence heavily favors the theory that lethal action of RF fields on insects results from thermal stress as a consequence of differential dielectric heating in which the insect absorbs energy from the electric field at a higher rate than the host material.

The respective dielectric properties of the insects and the grain which they infest are the principal factors influencing the degree of differential heating. Because the dielectric properties of most materials are frequency-dependent, the need is obvious to obtain data on the variation of the dielectric properties of the insects and the grain in order to identify regions of the RF spectrum which might be most profitably explored for insect control application.

Therefore, the problem selected for study was the determination of the dielectric properties throughout a wide range of the RF spectrum for the rice weevil, a widespread stored-grain insect useful for laboratory studies, and for hard red winter wheat, a commodity stored in large quantities and one which is most subject to infestation by stored-grain insects. Meeting this objective then required the selection and development of suitable and reliable methods of measurement by which the dielectric properties of insects and grain could be obtained. Because of the wide range of wavelengths of electromagnetic energy included in the RF spectrum and the nature of devices useful in generating and controlling such energy, a number of separate systems are required to cover any appreciable portion of the spectrum.

Interpretation of the resulting data and evaluation of its usefulness in identifying promising ranges of the spectrum for further study is a requirement for satisfactory solution of the problem.

II. SELECTION AND DEVELOPMENT OF DIELECTRIC-PROPERTIES MEASUREMENT METHODS

A. General Aspects

Many techniques and measurement systems have been developed for measuring the dielectric properties of various kinds of materials. The frequency range of interest dictates to some extent the type of measuring system which must be used. Also, the nature of the material on which data are to be obtained is important in designing a suitable specimen holder which is a part of the measurement system.

Several important reviews and discussions of dielectric-property measurement methods and techniques have been published. A frequently cited reference by Redheffer (1948) covers in a concise fashion most of the methods useful in the microwave range. Widely used microwave methods are covered in more detail by Altschuler (1963). Theory of dielectrics and measurement techniques are treated rather extensively in two books by von Hippel (1954a, 1954b), the latter including a chapter by Field (1954) covering lumped-circuit methods useful in the frequency range from 0 to 200 MHz, and a chapter by Westphal (1954) treating distributed-circuit methods useful at higher frequencies. A relatively recent book by Hill *et al.* (1969) includes a chapter by Vaughan (1969) with an extensive review of experimental methods useful in measuring the dielectric properties of various materials at frequencies from 0 to those of millimeter waves. Techniques useful for dielectric-properties measurements on biological materials have been reviewed by Schwan (1963) and Grant (1969). Bussey (1967) prepared a survey of RF-measurement methods, with emphasis on

accuracy achieved, for determination of dielectric and magnetic proper-
ties of materials. More details of the theory and techniques of RF meas-
urements of such properties have been presented by Bussey and Dalke (1967).
Surveys of methods and formulas useful in calculating dielectric and mag-
netic material constants have also been prepared by Eichacker (1958,
1961). Details for microwave measurements of permittivity and permeabil-
ity have also been considered by Franceschetti and Silleni (1964) and
Franceschetti (1967).

For frequencies of a few Hz or less than 1 Hz, transient methods in-
volving measurement of the charging or discharging current of a capacitor
containing the dielectric sample are employed. Various types of bridge
circuits have been used for measurements in the frequency range from a
few Hz to several MHz. The Schering bridge circuit is frequently employed
because of its wide frequency range. Problems with residual impedance in
the leads and bridge components usually render bridges impractical at fre-
quencies much above 10 MHz. Resonant circuits employing inductive and
capacitive components can be used in the range between about 10 kHz and
200 MHz, though special attention must be paid to design of instruments
and components near both extremities of this range. Transmission-line and
waveguide methods are used between about 200 MHz and about 75 GHz where
problems in fabricating sufficiently precise components currently set an
upper frequency limit. Such measurements employ not only reflection and
transmission concepts in lines and waveguide, but resonant-cavity tech-
niques are also very useful. For frequencies above this range, in the
millimeter-wave region, free-space methods and interferometric techniques

of the type employed in optical measurements have been developed.

For insect control possibilities using RF electric fields, it would not appear that the dielectric properties of insects and grain need be explored at the very low and very high ends of the frequency spectrum for which methods have been developed, but it would be desirable to obtain such data over a wide frequency range. The frequency range selected for study, determined to some extent by availability of suitable equipment, spans the region between 250 Hz and 12.2 GHz. Eight different measurement systems were developed to span this range, and each will be described in a separate section. Some of these methods were developed prior to the beginning of work on this dissertation, but all were reexamined, subjected to further scrutiny, and checked for reliability during the course of this research. Methods and techniques worked out during research for the dissertation will receive more attention in the appropriate sections to follow.

B. Audiofrequency Impedance Bridge System

1. General description

A method for measuring dielectric properties of grain and seed in the audiofrequency region, between 250 Hz and 20 kHz, was developed under the author's supervision and technical guidance (Corcoran *et al.*, 1970). A coaxial sample holder (Fig. 2-1), providing sufficient electrode area for necessary sensitivity in measurement of dielectric loss, was designed for use with a General Radio Type 1608-A Impedance Bridge. A detailed description of the sample holder and its construction is given in the

cited reference. A suitable insulated mounting block, also described in that reference, was attached to the impedance bridge to provide a platform to support the sample holder and to provide for proper electrical connection to the bridge (Fig. 2-2).

A Hewlett-Packard Model 200B Audio Oscillator was used for the external a-c source required for the bridge when other than 1-kHz measurement frequency was desired. A 600-ohm resistor in series with the oscillator output protected the bridge circuits from possible overload. Output frequency of the oscillator was set using a Hewlett-Packard Model 523C Electronic Counter, which continuously monitored the oscillator output frequency.

2. Determination of dielectric properties

Values for the capacitance and dissipation factor, or loss tangent, of the sample holder with and without the sample are obtained from the impedance bridge when it is properly balanced. The bridge employs two different bridge circuits for measurement of capacitive elements, one based on a parallel-equivalent circuit representation of the unknown, and the other on a series-equivalent representation. The choice of circuits depends upon the magnitude of the dissipation factor. The series-capacitance circuit is used for the dissipation-factor range from 0.0005 to 1.0, and the parallel-capacitance circuit is used for the range from 0.02 to 2.0. In the overlapping region, either circuit may be used. For grain and insect samples, measurements using both circuits are necessary.

The capacitance per unit length between two long coaxial cylindrical conductors is $C = 2\pi\varepsilon_o\varepsilon_r'/\ln(b/a)$ farads per meter, where b is the inside
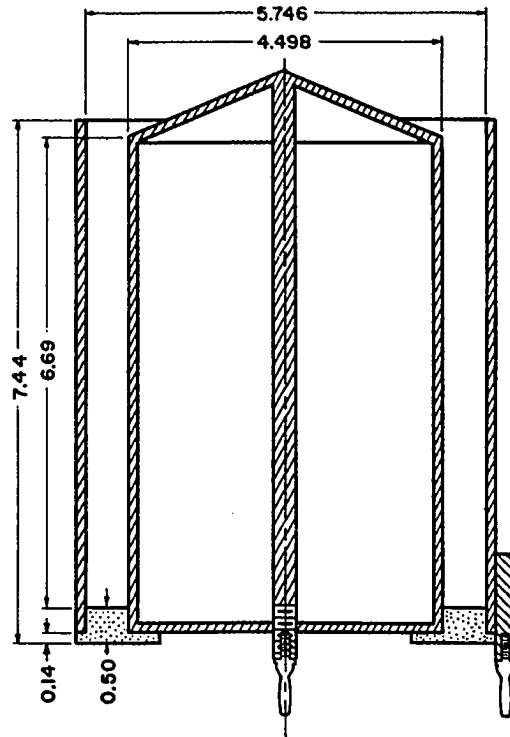
Fig. 2-1. Sectional view of coaxial sample holder for use
with impedance bridge, dimensions in inches
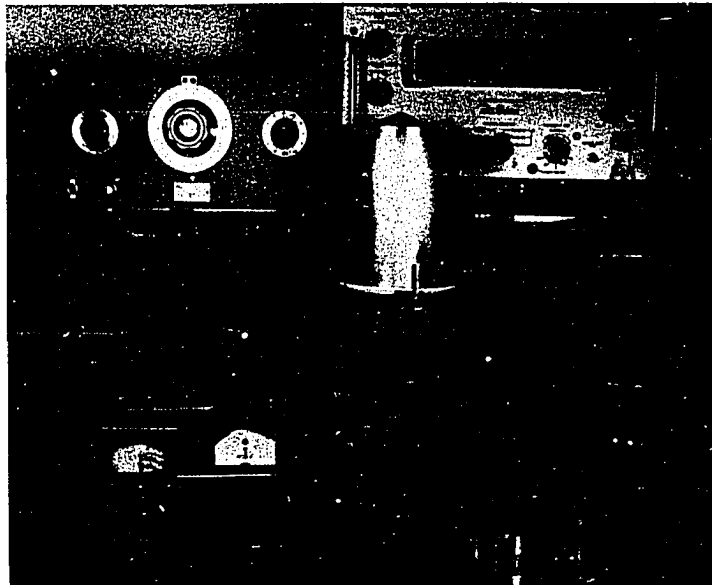
Fig. 2-2. Audiofrequency dielectric-properties measurement system,
including impedance bridge, coaxial sample holder,
sample-height gage, audiofrequency oscillator, and fre-
quency counter

diameter of the outer conductor and a is the outside diameter of the inner conductor. The change in capacitance of a coaxial sample holder due to the presence of a dielectric sample filling the holder to a height, h, (Fig. 2-3) may, therefore, be written $\Delta C = [2\pi\varepsilon_o h/\ln(b/a)]\ (\varepsilon_r' - 1)$. Therefore, when ΔC is determined by subtracting the capacitance measured for the empty sample holder from the capacitance measured for the sample holder with the sample present, ε_r' may be determined:

$$\varepsilon_r' = \frac{\Delta C\ \ln(b/a)}{2\pi\varepsilon_o h} + 1 \qquad\qquad [2\text{-}1]$$

Careful remeasurement of the dimensions of the sample holder and consideration of the fact that measurements are made in air rather than vacuum (see Appendix A, Sec. IX, D) resulted in slight revision of the constants of Eq. 2-1 as compared to those reported earlier (Corcoran *et al.*, 1970). For this sample holder (using 8.8599×10^{-12} farad per meter for air rather than $\varepsilon_o = 8.85419 \times 10^{-12}$) Eq. 2-1 becomes
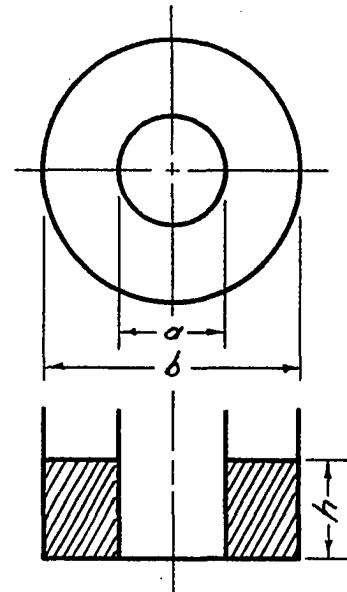
Fig. 2-3. Schematic diagram of a coaxial sample holder

$$\varepsilon_r' = \frac{0.1731\ \Delta C}{h} + 1 \qquad\qquad [2\text{-}2]$$

where h is measured in inches and ΔC is in picofarads (pF).

The loss tangent, or dissipation factor, D, for the sample material may be derived from the dissipation factors and capacitances measured for

the sample holder with and without the sample. Parallel-equivalent cir-

cuits for the empty sample holder and for the sample holder with sample

are represented in Figs. 2-4 and 2-5. For the empty holder, the dissipa-

tion factor at angular frequency,

ω, is $D_o = 1/\omega R_o C_o$, where the sub-

script, o, denotes conditions with

the sample holder empty. When a

quantity of material is placed in

the sample holder, additional re-

sistance and capacitance are added

in parallel as shown in Fig. 2-5.

The dissipation factor for the

sample holder and material com-

Fig. 2-4. Parallel-equivalent circuit of empty sample holder

bination is $D_c = (R_o + R)/[\omega(C_o + C)R_o R]$. Quantities measured using the

impedance bridge are D_o, C_o, D_c, and $C_o + C = C_p$. Since the dissipation
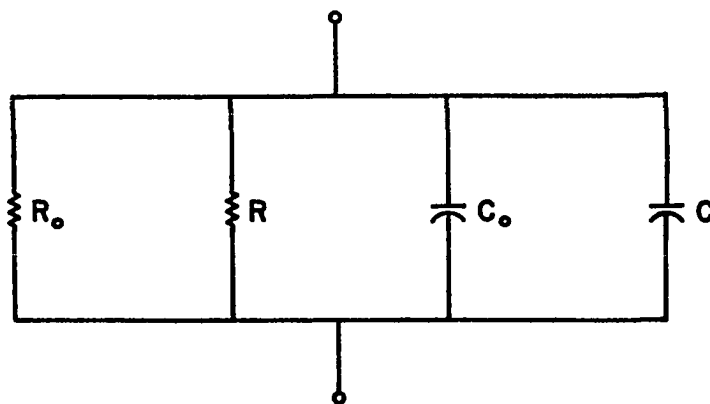
Fig. 2-5. Parallel-equivalent circuit of sample holder with sample

factor of the material itself is $D = 1/\omega CR$, suitable algebraic substitutions yield

$$D = (C_p D_c - C_o D_o)/(C_p - C_o) \qquad [2\text{-}3]$$

The D scales of the impedance bridge are calibrated for measurements at 1 kHz. D values read from the bridge must, therefore, be corrected if measurements are made at other frequencies. D values corrected for frequency are D_p/f for parallel-capacitance readings and $D_s f$ for series-capacitance readings, where f is in kHz (General Radio Company, 1965). Dissipation factors are the same whether derived from a series- or parallel-equivalent circuit. Therefore, the values obtained with the series- or parallel-capacitance bridge circuits should agree (within the accuracy of the measurement) after correction for frequency calibration. Since calculation of dielectric properties was based on parallel-equivalent circuit analysis, series-capacitance readings from the bridge were converted to equivalent-parallel capacitance using $C_p = C_s/(1 + D^2)$.

For measurements on grain and insect samples, both parallel and series measurements were obtained when balance of the bridge was possible, and they were averaged. Measurements recorded for the empty sample holder were C_{so} and D_{so}. Those recorded for the sample holder with the sample were C_p, D_p, C_s, and D_s. The calculations necessary to obtain the dielectric properties of samples are as follows (where double subscripts are used, the first denotes a series or parallel value, and the second indicates whether the sample holder is empty or filled with material):

$$D_o = f D_{so}, \quad C_{po} = C_{so}/(1 + D_o^2), \quad D_m = (D_p/f + D_s f)/2,$$
$$C_{pm} = [C_p + C_s/(1 + D_m^2)]/2, \qquad \bullet$$

$$\tan \delta = D = \frac{C_{pm} D_m - C'_{po} D_o}{C_{pm} - C_{po}} \qquad [2\text{-}4]$$

$$\varepsilon'_r = \frac{0.1731(C_{pm} - C_{po})}{h} + 1 \qquad [2\text{-}5]$$

where Eqs. 2-4 and 2-5 are restatements of Eqs. 2-3 and 2-2. Eqs. 1-6 and 1-8 then provide expressions for the relative dielectric loss factor and the conductivity:

$$\varepsilon''_r = \varepsilon'_r \tan \delta \qquad [2\text{-}6]$$

$$\sigma = 0.5567 \, f \, \varepsilon''_r \qquad [2\text{-}7]$$

where again the permittivity of air is used in figuring the constant rather than the free-space value, ε_o, and σ is expressed in nanomhos for a centimeter cube when f is in kHz.

Calculations were initially programmed for computation on an IBM 1130 computer. Later they were programmed for calculation on a Wang 700B programmable electronic calculator. Because the values for C_{so} and D_{so} measured on the empty sample holder consistently remained constant for measurements at a given frequency, repeated measurements on the empty sample holder were found unnecessary. By carefully determining these values at frequencies of 0.25, 0.5, 0.7, 1, 1.5, 2, 3, 5, 7, 10, 15, and 20 kHz and fitting a curve to these data, the values for C_{so} and D_{so} are calculated for any frequency in the 0.25- to 20-kHz range automatically by the program using the following equations: $C_{so} = 50.987 - 0.0657348 \ln f$ and $D_{so} = e^{(-5.92707 - 1.60705 \ln f)}$.

3. Verification of reliability

Measurements on benzene were conducted to check the reliability of the method. Measurements throughout the frequency range, 250 Hz to 20 kHz, at 76° F (24° C) yielded values ranging between 2.278 and 2.282 for the real part of the relative permittivity (dielectric constant). The actual value for Analytical Reagent Grade benzene, which allows up to 0.02 percent water, can be expected to lie within this range at this temperature. The accepted value for pure benzene is 2.276 at 24° C (Buckley and Maryott, 1958; Maryott and Smith, 1951).

Edge effects due to field fringing were not expected to be troublesome at audiofrequencies for the purposes of these measurements. The influence of such effects was checked, however, by introducing a small quantity of benzene (100 ml) into the empty sample holder before the initial readings and calculating the dielectric properties on the basis of the change produced in adding a larger quantity (400 ml) for the sample measurement. Comparison of data obtained starting with an empty sample holder and that obtained using a small quantity of material to minimize edge effects revealed very little difference in resulting values for the dielectric constant; so the influence of edge effects was negligible, at least for a sample size of 500 ml or more.

4. Filling the sample holder

For measurements on grain, 1 liter of grain was measured out and placed in the hopper of a standard weight-per-bushel apparatus (Fig. 2-6). An adapting base plate centered the sample holder under the funnel with the lower edge of the funnel spaced 1 inch vertically above the top edge
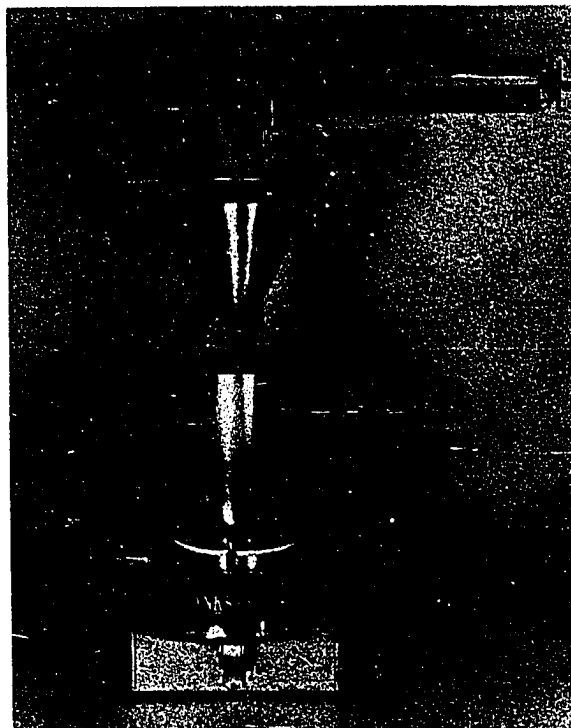
Fig. 2-6. Equipment for filling sample holder, including weight-per-bushel apparatus and removable adapting base plate

of the outer electrode of the sample holder. This provided a convenient

means for rapidly and uniformly filling the sample holder. A sample-

height gage, shown in Fig. 2-2, consisting of an aluminum ring with four

vertical posts on which a height scale was inscribed, provided a conven-

ient means for direct measurement of sample height. The sample height for

benzene was calculated from the known volume of the sample and the cross-

sectional area of the sample holder (64.755 cm^2).

C. Q-Meter System

1. General description

A suitable method for measuring dielectric properties of grain in the frequency range from 1 to 50 MHz was developed earlier (Nelson, 1952; Nelson et al., 1953), and the variation of the dielectric properties of various kinds of grain and seed with frequency and moisture content has been studied in some detail (Nelson, 1965). This method utilized a Boonton Type 160-A Q-Meter and a coaxial sample holder especially designed and constructed for use with this instrument. The method is an adaptation of the reactance-variation principle reported by Hartshorn and Ward (1936) and also utilized by Wangsgard and Hazen (1946). The Q-Meter provides a calibrated variable-frequency oscillator coupled to a series resonant circuit in such a way that the source impedance is negligibly small (Fig. 2-7). Calibrated, variable, air capacitors, C_1 with a range of 30 to 460 pF and a vernier capacitor, C_2 with a range from -3 to 0 to +3 pF, are an integral part of the instrument, and, with suitably wound inductance
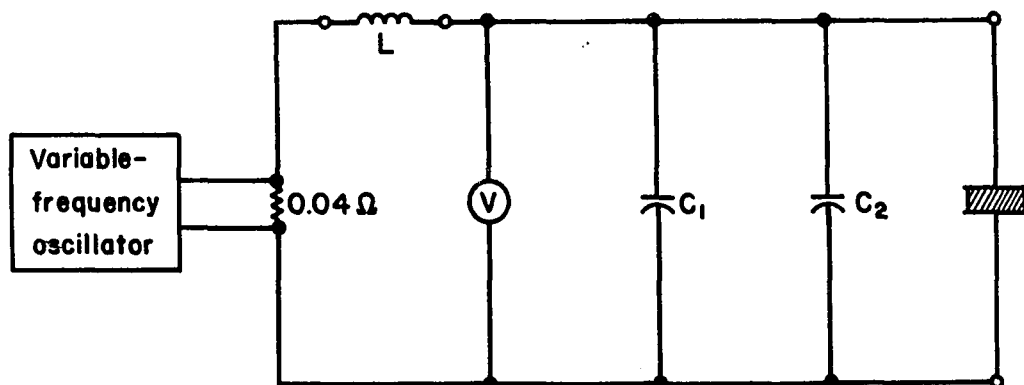
Fig. 2-7. Schematic diagram of Q-Meter circuit

coils, L, attached to the inductance terminals, series resonance can be achieved over a frequency range from 50 kHz to 75 MHz.

Earlier attempts to measure the dielectric properties of grain samples with the Q-Meter and simple coaxial sample holders were unsuccessful, particularly at frequencies above about 10 MHz, because of residual circuit and lead inductances. These problems were overcome with a coaxial sample holder equipped with a small, variable, air capacitor located near the sample chamber and calibrated so that capacitance lost when the sample was removed could be restored by adjustment of the variable, air capacitor (Fig. 2-8). A detailed description of the sample holder was
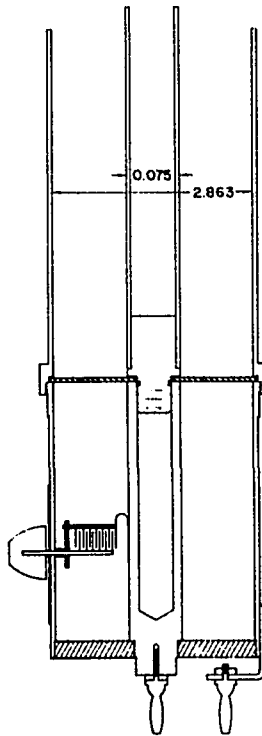
Fig. 2-8. Sectional view of coaxial sample holder for use with the Q-Meter, dimensions in inches

reported elsewhere (Nelson *et al.*, 1953). The Q-Meter, sample holder, and inductance coils are pictured in Fig. 2-9, where the sample holder is shown plugged into the capacitance terminals of the Q-Meter.
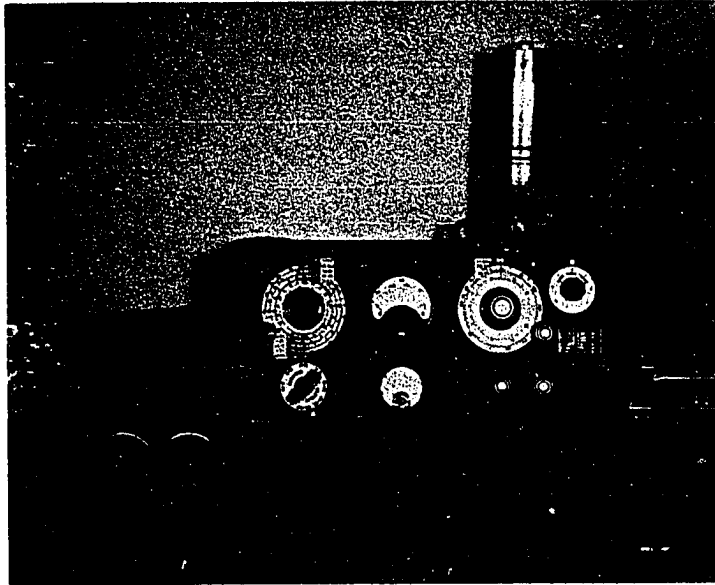
Fig. 2-9. Q-Meter, sample holder, coils, and associated equipment used for dielectric-properties measurements

With an appropriate coil for the desired frequency connected to the inductance terminals and the sample holder plugged into the capacitance terminals of the Q-Meter, the main tuning capacitor, C_1, can be adjusted until the resonant condition is indicated by the Q-Meter vacuum-tube voltmeter. The characteristic curve of the potential difference across the capacitive component is similar to that shown in Fig. 2-10. The peak or maximum voltage, V_m, is read on the Q-Meter voltmeter at resonance, or, more specifically, when the potential across the capacitor is maximum. The change in capacitance, ΔC, is produced by changing the vernier

capacitor, C_1, until the voltmeter
registers a value, V, on both sides
of resonance. ΔC is measured by the
total variation of capacitance as
indicated by the sum of the abso-
lute values of the $+C$ and $-C$ set-
tings of the vernier capacitor.

Measurements of V_m, V, and ΔC_s
are made with the sample holder vari-
able capacitor set to zero and with
a known volume or height of grain in

Fig. 2-10. Q-Meter
resonance curve

the sample holder. With the circuit carefully tuned to resonance, the
sample is then removed and the empty sample holder reconnected to the Q-
Meter. Then capacitance is added to restore resonance using the variable
capacitor of the sample holder, and its setting at resonance gives the
value C_x, which is the capacitance due to the presence of the sample in
the sample holder. With the empty sample holder in place, V_m, V, and ΔC_a
are obtained with air as the dielectric in the sample holder.

2. Determination of dielectric properties

Eq. 2-1 provides the means for calculating the dielectric constant,
and considering the permittivity of air rather than free space,

$$\varepsilon_r' = \frac{1.7964 \ C_x \ \ln(b/a)}{h} + 1 = \frac{1.4109 \ C_x \ (b^2 - a^2) \ \ln(b/a)}{v} + 1 \quad [2\text{-}8]$$

where h is the height of the sample in cm, v is the sample volume in cm^3,
a and b are in cm for purposes of calculating cross-sectional area, and

C_x is in pF. For the sample holder used,

$$\varepsilon_r' = (92.697\ C_x/v) + 1 \qquad\qquad [2\text{-}9]$$

The loss tangent is calculated as

$$\tan \delta = \frac{\dfrac{\Delta C_s}{\sqrt{(V_m/V)^2_s - 1}} - \dfrac{\Delta C_a}{\sqrt{(V_m/V)^2_a - 1}}}{2C_x} \qquad\qquad [2\text{-}10]$$

where the subscript s denotes measurements taken with the sample in the

sample holder, and subscript a denotes measurements taken with air in the

sample holder. Again, from Eqs. 1-6 and 1-8, $\varepsilon_r'' = \varepsilon_r' \tan \delta$, and

$\sigma = 0.5567\ f\ \varepsilon_r''$, where σ is the conductivity for a centimeter cube in mi-

cromhos when f is in MHz.

These calculations were initially programmed for a Wang 320 elec-

tronic calculator equipped with a Wang CP-1 card programmer. Later, they

were programmed for the Wang 700B programmable calculator, which permitted

much more versatility. Before running calculations with the earlier

method, the scale reading from the variable, air capacitor of the sample

holder had to be converted to capacitance using either the calibration

curve or tables prepared from the curve. In the latter program, the scale

reading is entered directly and the calculator computes the appropriate

capacitance from equations which were fitted to the calibration curve in

two sections. For scale values less than 30, $C_x = -0.930616 + 0.163333\ S$,

and, for scale values greater than 30 but less than 90, $C_x = -0.81071 + $

$0.15468\ S + 0.0001607\ S^2$, where S is the scale reading. Also, either h

or v may be entered on the calculator without concern, for h values will

never exceed 10 cm, v values will always exceed 10 cm^3, and the program

tests the value entered and performs the appropriate calculation for

either sample height or volume input.

3. Verification of reliability

The sample holder was originally constructed with carefully cut gas-

kets of Thiokol synthetic rubber in order to permit measurements on ben-

zene to check accuracy and reliability, and satisfactory results were ob-

tained at that time (Nelson *et al.*, 1953). Since dimensions of solid

materials are easier to determine than liquids, specimens were machined

from Rexolite 1422, a thermosetting cross-linked styrene copolymer used

for high-frequency insulating applications. It is a reasonably stable and

uniform material, and dielectric-properties calibrated stock is available

from the National Bureau of Standards (H. E. Bussey, personal communica-

tion. National Bureau of Standards, U. S. Department of Commerce. Boul-

der, Colo. 1971). Because of the costs of calibrated stock, specimens

were fabricated from uncalibrated stock on hand. Values of the dielectric

constant and loss factor were measured on several systems with higher ac-

curacy than can be expected with the Q-Meter system employed here, and

results agreed well with established values, $\epsilon_r' = 2.530 \pm .001$ between

10^6 and 10^{10} Hz, with the value 2.53 listed for frequencies from 10 Hz to

10 GHz, and tan δ ranging from 0.00012 at 1 MHz to 0.00066 at 10 GHz

(American ENKA Corporation, Brand-Rex Division, 1971).

Careful dimensional measurements of the sample holder were required

in order to specify dimensions of the Rexolite 1422 specimens to obtain

tightly fitting samples. These measurements and the use of the

permittivity for air rather than free space resulted in refinement of the constants in Eqs. 2-8 and 2-9. Measurements on Rexolite 1422 specimens in the range from 50 kHz to 50 MHz yielded values for the dielectric constant agreeing with the value 2.53 to within less than 1 percent. Values for the loss tangent were zero when rounded to two decimal places. For measurements on grain and insect samples, this accuracy is deemed adequate.

4. Modification of procedures and sample-height gage construction

This method was originally developed for the 1- to 50-MHz frequency range, and coils were wound to provide a high-Q resonant circuit for the measurements with the sample holder. For purposes of this study, the frequency range was extended to lower frequencies by simply obtaining suitable coils furnished by the manufacturer for use with the Q-Meter and providing a lateral conductor extension to permit their connection to the Q-Meter inductance terminals at the same time that the sample holder was plugged into the capacitor terminals.

Since comparisons were to be made of dielectric properties measured on the same material using several different sample holders of widely varying size, and because the dielectric properties depend upon the density to which a granular material may be settled in the sample holder, a means of determining the sample density was needed. Normally, measurements on grain samples taken with the Q-Meter and sample holder were obtained by measuring the sample volume using a 100-ml strike-off cup, and following consistent procedures to obtain a uniform settling of the sample in the sample holder. With the need for density values, a

sample-height gage was constructed for use with the sample holder (Fig. 2-9). An annular piece was machined from 3/4-inch Rexolite plate to fit loosely but squarely between the sample-holder electrodes. A recess was cut into one side of the Rexolite plate around the center hole while still chucked in the lathe to receive one end of a clear acrylic plastic tube whose inside diameter was just large enough to allow it to slip over the central conductor of the sample holder. A scale with cm and mm subdivisions was then scribed on the acrylic tube so that the top edge of the inner conductor, when aligned with scale markings, provided a direct reading of sample height in the sample holder.

Scribing of the scale was accomplished by chucking the acrylic tube in a lathe, supporting the other end with a live center, and mounting the scriber in the tool rest. The scriber could then be accurately positioned while viewed through a magnifier to align each mark with those of a metric steel rule. For ease in reading the scale, cm marks were scribed around the complete circumference of the tube, 5-mm markings were scribed through a limited arc, and the intermediate mm markings were scribed somewhat shorter. The head-stock spindle was rotated manually as marks were scribed, and pins inserted in appropriate indexing holes in the face of the front spindle gear served to limit the spindle rotation for the length of mark desired. Black India ink was rubbed into the scribed markings to improve contrast for easier reading.

D. RX-Meter System

1. General description

A method for measuring dielectric properties of grain and seed samples in the 50- to 250-MHz range, developed under the author's general supervision, was reported by Jorgensen *et al.* (1970). The Boonton Type 250-A RX Meter served as the basic measuring instrument, and a coaxial sample holder with an open-circuit termination was designed and constructed for use with the RX Meter to obtain the necessary measurements on grain and seed samples (Fig. 2-11).
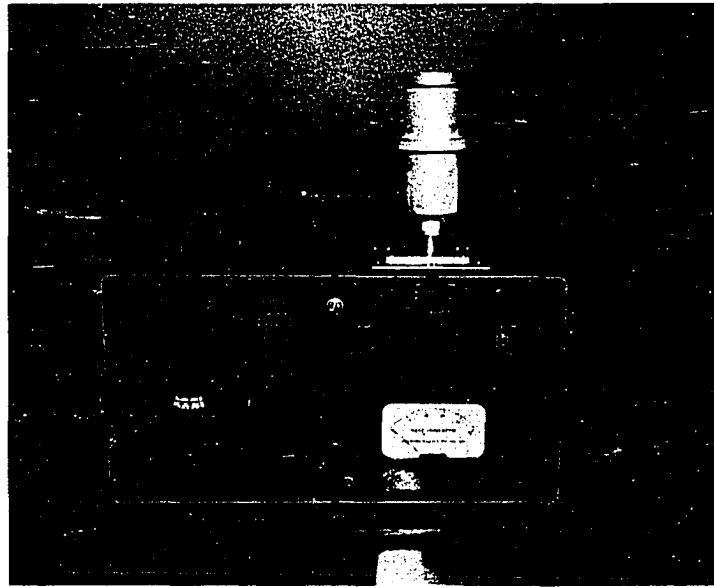
Fig. 2-11. RX Meter and coaxial sample holder

The RX Meter employs two modified Colpitts oscillators and a refined Schering bridge circuit combined in a special way to permit measurement of parallel-equivalent resistance and capacitance of elements connected

to the "unknown" terminals of the bridge over the frequency range from 0.5 to 250 MHz. A Type-N coaxial terminal supplied for the RX Meter served for connecting the sample holder which was constructed with a matching connector. Parts of the sample holder are shown in the sectional drawing (Fig. 2-12), and it is described in further detail in the reference cited.
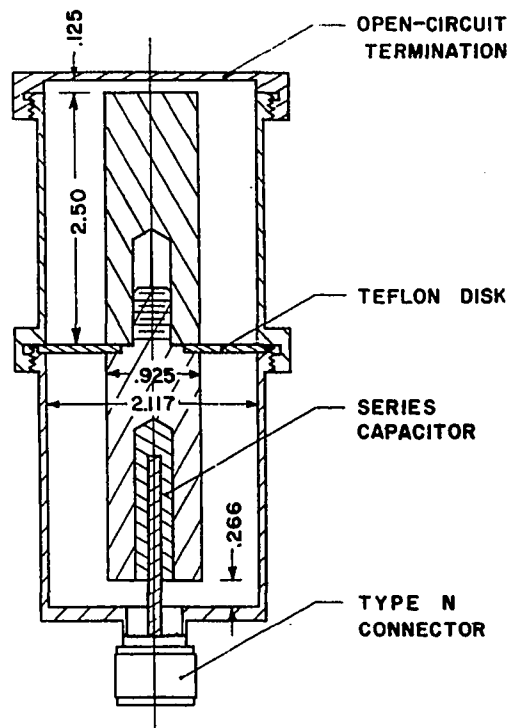
Fig. 2-12. Sectional view of coaxial sample holder
for use with the RX Meter, dimensions in inches

Care was taken in its design to maintain a 50-ohm characteristic imped-ance, and an open-circuit termination in the form of a threaded cap was provided to confine the electric fields, preventing radiation from the open end of the coaxial line and providing a dependable open-circuit ter-mination for the line. Since the capacitance of a coaxial sample holder

of the size necessary for measurements on grain samples exceeded the RX-Meter capacitance range when filled with grain, a series capacitance was built into the central conductor in order to limit the equivalent capacitance to a value within the range of the instrument. In fact, two different lower central conductor parts were constructed, each with a different series capacitance, in order to cover the desired frequency range for measurements on grain samples. A Teflon sleeve separating the two silver-plated brass conductors formed this series capacitor.

The sample holder filled with the sample to a plane parallel with the top surface of the central conductor was then modeled in terms of lumped-parameter transmission-line sections (Fig. 2-13), and its input impedance was equated to the impedance of the sample holder measured by the RX Meter. Separating the resulting equation into real and imaginary compo-
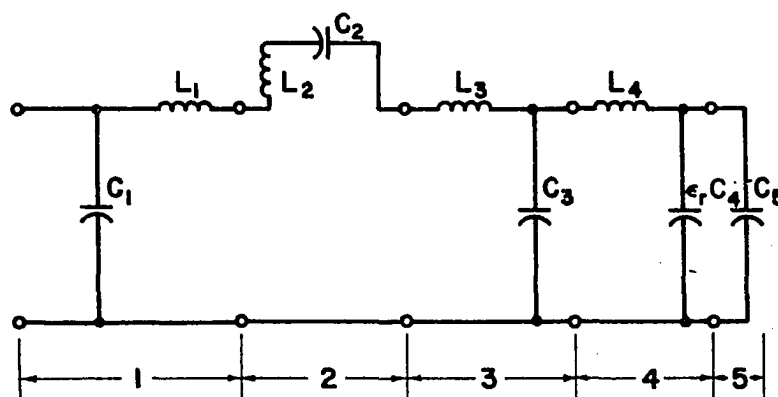
Fig. 2-13. Lumped-parameter model of the coaxial sample holder

nents yields the following expressions for the real and imaginary parts of the relative permittivity:

$$\varepsilon_r' = \frac{(Q_4 - \omega C_p' Q_3)(Q_1 + \omega C_p' Q_2) - G_p^2 Q_2 Q_3}{(Q_1 + \omega C_p' Q_2)^2 + (G_p Q_2)^2} \qquad [2\text{-}11]$$

$$\varepsilon_r'' = \frac{- G_p[Q_3(Q_1 + \omega C_p' Q_2) + Q_2(Q_4 - \omega C_p' Q_3)]}{(Q_1 + \omega C_p' Q_2)^2 + (G_p Q_2)^2} \qquad [2\text{-}12]$$

where $G_p = 1/R_p$, R_p being the parallel-equivalent resistance measured with the RX Meter, and $C_p' = C_p - C_1$, C_p being the parallel-equivalent capacitance measured with the RX Meter, and C_1 is the value identified in Fig. 2-13. The quantities Q_1, Q_2, Q_3, and Q_4 are constants for the sample holder defined as follows in terms of frequency and lumped-parameter values identified in Fig. 2-13:

$$Q_1 = \omega C_4(\omega^2 L_4 C_3 - 1)$$

$$Q_2 = [\omega L_3 - 1/(\omega C_2')]\omega C_4(\omega^2 L_4 C_3 - 1) - \omega^2 L_4 C_4$$

$$Q_3 = [\omega L_3 - 1/(\omega C_2')][\omega C_5(\omega^2 L_4 C_3 - 1) - \omega C_3] + 1 - \omega^2 L_4 C_5$$

$$Q_4 = \omega C_3 - \omega C_5(\omega^2 L_4 C_3 - 1)$$

where $C_2' = C_2/(1 - \omega^2 L_t C_2)$ and $L_t = L_1 + L_2$.

Values for the parameters of Fig. 2-13 were arrived at by initial calculation and a series of procedures outlined by Jorgensen (1966). The values used in this work for the low-frequency and high-frequency models are listed in Table 2-1.

Table 2-1. Values for lumped-circuit parameters of the model (Fig. 2-13) for the RX-Meter sample holder with low-frequency and high-frequency central conductors

Parameter	Low-frequency range 50 - 130 MHz	High-frequency range 130 - 250 MHz
C_1	2.48 pF	2.39 pF
C_2	13.00 pF	7.69 pF
C_3	4.15 pF	4.15 pF
C_4	4.15 pF	4.15 pF
C_5	1.86 pF	1.86 pF
$L_t = L_1 + L_2$	0.0140 µH	0.0148 µH
L_3	0.0107 µH	0.0107 µH
L_4	0.0107 µH	0.0107 µH

2. Verification of reliability

This method should be expected to provide reliable values for the dielectric constants of materials in the range from 1 to 2.28, respectively, the dielectric constants for air and benzene, because these dielectrics were used in measurements to arrive at the values for the parameters of the model. Therefore, additional measurements were needed to assess the reliability of the method for materials with higher dielectric constants. Dielectric constants obtained on n-decyl alcohol (Sec. II, I, 4, c), $\varepsilon'_r = 7$ and $\varepsilon''_r = 1.9$ at 50 MHz, agreed, to within 2 percent, with values reported in the literature (Buckley and Maryott, 1958) for data taken at 10, 48, and 160 MHz. Agreement of dielectric loss factors was also good (Jorgensen *et al.*, 1970).

In further checking for the current studies, rings of Rexolite 1422

(Sec. II, C, 3) were machined with proper dimensions and surfaces ground

to close tolerances so as to fit very closely in the sample space of the

sample holder. Measurements were taken at 10-MHz intervals between 50 and

240 MHz, and the resulting dielectric properties are listed in Table 2-2.

Table 2-2. Values obtained for the dielectric properties of Rexolite 1422
using the RX Meter and sample holder as modeled (Fig. 2-13,
Table 2-1)

Frequency (MHz)	Dielectric constant	Loss factor	Loss tangent
50	2.533	0.000	0.000
60	2.539	0.000	0.000
70	2.539	0.000	0.000
80	2.520	0.000	0.000
90	2.536	0.000	0.000
100	2.552	0.000	0.000
110	2.525	0.000	0.000
120	2.543	0.000	0.000
130	2.605	0.000	0.000
140	2.564	0.000	0.000
150	2.604	0.000	0.000
160	2.613	0.000	0.000
170	2.653	0.014	0.005
180	2.453	0.014	0.006
190	2.476	0.044	0.018
200	2.477	0.028	0.011
210	2.487	0.030	0.012
220	2.450	0.045	0.018
230	2.331	0.062	0.026
240	2.275	0.056	0.025

These values must be compared to accepted values for this material, ε'_r =

2.53 throughout this frequency range, tan δ = 0.0004 at 50 MHz to 0.0005

at 240 MHz (American ENKA Corporation, Brand-Rex Division, 1971). At fre-

quencies below 230 MHz, the resulting values for the dielectric constant

fall within ± 5 percent of the true value as expected, but at the high end of the range the values are too low. Problems are also evident with the model of the sample holder equipped with the high-frequency central conductor in the values obtained for the loss tangent and loss factor at the higher frequencies, particularly with very low-loss samples such as Rexolite. Sensitivity of the method is not suitable for accurate determinations of such small loss tangents, but those expected for insects and grain will be much larger.

Because the sample volume is constant for measurements using the RX-Meter sample holder, density of samples may be calculated if the weight of the sample is obtained.

E. Admittance-Meter System

1. General description

Another method developed under the author's supervision utilizes the General Radio Type 1602-B Admittance Meter and a special sample holder for measuring dielectric properties of grain and seed in the 200- to 500-MHz range (Stetson and Nelson, 1970). A block diagram of the admittance measuring system is shown in Fig. 2-14. Components of the system, in addition to the General Radio 1602-B Admittance Meter, include the following General Radio equipment: 874-LTL Trombone Constant-Impedance Adjustable Line; 1208-B, 1209-B, and 1215-B Unit Oscillators and necessary power supplies; 10-, 20-, and 30-cm sections of Type 874 Coaxial Air Line; and a Type DNT Detector consisting of a Type 874-MR Mixer-Rectifier, 1216-A Unit I-F Amplifier, and an appropriate Unit Oscillator. The assembled equipment is pictured in Fig. 2-15.
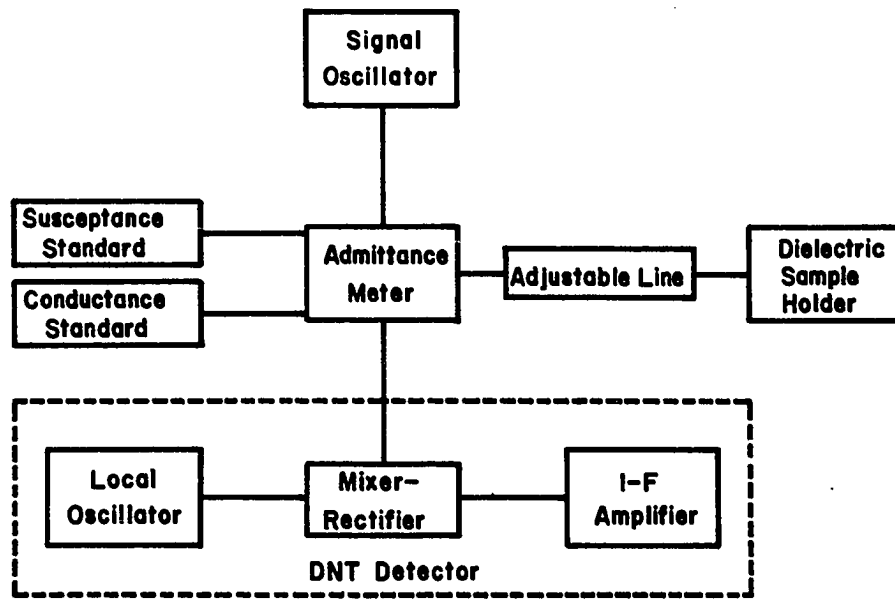
Fig. 2-14. Block diagram of admittance measuring system
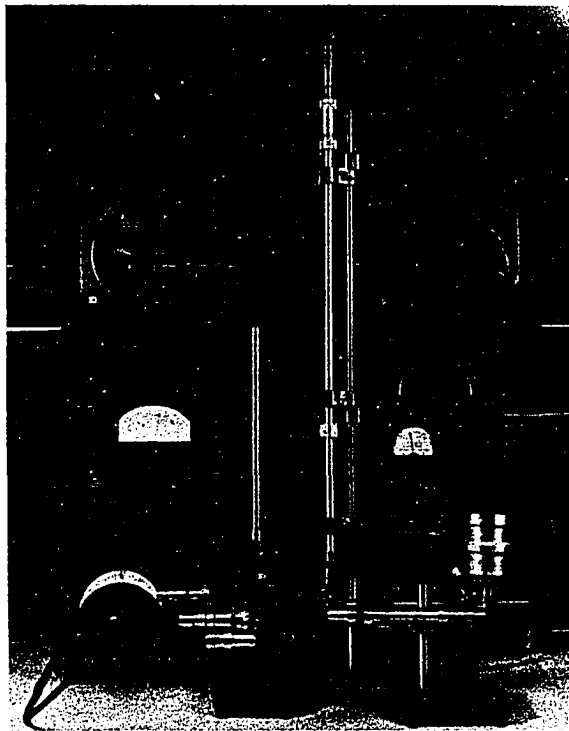
Fig. 2-15. Admittance measuring system including Admittance Meter, trombone line, coaxial sample holder, and auxiliary oscillators, power supply, and detector

The coaxial sample holder shown connected to the system in Fig. 2-15 is described in detail in the cited publication, and a sectional drawing illustrates its construction (Fig. 2-16). The length of the sample
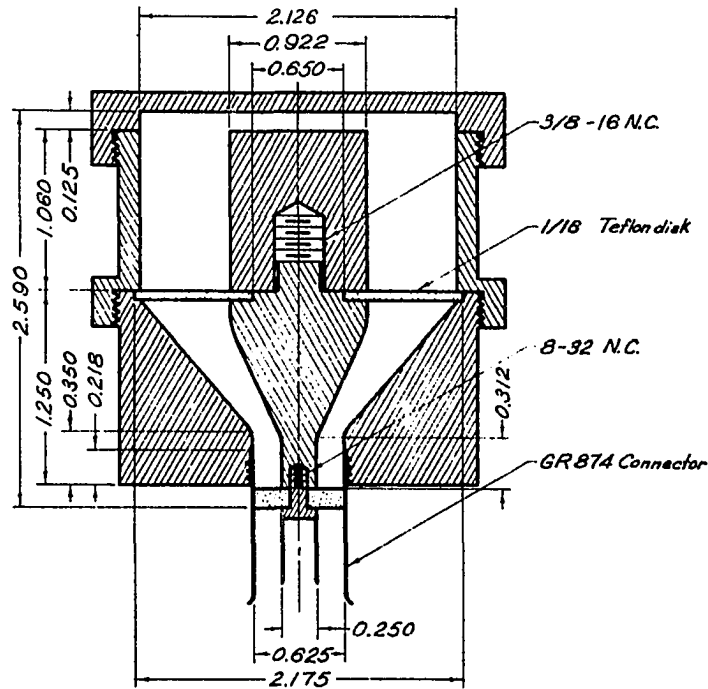
Fig. 2-16. Sectional view of coaxial sample holder for use
with the Admittance-Meter system, dimensions in inches

holder was limited to a small fraction of a wavelength at the highest fre-
quency to be used, and care was taken to maintain a 50-ohm characteristic
impedance in its design. It was constructed with a General Radio Type 874
50-ohm Connector to facilitate proper connection to the Type 874 50-ohm
line. A threaded cap served to provide an open-circuit termination for
the sample holder. The sample to be measured occupies all space between
the Teflon disk on which it rests and the plane parallel to the top

surface of the central conductor.

The sample holder with sample in place was modeled as lumped-circuit equivalents of a series of transmission-line sections (Fig. 2-17), where
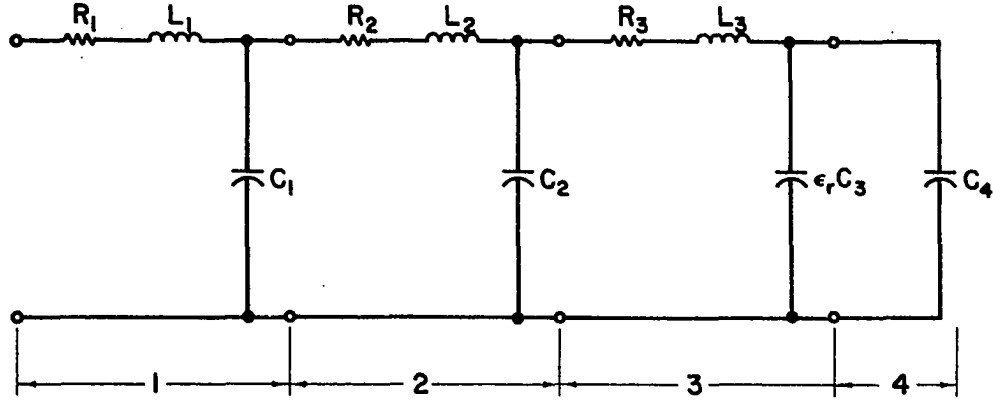
Fig. 2-17. Lumped-circuit model of coaxial sample holder

$\epsilon_r C_3 = (\epsilon_r' - j\epsilon_r'')C_3$ represents the complex capacitance of that section of the coaxial line holding the sample. The input admittance of the sample holder, Y_i, is equated to the measured admittance $Y_m = G + jB$, where G and B are the conductance and susceptance measured with the Admittance Meter. Separation of the real and imaginary parts of the resulting equation yields the following expressions for the dielectric constant and loss factor:

$$\epsilon_r' = \frac{(\omega Q_3 + BQ_8 - GQ_7)(GQ_5 - BQ_6 - \omega Q_1) + (\omega Q_4 - GQ_8 - BQ_7)(GQ_6 + BQ_5 - \omega Q_2)}{(GQ_5 - BQ_6 - \omega Q_1)^2 + (GQ_6 + BQ_5 - \omega Q_2)^2} \qquad [2\text{-}13]$$

$$\epsilon_r'' = \frac{(\omega Q_3 + BQ_8 - GQ_7)(GQ_6 + BQ_5 - \omega Q_2) + (\omega Q_4 - GQ_8 - BQ_7)(GQ_5 - BQ_6 - \omega Q_1)}{(GQ_5 - BQ_6 - \omega Q_1)^2 + (GQ_6 + BQ_5 - \omega Q_2)^2} \qquad [2\text{-}14]$$

where the quantities Q_1 through Q_8 are frequency-dependent constants of the sample holder defined as follows:

$$Q_1 = C_3 + \omega^2(\omega^2 L_2 L_3 C_1 C_2 C_3 - L_3 C_2 C_3 - L_3 C_1 C_3 - R_2 R_3 C_1 C_2 C_3 - L_2 C_1 C_3)$$

$$Q_2 = \omega(R_3 C_2 C_3 + R_3 C_1 C_3 + R_2 C_1 C_3 - \omega^2 R_2 L_3 C_1 C_2 C_3 - \omega^2 R_3 L_2 C_1 C_2 C_3)$$

$$Q_3 = C_1 + C_2 + C_4 + \omega^2(\omega^2 L_2 L_3 C_1 C_2 C_4 - L_3 C_1 C_4 - R_2 R_3 C_1 C_2 C_4 - L_2 C_1 C_2 -$$
$$L_2 C_1 C_4 - L_3 C_2 C_4)$$

$$Q_4 = \omega(R_3 C_2 C_4 + R_3 C_1 C_4 + R_2 C_1 C_2 + R_2 C_1 C_4 - \omega^2 R_2 L_3 C_1 C_2 C_4 - \omega^2 R_3 L_2 C_1 C_2 C_4)$$

$$Q_5 = \omega(R_1 Q_1 - \omega L_1 Q_2 + R_3 C_3 + R_2 C_3 - \omega^2 R_2 L_3 C_2 C_3 - \omega^2 R_3 L_2 C_2 C_3)$$

$$Q_6 = \omega R_1 Q_2 + \omega^2(L_1 Q_1 + L_3 C_3 + R_2 R_3 C_2 C_3 + L_2 C_3 - \omega^2 L_2 L_3 C_2 C_3)$$

$$Q_7 = \omega (R_1 Q_3 - \omega L_1 Q_4 + R_3 C_4 + R_2 C_4 + R_2 C_2 - \omega^2 R_2 L_3 C_2 C_4 - \omega R_3 L_2 C_2 C_4)$$

$$Q_8 = \omega R_1 Q_4 - 1 + \omega^2(L_1 Q_3 + L_3 C_4 + R_2 R_3 C_2 C_4 + L_2 C_2 + L_2 C_4 - \omega^2 L_2 L_3 C_2 C_4)$$

Determination of values for lumped-circuit parameters shown in Fig. 2-17 and procedures for adjusting them are described briefly by Stetson and Nelson (1970). Values used for this work are listed in Table 2-3. Calculated and adjusted values were based on measurement data taken with air and benzene as known dielectrics in the sample holder. Values were required for the parameters which minimized the rms percentage error in the resulting dielectric constant over the 200- to 500-MHz frequency range. Therefore, the method can be expected to provide proper values for the dielectric constant (within about ± 5 percent) for materials with ε'_r in the range from 1 to 2.28. Reliability checks were run using n-decyl and dodecyl alcohols at 288 and 500 MHz where published values (Lebrun, 1955) ranged between 3.0 and 3.5 for the dielectric constant and between 0.7 and 1.4 for the loss factor. Measured values for the dielectric constant of these compounds agreed with Lebrun's values to within less than

4 percent and agreement of loss factors was also very good.

Table 2-3. Values for lumped-circuit parameters of the sample holder model of Fig. 2-17

Parameter	Value
R_1	0.25 ohm
R_2	0.40 ohm
R_3	0.40 ohm
L_1	1.234 nH
L_2	3.000 nH
L_3	4.250 nH
C_1	1.470 pF
C_2	2.770 pF
C_3	1.815 pF
C_4	1.280 pF

2. Verification of reliability

In preparation for these studies, further reliability checks were conducted by taking measurements on accurately machined samples of Rexolite 1422 (Sec. II, C, 3). Parts of the Admittance-Meter sample holder were carefully measured, and two Rexolite rings were machined and ground to the following specifications: outside diameter, b = 2.126 + 0 or - 0.001 inches; inside diameter, a = 0.922 + 0.001 or - 0 inches; and combined height, h = 1.063 ± 0.001 inches. These two rings provided a sample fitting tightly around the central conductor and tightly inside the outer

conductor filling the sample space of the sample holder.

Two separate sets of measurements were made at 20-MHz intervals throughout the frequency range from 200 to 500 MHz. The average values obtained are listed in Table 2-4. Resulting values for the dielectric

Table 2-4. Values obtained for the dielectric properties of Rexolite 1422 using the Admittance Meter and sample holder as modeled (Fig. 2-17, Table 2-3)

Frequency (MHz)	Dielectric constant	Loss factor	Loss tangent
200	2.54	0.00	0.00
220	2.67	0.00	0.00
240	2.59	0.00	0.00
260	2.59	0.00	0.00
280	2.64	0.00	0.00
300	2.60	0.00	0.00
320	2.55	0.00	0.00
340	2.63	0.00	0.00
360	2.63	0.00	0.00
380	2.70	0.04	0.01
400	2.68	0.04	0.01
420	2.64	0.06	0.02
440	2.63	0.08	0.03
460	2.67	0.09	0.03
480	2.69	0.09	0.03
500	2.86	0.14	0.05

constant of Rexolite 1422 were all a bit high, but, except for the 500-MHz value, all lie within less than 7 percent of the proper value 2.53. The loss tangent of Rexolite 1422 in this frequency range is about 0.0005. While the method is not sensitive enough for accurate determination of such low loss tangents, a problem is indicated in the values of loss tangents obtained at the higher frequencies of this range. The expected loss tangents of grain and insect samples, however, are so high that

errors of the magnitude indicated in loss-tangent determination should not be of any real concern.

F. Slotted-Line System

1. General description

A Rohde & Schwarz instrument system consisting of a Type SLRD (BN 41004/2) Power Signal Generator, LMD (BN 3926/50) Slotted Line, UBK (BN 12120) VSWR/Null Indicator, and Short-Circuit Specimen Container (BN 39318/50) was assembled, which is useful for dielectric-properties measurements over the range of the signal generator, 275 to 2,750 MHz. Specifications for the LMD slotted line list a range of 300 to 3,000 MHz because the range of the probe carriage is limited to approximately 50 cm, and 300 MHz is about the lowest frequency at which a half-wavelength can be measured. The slotted line and 15-cm long coaxial specimen container are designed for a 50-ohm characteristic impedance with a 9.12-mm-diameter central conductor and an outer conductor of 21.00-mm inside diameter. This physical size provides sufficient space to accommodate wheat kernels with a random orientation, though it approaches the lower limit of such dimensions.

The measurement system is pictured in Fig. 2-18, where the vertical mounting of the slotted line may be noted. A base plate (BN 39310) on which the slotted line can be mounted was fastened to the laboratory wall and carefully aligned using a spirit level to insure a truly vertical or plumb orientation for the slotted line. Then, when the specimen container is attached to the load end of the slotted line, liquid or granular
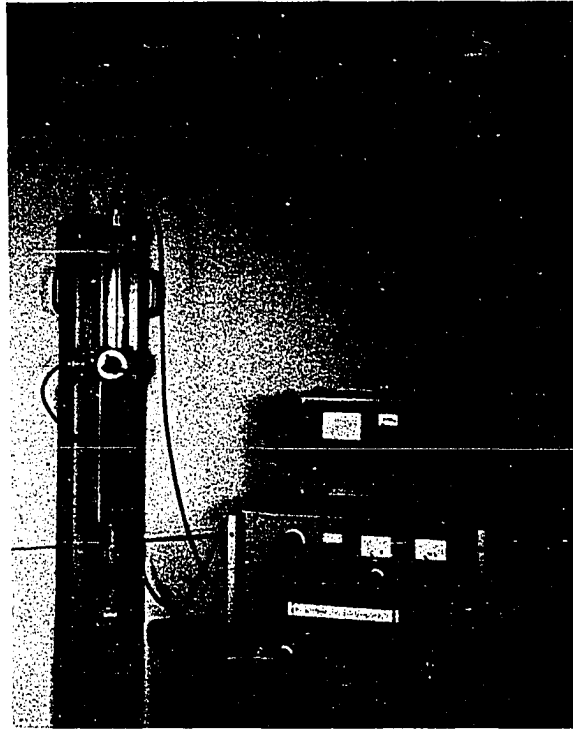
Fig. 2-18. Rohde & Schwarz LMD Slotted Line, SLRD Signal
Generator, and UBK Indicator, showing vertical
mounting and counterweight for slotted line
and sample holder connected to the line

samples may be measured with the plane of the air-sample interface per-

pendicular to the axis of the coaxial line.

Use of the slotted line in the vertical orientation presented a

problem, because the weight of the movable probe carriage would cause it

to move to the lower end of the line whenever the operator's hand released

the positioning knob. This problem was overcome by building the counter-

weight and pulley assembly shown in Fig. 2-18 and constructing a clamp to

secure the end of the braided nylon chalk line, used as a cord for the

counterweight assembly, to the probe carriage of the slotted line. The

counterweight consisted of a 7-inch length of 1-1/2-inch brass rod

machined on a lathe and provided with an axially drilled hole to receive the nylon cord.

The SLRD signal generator employs a single-stage, grounded-grid, tuned-plate, tuned-cathode oscillator circuit using a disk-seal triode and tunable coaxial lines as resonant circuits. The plate and cathode tuning circuits are mechanically coupled for ease in changing frequencies, with provision for separate tuning of the cathode circuit for final adjustment for proper oscillation. The frequency range from 275 to 2,750 MHz is covered in two subranges, inductive feedback being used for the 275- to 950-MHz range, and capacitive feedback being utilized for the 850- to 2,750-MHz range. Power is coupled out from the anode circuit by means of a calibrated piston attenuator, and a directional coupler, amplifier, and output power meter provide a reliable indication of power to the connected equipment. Output power is adjustable from 1×10^{-8} W to 30 W with maximum power available dropping off at the higher frequencies. Power levels greater than 9 dBm are read from the panel meter while lower levels are read from the calibrated attenuator dial. Calibration accuracy of the frequency scales is ± 2 percent, and frequency stability is good (drift less than 5×10^{-5}/15-min period at constant supply voltage and ambient temperature). The unit also has low residual FM characteristics.

The LMD slotted line was equipped with a crystal detector and tunable probe circuit. The scale, indicating location of the probe, is calibrated in cm with mm subdivisions and is equipped with a vernier reading to 0.1 mm. In using the vernier, possible errors due to parallax were noted. To remedy this, a small rectangular piece was cut from a thin glass mirror

and cemented on a plane surface adjacent to the vernier scale so that the image of the eye might be observed while reading the scale to insure that the observer's eye is viewing the scale from an angle perpendicular to the scale.

The UBK indicator is a five-stage amplifier employing low-noise audiofrequency pentodes in the first three stages with a narrow-band 1-kHz section in the plate circuit of the third stage which is tunable through a limited range in 2-percent steps to match the modulation frequency of the signal generator. A cathode-follower output delivers 10 V ac to a rectifier circuit for full-scale deflection of the main meter.

An attenuator in the input circuit provides for 120-dB attenuation in 10-dB steps referenced to 2 μV. The instrument is calibrated for direct reading when used with square-law detectors. Scales provided include voltage standing-wave ratio (VSWR), inverse VSWR, and dB scales for voltage ratios. Half-power- or double-power-point readings must, therefore, be 6 dB apart on the scale of the main meter. Attenuator settings where the inverse square law can no longer be used because of high RF signal amplitudes are marked with a red arc as a reminder. A second panel meter, useful in searching for voltage null locations when the main meter is overloaded, is also provided for convenience. The indicator has a switch for expanding the scale to provide more accurate measurement of half-power or double-power widths and low standing-wave ratios.

2. Development of procedures

Procedures recommended for measurement of the dielectric constant, ε'_r, and the loss tangent, tan δ, of insulating materials are outlined by

Rohde & Schwarz (1962). These procedures, employing a short-circuited sample holder, require adjustment of the signal generator frequency until the distance from the sample surface to the slotted-line probe is exactly an integral number of half-wavelengths (termed $\lambda/2$ resonance, because an integral number of half-wavelengths will then exist in the sample) or until that distance is an odd-multiple quarter-wavelength (termed $\lambda/4$ resonance, because there would then be an odd number of quarter-wavelengths in the sample). Equations are provided for the simple calculations then required to obtain ε_r' and tan δ. For the planned studies, measurements on numerous samples at a given frequency were desired, and it appeared that the procedure just described would be rather time-consuming. Therefore, another procedure requiring less time for taking data was selected. This procedure, which is applicable to a rather wide variety of dielectric materials, was first reported by Roberts and von Hippel (1946) and has since been refined and adapted for many kinds of dielectric measurements. Because this method is applicable to four different measurement systems used in this study, it is explained in detail in Appendix A. Other than frequency determination and physical length of the sample, the only observations required by this method, referred to hereinafter as the short-circuited line or waveguide method, are the voltage null widths and locations, as measured with the slotted line, with and without the sample at the shorted end of the line.

Numerous measurements on several different materials were made using the SLRD-LMD system in gaining familiarity with the equipment. One problem encountered appeared to be either a frequency or output level

instability in the signal generator. An extremely sharp voltage minimum
is obtained with this equipment when observing the voltage standing-wave
pattern in an empty short-circuited line. When operating the signal gen-
erator at frequencies between about 1,350 and 1,650 MHz, it was impossible
to set the slotted-line probe at an exact voltage minimum because of ap-
parently random fluctuation of the UBK indicator meter reading. Checks
of the oscillator stability using a Hewlett-Packard Model 5246L Electronic
Counter equipped with a 5254B Plug-In Frequency Converter showed that the
signal generator was operating within its specified frequency stability.
The problem was finally identified as one of radiated energy coupling
between the power signal generator and the slotted line, and moving the
signal generator as far as possible from the slotted line with the avail-
able connecting cable reduced the problem sufficiently that measurements
could be taken.

3. Verification of reliability

Benzene was used as the first standard material to check the reli-
ability of measurements obtained on this system. Benzene was measured
into the sample holder using a pipette held in a stand, and the volume was
read to 0.01 ml. Normally, 20-ml samples were used and the sample length
was calculated from the dimensions of the sample holder. Resulting di-
electric-constant values for frequencies of 1 GHz and higher averaged
about 2.27 or 2.28, and the loss-tangent values were on the order of
0.0001. The accepted value of ϵ_r' for pure benzene is 2.276 at 24° C (75°
F) (Maryott and Smith, 1951), and reported values for tan δ (Buckley and
Maryott, 1958) are of about the same magnitude as that obtained. At

frequencies less than 1 GHz, the dielectric-constant values were not as reliable and the tan δ values were much too large. The reasons have not been satisfactorily explained.

Samples of Rexolite 1422 (Sec. II, C, 3) were machined on a lathe to fit the coaxial sample holder, and measurements on these specimens were made as a further reliability check. Measurements at 1 and 2 GHz on a sample 32.781 mm long yielded $\varepsilon'_{rm} = 2.527$, and $\tan_m \delta = 0.0005$, where the subscript, m, denotes measured values. Corrections for air gaps between specimens and conductors of coaxial lines are treated by Eichacker (1958), who presents an expression for the error in the determination of the dielectric constant, which reduces to the following for small air gaps: $\Delta\varepsilon'_r/\varepsilon'_{rm} = (\varepsilon'_{rm} - 1)(\Delta a/a + \Delta b/b)$. The corrected value is then

$$\varepsilon'_r = \varepsilon'_{rm}[1 + (\varepsilon'_{rm} - 1)(\Delta a/a + \Delta b/b)] \qquad [2\text{-}15]$$

for a specimen of outside diameter $b - \Delta b$ with a coaxial hole of diameter $a + \Delta a$ in a coaxial line with central conductor of diameter a and outer conductor of inside diameter b. The Rexolite 1422 specimens used for these measurements fit tightly on the central conductor, but measured 20.97 mm in diameter compared to 21.00 for the coaxial line. Applying the correction for the air gap, Eq. 2-15 yields 2.533 for the dielectric constant, which agrees quite closely with the expected value (Sec. II, C, 3), and very closely with the value 2.5332 reported by Bussey and Gray (1962) for an unidentified plastic which was in fact Rexolite 1422. Eichacker also gives an expression for the error in tan δ resulting from air gaps, but the correction is insignificant in this case, and Bussey

and Gray (1962) expressed doubt that such a correction should be applied for the loss factor and loss tangent. They reported tan δ = 0.00057 for the plastic known to be Rexolite, with which the value 0.0005 obtained here is in close agreement.

Problems were again encountered using the SLRD-LMD system for measurements on the Rexolite sample at frequencies below 1 GHz. The dielectric-constant value obtained at 500 MHz was close, but the loss-tangent value was about 0.05. At 300 MHz, the value obtained for the dielectric constant was very bad and the loss factor was indicated as 0.9. This method with this particular equipment, therefore, cannot be used reliably at frequencies much below 1 GHz. The problem has not been identified, though the influence of a stationary Teflon support in the end of the slotted line between the sample and the probe is suspect, because the theoretical basis for the short-circuit method (Appendix A) does not provide for the presence of a third medium.

4. Sample height determination

In order to measure the length of the sample for measurements on insects and grain, a sample-height gage was constructed for use with the specimen container or sample holder. It was machined from Kel-F rod to fit closely, but with enough clearance to slide freely into the coaxial sample holder. Using the procedure outlined in Sec. II, C, 4, an accurately divided metric scale with cm and mm divisions was scribed on the surface of the height gage in correct position to read the sample height directly on the scale at the top edge of the sample holder outer conductor. The sample holder and height gage are pictured in Fig. 2-19.
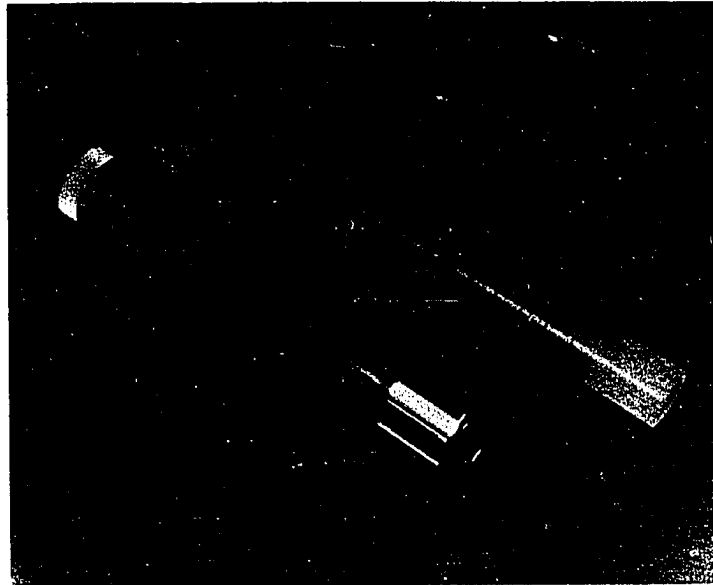
Fig. 2-19. Coaxial sample holder and sample-height gage for use
with Rohde & Schwarz Slotted-Line system

Knowing the height of the sample and the cross-sectional area of the sample holder also permitted sample density to be calculated when the sample weight was known.

G. Non-Slotted-Line System

1. General description

Another system of Rohde & Schwarz instruments was used for measurements in the range from 2.3 to about 6.3 GHz. A Type SLRC (BN 41005) Power Signal Generator with a frequency range of 2.3 to 7.0 GHz provided the source of power to the Type LMC Non-Slotted Line (BN 3931/50), useful from 1.65 to 6.35 GHz. The Short-Circuit Specimen Container (BN 39318/50) was then attached to the load end of the non-slotted line, and the Type UBK

VSWR/Null Indicator was connected to the detector output from the non-slotted line. The UBK Indicator and the specimen container have been previously described in Sec. II, F, 1. The instrument assembly for measurements in this frequency range, 2.3 to 6.3 GHz, is shown in Fig. 2-20.
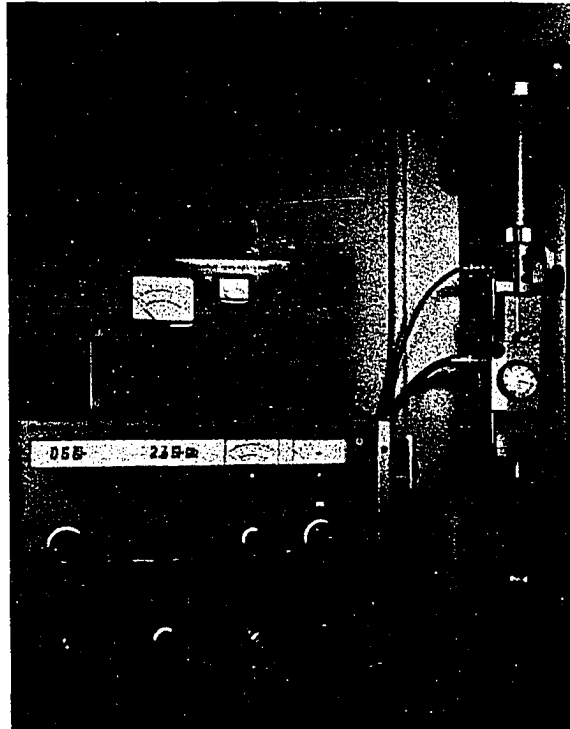
Fig. 2-20.   Rohde & Schwarz LMC Non-Slotted Line, SLRC Signal
Generator, UBK Indicator, and sample holder

The non-slotted line was fastened to a mounting base in the same way that the Rohde & Schwarz LMD Slotted Line was mounted (Sec. II, F, 1) to provide vertical mounting for work with liquid and granular materials.

Like the Rohde & Schwarz SLRD Power Signal Generator, the SLRC unit employs a disk-seal triode in a grounded-grid, tuned-plate, tuned-cathode circuit with shorting plungers tuning the coaxial-line resonant circuits.

Tuning plungers of the plate and cathode circuits are mechanically coupled through a unique nonlinear system so that single-knob tuning of the oscillator is achieved. Provision for separate limited tuning of the cathode resonant line permits adjustment for proper oscillation and maximum power output. Power is coupled out of the plate resonator by means of a loop, and an output attenuator is provided to adjust the output power level. A directional coupler and power meter also indicate the level of power delivered to attached equipment.

Calibration accuracy of the frequency dial is specified as ± 1.5 percent, and the SLRC has the same frequency stability as the SLRD and low residual FM characteristics.

The Type LMC Non-Slotted Line is a precision instrument built around an accurately machined and finished coaxial line. A movable short-circuiting piston serves to tune the line to resonance when desired. The power from the signal generator is fed through a tunable harmonic filter which functions as a low-pass filter and voltage transformer in coupling energy into the coaxial-line section by means of two symmetrically opposed capacitive probes near the load end of the non-slotted line. A coupling loop mounted in the face of the shorting piston provides a voltage proportional to the current flowing in the short-circuit plane. This signal is rectified by a coaxial crystal diode inside the piston and is available at the connection for the UBK VSWR/Null Indicator. In this way the current standing-wave pattern may be observed as the shorting piston traverses the length of the non-slotted line in the same way that the voltage standing-wave pattern is obtained with a slotted line using a moving capacitive probe.

Because the central conductor of the non-slotted line is supported only at the shorted end of the line, there are no supports between the probe and the sample holder, which is simply a smoothly connected extension of the coaxial line. Therefore, a reflection-free connection between the non-slotted line and the sample-holding line section is achieved providing an ideal arrangement for making measurements.

An accurate worm drive actuated by a hand-operated spindle provides precisely controlled movement of the shorting piston. A scale is provided for measurement of the probe (short-circuit plane) location and a vernier permits readings to be taken to 0.05 mm. For more precise measurements, a dial gage is provided as an integral part of the instrument permitting readings to 0.001 mm. Gage blocks are provided for use with the dial gage for greater accuracy in wavelength measurements.

2. Verification of reliability

Measurements on benzene samples of the same type described in Sec. II, F, 3 at 3, 4, 5, and 6 GHz yielded the same dielectric-constant and loss-tangent values as obtained with the SLRD-LMD system, which were in good agreement with accepted values. Measurements on the same Rexolite 1422 samples described in Sec. II, F, 3 at 6 and 2.44 GHz gave a measured value of 2.525 for the dielectric constant, which, when corrected for the air gap according to Eq. 2-15, became 2.531. Loss tangents obtained were of the same order of magnitude as those given in Sec. II, F, 3. Reliable values were obtained throughout the frequency range with the SLRC-LMC system. The same sample holder and sample-height gage were used with both Rohde & Schwarz systems.

H. Microwave Dielectrometer System

1. General description

A Central Research Laboratories Model 2 Microwave Dielectrometer was available for the studies. This instrument was designed especially for utilizing the shorted-line or shorted-waveguide technique originally reported by Roberts and von Hippel (1946) for dielectric-properties measurements on solid and liquid materials at frequencies of 1, 3, and 8.5 GHz. The underlying principles of this method and techniques for obtaining such measurements were thoroughly explored, mathematical relationships verified, and a general computer program developed for the calculation of dielectric properties from measurements data. This work is summarized in Appendix A.

The Microwave Dielectrometer with an auxiliary Model 2 Dielectrometer Temperature Control Unit is shown in Fig. 2-21. The dielectrometer proper rests on the table top of the temperature control unit. The dielectrometer consists of a slotted cylindrical waveguide section, precision traveling probe, probe-output amplifier and indicating meters, three separate klystron oscillators, and associated modulators, power supplies, switches, and coupling devices. For frequencies of 1 and 3 GHz, a central conductor is used in the slotted section so it operates as a coaxial line (TEM mode). At 8.5 GHz, the slotted section is utilized as a cylindrical waveguide operating in the TE_{11} mode. Energy from the klystrons is coupled into the waveguide through a loop in a shorting plunger in the upper section which serves to tune the waveguide to resonance. The sample holder, which is a section of waveguide or coaxial line, connects to the
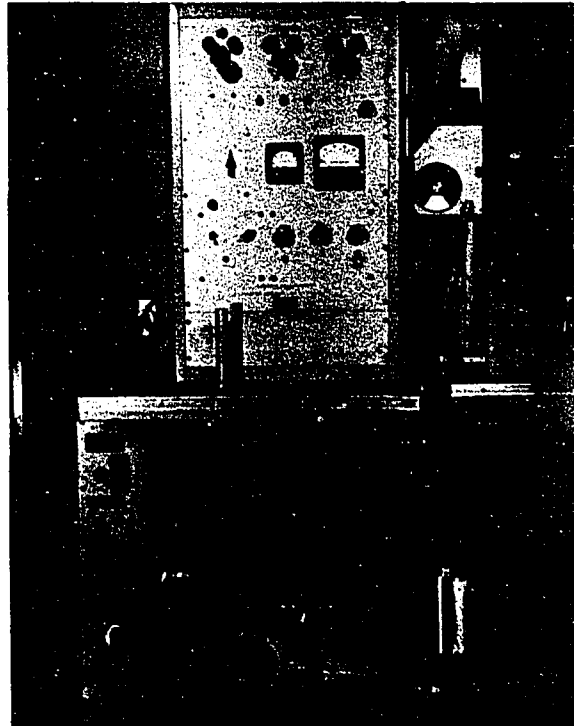
Fig. 2-21. Central Research Laboratories Microwave Dielectrometer
and auxiliary Temperature Control Unit with long sample
holder attached to the line and sample-height gage
standing on the table

lower end of the slotted section and terminates the line in a short cir-

cuit. Solid samples are placed in the line against the short-circuit

termination, and granular materials are simply poured into the sample

holder and properly leveled. Special provisions have been made in the

design of sample holders to permit external filling with liquids through

capillary lines. Half-wavelength-long Teflon plugs equipped with fine

air relief tubes are provided which serve as covers for liquid samples.

For studies of material properties at other than room temperature, a long

sample holder is provided which extends far enough that the temperature

control jacket assembly may surround the sample-holding section. A

water-cooled heat sink is used around the upper section of the sample

holder to reduce transfer of heat from the sample holder to the slotted

section. Sections of silver-plated stainless steel are also used in the

sample holder construction to reduce the heat conduction that normally

takes place in copper or brass.

A tunable crystal detector is employed with the probe, and the probe

carriage drive mechanism is of precision design, with a probe position

dial vernier permitting readings to 0.001 mm. The probe-output amplifier

is designed for convenience in recording double-power points for measure-

ment of voltage null widths. An auxiliary meter is provided to register

indications, when the main meter is overloaded, for convenience in locat-

ing voltage nodes without changing sensitivity switch settings as the

probe traverses the slotted section.

Dimensions of the waveguide and sample holders are nominally 1 inch

for the inside diameter of the outer conductor and 3/8 inch for the out-

side diameter of the inner coaxial conductor. This sample holder size

will accommodate insect and wheat samples satisfactorily. A sample-

height gage made from Plexiglas rod, shown with the dielectrometer in Fig.

2-21, serves to level the top surface of granular samples and provides for

direct reading of the sample height.

Considerable time was required for complete checking out of the di-

electrometer. Replacement of one of the klystron tubes was necessary,

and, since the type was no longer manufactured, a replacement was obtained

from surplus electronic supply sources. The rubber tubing which inter-

connects four water-cooling capillary tubes for each klystron had

deteriorated and was replaced with sections of plastic line. This line ruptured when a plug developed in the capillary tubing while the equipment was operating, so all chassis were removed from the cabinet for drying and inspection of components. High-pressure tubing was obtained to replace the plastic tubing, and the unit was restored to proper operation after clearing the plugged cooling line and replacing two Helipots which were damaged when the water line ruptured. Initially, the lack of any probe-output signal was traced to an incorrectly positioned probe wire which resulted when a locking sleeve had slipped. The probe wire was also found to be bent. It was satisfactorily straightened after numerous measurements and adjustments. Discrepancies in probe-scale readings were traced to a barely visible kink in a steel tape which is part of the carriage drive mechanism. It was found that errors as a result of this defect could be avoided by properly selecting the nodes for the measurements needed in this study, but a replacement tape was obtained. A parallax problem in reading the vernier on the fine probe-carriage-positioning-knob drum scale was remedied by making and installing a 0.010-inch shim under the vernier scale block.

2. Verification of reliability

According to the manufacturer, the dielectrometer is capable of measuring dielectric constants in the range from 1 to 100 and loss tangents between 0.0001 and 1.0 with an accuracy of 1 or 2 percent with ordinary care in sample preparation, when the product of these two quantities, ϵ_r' tan δ, is less than 0.5. Measurements on Rexolite 1422 samples at 3 GHZ gave a dielectric-constant value of 2.505; however, the sample fit the

line a bit loosely, both diameter dimensions of the sample being about
0.002 inch different from the dimensions of the line. Applying the cor-
rection for air gaps, Eq. 2-15, corrected the value to 2.533 which agrees
very well with the values obtained with the Rohde & Schwarz instruments.
The loss-tangent values obtained were near 0.0007, which also agree fairly
well. These results were obtained by inserting the sample directly into
the end of the slotted section in contact with a short-circuit termina-
tion.

The same Rexolite samples were also measured in the end of the 30-
cm-long sample holder, which is used with the temperature control unit.
Slightly larger loss tangents (about 0.0012) were obtained in this case,
but the error would be negligible for grain and insect samples. Measure-
ments at 1 and at 8.5 GHz gave slightly higher dielectric-constant values
ranging, when corrected for air gaps, between 2.537 and 2.541. The cor-
rection for an air gap between the sample and the waveguide walls in a
cylindrical waveguide operating in the TE_{11} mode was presented by Bussey
and Gray (1962). The correction equation for the cylindrical waveguide
case, in form similar to Eq. 2-15, is

$$\epsilon_r' = \epsilon_{rm}'[1 + (\epsilon_{rm}' - 1)(0.8368)\Delta b/b]$$

[2-16]

Eq. 2-16 was used for 8.5-GHz measurements while Eq. 2-15 was applied for
1- and 3-GHz measurements. Closer agreement among measurement results at
the three different frequencies might be achieved with better fitting sam-
ples or with more accurate measurements of the air gaps, but further work
at this time did not appear justified because of the variation expected
to be encountered with insect and grain samples.

I. X-Band System

1. *General*

In order to extend dielectric-properties measurement capability to higher frequencies, a collection of X-band (8.2 to 12.4 GHz) and WR-90 waveguide components was assembled in an effort to develop a suitable measuring system. Initially, components were obtained for a microwave bridge system as the first technique to be tried. Major items included a Varian X-13A reflex klystron, a klystron tube mount, klystron power supply, microwave power meter, slotted section, VSWR meter, cavity-type frequency meter, precision attenuator, precision phase shifter, isolators, 20-dB directional couplers, waveguide shorting switch, slide-screw tuner, and hybrid or magic tee.

In order to safely mount the X-13A klystron in the Narda Model No. 990 Tube Mount, the klystron was mounted on one flange of a 6-inch, straight, WR-90 waveguide section, and a mounting bracket was constructed of aluminum angle and attached rigidly with screws to the frame of the tube mount (Fig. 2-22). A notch to accommodate the waveguide section was cut in the mounting bracket and a piece of aluminum plate was attached to the aluminum angle clamping the waveguide section securely in position when the klystron was plugged into the tube socket of the tube mount. A power cable was then made up for proper connection of the Narda tube mount to the Hewlett-Packard Model 716B Klystron Power Supply. In this way, 115-V a-c power is supplied for operation of the cooling fan in the tube mount when the klystron power supply switch is set to the standby position to energize the klystron filament. After suitable warm-up time, the power
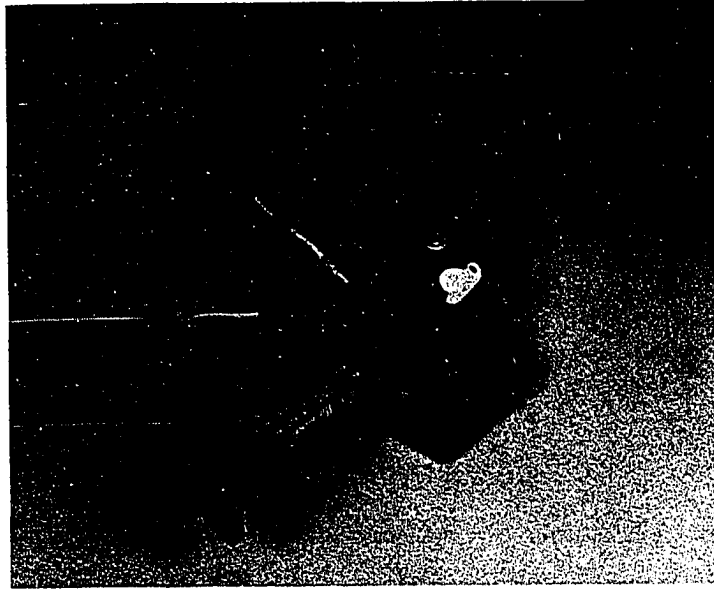
Fig. 2-22. Klystron, connecting waveguide section, and klystron
tube mount, showing bracket constructed for rigid
support of waveguide section

supply switch may be set to the "high-voltage" position and beam, or

anode, and repeller, or reflector, voltages are supplied to the klystron.

The 716B power supply has a panel meter which registers klystron beam

current and has provisions for modulation of the klystron output when de-

sired. Cooling of the klystron by the fan in the tube mount is necessary

in order to maintain a constant operating temperature for the klystron

and desired frequency stability. The klystron is the microwave power

source for the system. The X-13A klystron is tunable over the X-band

range. A micrometer gage calibrated to read in thousandths of an inch

is an integral part of the klystron and serves to permit approximate set-

ting of the klystron operating frequency when a calibration curve is

available.

2. Consideration of bridge measurements

Some time was spent gaining familiarity with the various instruments. Standing-wave ratios for various components, joints, etc., were checked, and wavelength measurements with the slotted section were checked against guide wavelengths calculated from frequency meter readings, etc. These preliminary measurements served to identify sources of errors and problems in obtaining meaningful microwave measurements.

As originally planned, components were assembled into a microwave bridge system. Starting with the klystron and attached straight waveguide section, an isolator was connected to provide required isolation of the klystron oscillator. Next, a variable attenuator was added for use in adjusting the power level to the system. A cavity-type frequency meter was the next component in the line, and a waveguide shorting switch was added just before the shunt tee, which divided the signal for the two arms of the bridge. Ninety-degree H-plane bends were connected to the tee for each bridge arm. A precision attenuator and a precision phase shifter were installed in one arm of the bridge, and another variable attenuator and sample-holding waveguide section were installed in the other arm. Each arm of the bridge was then connected through an isolator and 90° H-plane bend to a hybrid tee. A matching termination was connected to the shunt port of the hybrid tee, and a thermistor mount for use with the microwave power meter was connected to the series port. When the variable attenuator in the sample-holding arm of the bridge (without any sample in place) was set to match the residual attenuation of the precision attenuator and phase shifter (set for zero phase shift) in the other arm,

the waves arriving at the hybrid tee from the two arms of the bridge were in phase and of the same amplitude, giving a sharp null indication on the power meter. Any phase shift or difference in amplitude between signals from the two arms of the bridge resulted in a measurable power indication at the series port of the hybrid tee which was detected by the power meter. Later, a crystal detector mount was obtained and used with the VSWR meter instead of the thermistor mount and power meter to obtain a more sensitive indication of bridge balance. One-kHz square-wave modulation of the klystron output was then employed in order to use the VSWR meter.

The plan for using the bridge to determine dielectric properties involved placing a sample in a straight waveguide section in the "sample" arm of the bridge and adjusting the precision attenuator and precision phase shifter in the other arm to restore balance. It was then expected that the dielectric properties of the sample could be calculated from the attenuation and phase shift data and the sample length. The complex propagation constant in lossy media may be expressed as $\gamma = \alpha + j\beta = j\omega\sqrt{\mu\varepsilon}$. If there are no magnetic losses and the permeability of the medium is the same as free space, this expression becomes

$\alpha^2 + j2\alpha\beta - \beta^2 = -\omega^2\mu_o\varepsilon' + j\omega^2\mu_o\varepsilon''$. Separating the equation into real and imaginary parts, noting that $\varepsilon_r = \varepsilon/\varepsilon_o$, and that $c = 1/\sqrt{\mu_o\varepsilon_o} = \lambda_o f$, we obtain $\varepsilon_r' = (\beta^2 - \alpha^2)(\lambda_o/2\pi)^2$ and $\varepsilon_r'' = 2\alpha\beta(\lambda_o/2\pi)^2$. Knowing the frequency or free-space wavelength λ_o and values for α and β permits calculation of the dielectric properties. Attenuation measured in dB by the precision attenuator and phase shift, ϕ, measured in degrees by the precision phase

shifter are converted to values for α and β by the following relations: $\alpha = dB/(8.68L)$ nepers/m, $\beta = \phi/(57.296L)$ radians/m, where L is the sample length in meters.

The intention was to confine grain or insect samples of a few centimeters length between thin polystyrene windows in a straight waveguide section and measure the phase shift and attenuation due to the presence of the sample in the waveguide. Hopefully, the attenuation and phase shift attributable to the polystyrene windows could be neglected. Initial measurements were attempted with pieces of polystyrene and Teflon as sample material, but the calculated dielectric properties made little sense, and values obtained were dependent upon the position of the sample in the waveguide. Slotted-section measurements in the sample arm of the bridge revealed high standing-wave ratios. A number of ideas were tried in attempts to improve the situation. Some tapered wedges made of Rexolite and Plexiglas were used in an effort to better match the impedance of grain samples in the waveguide, but these efforts were not very successful. Since the reflections appeared difficult to handle, especially for samples of widely varying dielectric properties as anticipated, the bridge technique was abandoned in favor of the short-circuited waveguide method.

3. Investigation of procedures

A long series of trials and measurements with different equipment assemblies and studies of the influences of various factors finally led to the combination of components and connections shown in Fig. 2-23. The system will be described in detail later. The evolution of this system
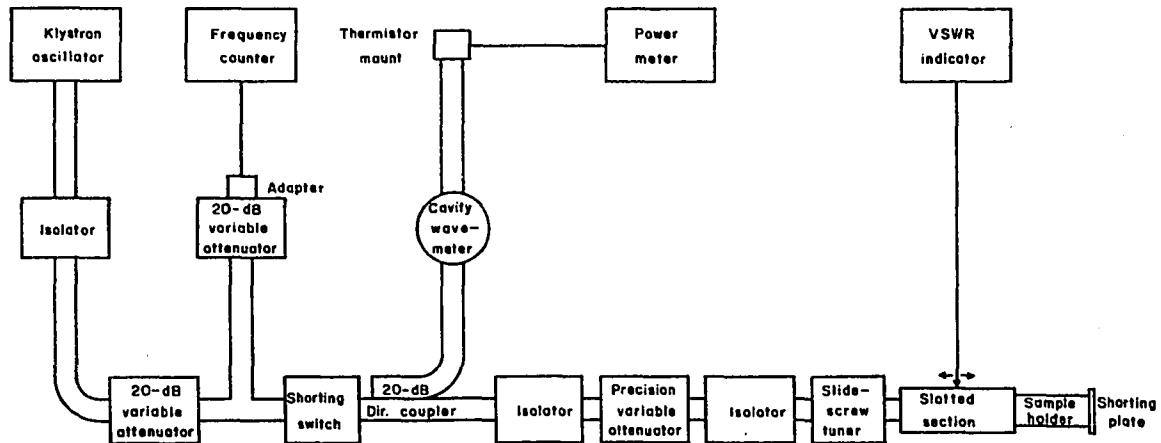
Fig. 2-23. Diagram of X-band system for short-circuited
waveguide measurement of dielectric properties

will not be detailed here, but some of the more important findings will be

summarized very briefly, and others are evident in the material of Appen-

dix A. Information in Appendix A details the principles of the method,

the derivation of the mathematical expressions, measurement and calcula-

tion considerations, and a description of a computer program to properly

carry out the calculations for measurements on a shorted coaxial line,

rectangular waveguide, or cylindrical waveguide.

Because measurement of voltage node locations and node widths is im-

portant for the method selected, the slotted-section carriage was equipped

with a dial gage with 0.01-mm divisions. Comparison of guide-wavelength

data taken with the slotted section and the guide wavelengths calculated

from frequency meter readings, $\lambda_g = \lambda_o / \sqrt{1 - (\lambda_o/\lambda_c)^2}$, where λ_o is free-space wavelength, $\lambda_o = c/f$ (c = velocity of light in free space), and $\lambda_c = 4.5720$ cm for WR-90 waveguide, revealed discrepancies. Calibration of the cavity-type frequency meter was suspected at first, so it was checked against a Hewlett-Packard Model 5246L Electronic Counter equipped with a 5255A Frequency Converter for direct reading of X-band frequencies. In order to use the counter, CW (continuous-wave) or unmodulated operation of the klystron was necessary. When the klystron power supply modulation switch is changed from CW to 1-kHz square-wave operation, there is a slight shift in frequency, but, since the klystron is tunable, the calibration of the wavemeter scale can be checked at any desired point. Results of these measurements showed that calibration of the cavity-type frequency meter, or wavemeter, was well within the limits of specified accuracy, 0.08 percent over-all. Because the electronic frequency counter provided much higher accuracy, calibration corrections were determined and used for all wavemeter frequency settings used thereafter.

With these corrections applied, rather consistent discrepancies, on the order of 0.05 percent, still remained between guide-wavelength determinations based on slotted-section measurements and those based on frequency measurement. The problem was resolved on realization that the slot in the slotted section does influence the propagation constant of the guide, and corrections of measured guide wavelength, in accordance with Eq. 9-30, Appendix A, brought the two measurements into agreement.

Ordinarily, slotted lines and slotted sections are used with the minimum probe penetration necessary for the measurement. For exploration of

the voltage null region in a short-circuited line, however, the voltage minimum has a very low value. With limited input power to the line, therefore, it was necessary to increase the probe penetration to nearly the maximum value to bring the voltage minimum to midrange readings even with the higher sensitivity settings of the VSWR meter. Therefore, the influence of probe penetration on the measured width of the voltage minimum at points 3 dB above the minimum was checked. It was found that full probe penetration provided the same node-width measurement data that were obtained with lesser probe-penetration settings. Therefore, full probe penetration was employed, because this usually permitted using less than maximum sensitivity settings for the VSWR meter where meter indications were more stable. Influence of probe penetration was also checked in later measurements on a high-loss dielectric sample, n-decyl alcohol, and full probe penetration gave the same results as lesser probe-penetration settings (Sec. II, I, 4, c).

Such comparisons were also made using Eq. 9-36 for calculating VSWR values from node-width measurements and the approximation formulae, Eqs. 9-40 and 9-38. For measurements with the empty waveguide terminated in a 45-dB short circuit, i.e., the voltage minimum 45 dB below the voltage maximum, the approximation, Eq. 9-40, gave values within about 0.01 percent of the true value as calculated from Eq. 9-36. With a grain sample in the waveguide, however, Eq. 9-36 must be used to avoid serious errors. Since a computer program was used, all VSWR values were calculated using the exact relation, Eq. 9-36.

4. <u>Short-circuited waveguide measurement system</u>

    a. <u>General description</u>   The measurement system already referred

to, which finally evolved from all of the preliminary work, is shown sche-

matically in Fig. 2-23 and is pictured in Fig. 2-24. A Hewlett-Packard

Fig. 2-24. X-band system for short-circuited waveguide
measurement of dielectric properties

(HP) Model 716B Klystron Power Supply was used to provide the filament,

beam, and reflector voltages needed for operation of the Varian X-13A re-

flex klystron which provided the microwave power source for the system.

The klystron was mounted in a Narda Model 990 Klystron Tube Mount equipped

with a cooling fan. Electrical connections for the tube mount and the

waveguide-holding bracket constructed for the tube mount were described

in Sec. II, I, 1. Narda Microline Model 1210 Ferrite Isolators were used

in the system, one for isolation of the klystron and two others for pre-

cision attenuator isolation.

Two FXR X155A Variable Attenuators were used, one to set the power level to the system from the source, and the other to adjust the signal level to an HP X281A waveguide-to-coax adapter which coupled energy out for frequency measurement by an HP Model 5246L Electronic Counter equipped with a 5255A Frequency Converter plug-in-unit. The time-base accuracy of about 1 part in 10^7 permits direct reading of frequency to about the nearest 100 kHz with this frequency counter. The counter can, therefore, be used to obtain calibration corrections at any point for the scale of the HP Model X532B Frequency Meter, which is a tuned-cavity, absorption-type wavemeter with a specified accuracy of 0.08 percent over the entire X-band range, 8.2 to 12.4 GHz. This frequency meter is convenient to use in checking the klystron operating frequency and must be used in this system to measure frequency when the klystron output is modulated. The electronic counter is useful only when the klystron is operating in the CW mode (unmodulated). Since 1-kHz square-wave modulation is used for the measurements, the wavemeter is employed to monitor the klystron frequency during measurement sequences. Minor adjustments of klystron frequency can be accomplished by adjusting the reflector voltage to maintain a set frequency.

An HP X752D 20-dB Directional Coupler is used to isolate the frequency meter from the system. In this way the frequency meter may be left set at the resonant frequency without affecting the power level in the rest of the system. The frequency meter, when set at the resonant frequency, absorbs some energy, and a dip in the power, registered by the power meter as the frequency meter cavity is tuned, serves as the indication for resonance. An HP Model 430C Microwave Power Meter was used with

an X487B Thermistor Mount to measure the power level transmitted by the frequency meter. With the frequency meter set off resonance, the power meter also then indicates 1 percent of the power being transmitted through the waveguide of the main system.

An HP X930A Waveguide Shorting Switch is used just ahead of the directional coupler to short-circuit the waveguide to insure zero-level power for adjusting the zero-set of the power meter and for safety when the end of the waveguide is opened as the sample holder is removed. Normal power levels ranged between 30 and 100 mW for measurements, but levels several times this are possible under certain conditions.

Known attenuation levels are inserted in the system using an HP Model X382A rotary-vane type Precision Attenuator as part of the measurement procedure to be discussed later. A Budd-Stanley Model X1636A Slide-Screw Tuner was inserted in the line ahead of the slotted section to provide for better matching of the line to increase the signal available from the slotted section. An HP Model X810B Slotted Section mounted in the HP 809C Universal Probe Carriage was used for measurements associated with the voltage standing-wave patterns in the waveguide. The probe carriage was equipped with a Starrett No. 655-2081 Dial Gage which has a 50-mm range with 0.01-mm scale divisions (Fig. 2-25). This dial gage was not listed by Hewlett-Packard for use with the probe carriage, though one with a 25-mm range was, and neither was it listed in the Starrett general catalog. The 50-mm range, however, is very much worthwhile for this application.

Adjustment of the probe position using the probe carriage knob is
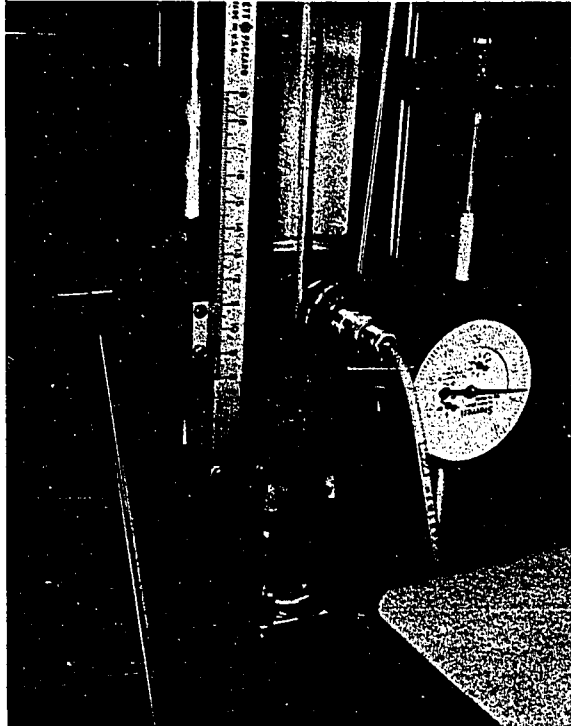
Fig. 2-25. X-band slotted section in probe carriage equipped
with dial gage showing sample holder attached and
extension rod used for fine adjustments

quite critical when measuring the width of the voltage null for a short-
circuited empty waveguide. Therefore, an extension rod was made from 1/4-
inch polystyrene rod by machining one end of the rod in a lathe to fit
snugly into the set-screw access holes in the side of the knob (Fig. 2-25).
Insertion of this extension rod whenever needed greatly facilitated the
fine adjustments necessary for these readings.

The crystal detector in the carriage probe unit provides a d-c signal
proportional to the square of the input signal over a limited range, and
the HP 415E SWR Meter is calibrated for this square-law response of the
crystal detector. The SWR Meter is a high-gain amplifier tuned to accept

1-kHz signals and provides meter readings directly on either SWR or attenuation scales. This is the reason for using 1-kHz modulation of the klystron output.

Sample holders, to be described later, were attached directly to the end of the slotted section. Measurements of the shift in the voltage node and changes in the width of the node due to the presence of the sample in the shorted end of the waveguide provide the means for determining the dielectric properties of the sample. The underlying theory, methods, and principles for calculation are discussed in detail in Appendix A. Procedures adopted for the measurements are outlined in Sec. III, E, 9.

b. <u>Sample holders</u> For some of the preliminary work, short, straight waveguide sections were used as sample holders, and a shorting plate was made from 3/16-inch brass plate stock. None of the short sections in the available collection, however, had been fabricated with enough care that they could be considered for any precision measurements. Also, a liquid-tight sample holder was needed for some measurements on benzene and other liquids. Therefore, a length of WR-90 copper waveguide stock and some UG-39/U waveguide cover flanges were obtained for construction of the desired sample holders. These flanges permit the waveguide stock to slip completely through the flange rather than providing a butt joint inside the resulting waveguide section.

A 5.0-cm straight-section sample holder for use with the shorting plate was fabricated from these materials (Fig. 2-26). There was sufficient clearance between the waveguide and the flanges that some care was necessary to assure that the flanges were soldered on with the plane
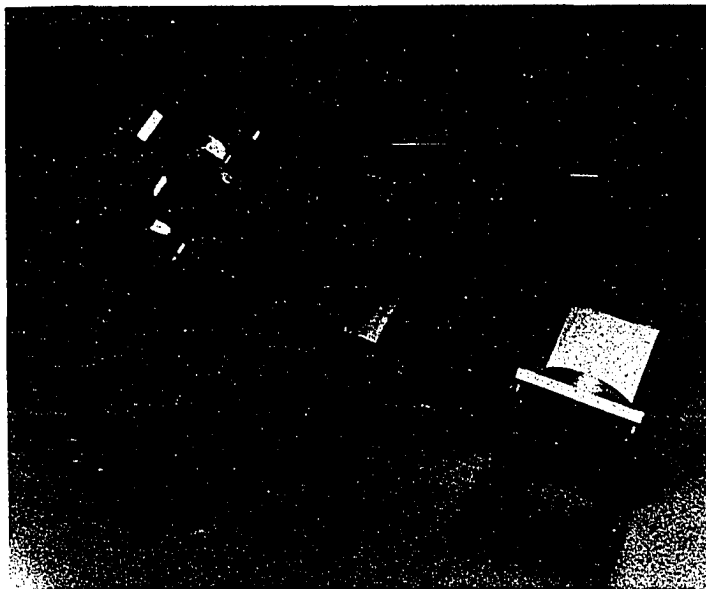
Fig. 2-26. Straight-section sample holder, plunger with height gage, and liquid sample holder for X-band measurements

surface of the flange truly perpendicular to the axis of the waveguide.

This was accomplished by inserting 0.003-inch brass shim stock between

the outside surface of the waveguide walls and the mating flange sur-

faces on all four sides, providing a tightly fitting flange, before it

was soft-soldered to the waveguide. Ends of the waveguide were squared

off in a milling machine before the flanges were mounted, but the wave-

guide was permitted to extend slightly beyond the face of the flange.

After soldering was completed and the section had cooled, it was lightly

chucked in a lathe, carefully adjusted to run true with a dial gage, and

the flange surface was faced off to remove the excess waveguide and pro-

vide a plane surface.

A liquid sample holder (Fig. 2-26) was made in a similar fashion,

except that a shorting plate was cut from brass plate, and the corners were milled out on one side to fit the inside dimensions of the waveguide before it was soldered in place to provide the liquid-tight short circuit.

Both the liquid sample holder and the 5-cm straight waveguide-section sample holder and its shorting plate were silver-plated to reduce wall losses for measurements on low-loss samples.

In order to provide a means for leveling granular samples in the 5-cm sample holder, for measuring the sample height, and for compressing samples in the sample holder to study effects of sample density, a rectangular cross-section plunger was machined from brass bar stock to fit the waveguide (Fig. 2-26). Initially, height of grain samples in the sample holder was obtained by subtracting the combined length of the plunger, the shorting plate thickness, and the clearance between the shorting plate and the end of the plunger, when the plunger was completely inserted in the empty sample holder, from an over-all length of the assembled sample holder and plunger with a sample in place and the plunger in contact with the sample. This proved somewhat unsatisfactory for some samples because the plunger could shift after the caliper reading was taken, before the plunger was removed. Compression of some samples while using the caliper was also difficult to avoid; therefore, a scale was scribed on an edge surface of the plunger to read sample height directly when the plunger was in contact with the sample (Fig. 2-26).

c. <u>Verification of reliability</u>   Benzene was the first material selected as a standard to check the reliability of resulting dielectric properties obtained with this system. The liquid sample holder was used

and sample height was determined by measuring the distance to the sample

surface and subtracting this distance from the depth of the sample holder.

Because of surface tension and adhesion between the benzene and the sample

holder, the top of the sample was not a plane surface. This presented a

problem in determining sample length, but the effective sample length was

estimated to lie one-third of the distance between the low point and high

point, measured with the depth-gage micrometer, above the low point. Re-

sulting values obtained from measurements on benzene at 8.361, 9.412,

10.885, and 12.164 GHz were, respectively, 2.287, 2.281, 2.282, and 2.296

for the dielectric constant, ε_r', and 0.0006, 0.0001, 0.0002, and 0.0005

for the loss tangent. Differences between values obtained for ε_r' and the

accepted value of 2.276 at 76° F could easily be accounted for by uncer-

tainty in sample length. Tan δ values are of the right order of magni-

tude. Separate measurements which were performed on the benzene samples

using 3-, 6-, and 10-dB levels for node-width measurement gave practically

identical results.

In order to check the method for high-loss samples, measurements were

made on n-decyl (1-decanol) and dodecyl (1-dodecanol) alcohols, respect-

ively, $CH_3(CH_2)_9OH$, molecular weight: 158.29, and $CH_3(CH_2)_{11}OH$, molecular

weight: 186.34. Measurements at 9.368 GHz yielded respective values of

2.51 and 2.42 for ε_r' and 0.235 and 0.161 for ε_r''. Values reported by

Lebrun (1955) for the same frequency (Buckley and Maryott, 1958) were, re-

spectively, 2.48 and 2.44 for ε_r' and 0.20 and 0.167 for tan δ at 25° C

(77° F). These values are in reasonably good agreement considering pos-

sible differences in purity of the materials. For the measurements on

n-decyl alcohol, four different probe-penetration settings were used to

see whether the probe penetration had any influence on resulting loss-tangent values for high-loss materials. All probe-penetration settings gave identical results showing that the probe penetration presents no problem in these measurements.

Because of the uncertainty of sample length when working with liquid materials, a search was begun for a suitable solid standard material. Correspondence with the National Bureau of Standards identified Rexolite as a material suitable for this work (Sec. II, C, 3). A Rexolite 1422 sample was cut from sheet stock and filed and sanded by hand to fit the sample holder. Measurements on this sample gave dielectric-constant values of 2.47 consistently, while the expected value is near 2.53. Because the handmade sample was not exactly square (sample length variation of 0.004 inch across the width), some new samples were prepared in a commercial machine shop. Cross-sectional dimensions were 0.4000 by 0.9000 ± 0.0002 inch. Machining to these tolerances was achieved using a vacuum chuck and grinding procedures. Dielectric-properties measurements on these samples which fit tightly in the waveguide gave about the same value for the dielectric constant, 2.47. This discrepancy prompted a check of all procedures used in the measurement and review of all sources of error. Finally, a bulge in the walls of the sample holder was discovered, which had resulted from tests in which grain samples were pressed into the sample holder. By using a press and wooden blocks of appropriate sizes and shapes, and utilizing light reflected from internal surfaces of the sample holder, the bulges were removed quite successfully from the walls of the waveguide. New measurements then gave the proper values.

Measurements at 8.5, 9.0, 10.0, 11.0, 12.2, and 12.4 GHz resulted in values for ε_r' ranging between 2.524 and 2.538 and tan δ values ranging from 0.0005 to 0.0012. These are very close to the probable values of 2.532 and 0.0007 for this particular sample of Rexolite 1422.

III. MATERIALS AND PROCEDURES

A. Wheat

Upon completing the development of methods for reliable measurement of dielectric properties throughout the frequency range from 250 Hz to 12.4 GHz, a suitable lot of wheat was selected for study. The wheat selected was Scout 66, a hard red winter wheat variety, *Triticum aestivum* L., grown in Saunders County, Nebraska, and combine-harvested in July 1970. It was obtained from the University of Nebraska Foundation Seed Division in August 1970 after it had been cleaned along with other seed stock, but not treated with any fungicide as is customary for seed stock. The wheat was stored in a walk-in refrigerator in which temperature was held at $40° \pm 2°$ F and relative humidity was controlled at 50 ± 4 percent, with periodic excursions to about 58 percent during reactivation of the dehumidifier desiccant bed. In April 1971, wheat for measurements was removed from refrigerated storage and conditioned to equilibrium moisture content in the laboratory at $76° \pm 2°$ F and 40 ± 3 percent relative humidity. Five weeks later, the wheat was sealed in glass jars with airtight lids to prevent any further change in moisture content or possible insect infestation and stored at 76° F for the remainder of the study.

The wheat lot was tested at 10.7-percent moisture (wet basis) for certain physical and chemical characteristics. The wheat was Grade No. 1 (U. S. Department of Agriculture, 1970) and the official test weight was 61.3 lb./bu. Individual kernel weight, based on replicated weighings of 1,000 kernels, was 30.86 mg. Wheat-kernel density, as determined by

replicated air-comparison pycnometer measurements to be described later, was 1.434 g/ml. Chemical analyses of the wheat gave 15.30-percent protein and 1.52-percent ash, reported on a 14-percent-moisture basis for the wheat (American Association of Cereal Chemists, 1962).

B. Rice Weevils

The insect chosen for the study was the rice weevil, *Sitophilus oryzae* (L.). Rice weevil cultures were set up using a laboratory strain which had been maintained for several years at the University of Nebraska Insectary from an original source culture obtained from the Stored-Product Insects Laboratory, ARS, United States Department of Agriculture, Manhattan, Kansas. Young adults from several culture jars were mixed to minimize inbreeding and introduced into fresh hard red winter wheat, 1968-grown Lancer variety, to produce new infestations. In establishing new cultures, one pint of wheat at about 12-percent moisture was placed in quart-size Mason jars. A quantity of approximately 1 to 2 ml of adult insects, depending upon the infestation density desired, was placed in each jar with the wheat. The sealing metal lid inserts for the screw-on lids were replaced with three thicknesses of 7.5-cm filter paper, Eaton-Dikeman Grade 613, to provide ventilation while preventing the insects from escaping from the jars. Normally, a period of 1 week was allowed for the adults to infest the wheat, and they were then screened from the wheat and discarded.

The cultures were maintained in a cabinet at the Insectary, where the temperature was held at $85° \pm 3°$ F and the relative humidity at $65 \pm$

5 percent. A thermostatically controlled heating and cooling system for a battery of cabinets provided the temperature control, and forced-air circulation within the cabinet was provided by a fan. The relative humidity level was maintained through evaporation of moisture from a length of 36-inch-wide Curity Grade 80 cheesecloth folded twice longitudinally and suspended by a wooden frame between two battery jars so that both ends of the cheesecloth were submerged in water maintained near the full level in the battery jars. The cheesecloth was cut in about 4-foot lengths as it came already double-folded from the bolt, so that such a length, draped over a 5-inch-wide wooden support, provided two vertical evaporative strips of four thicknesses each 9 inches wide and about 5 inches apart, drawing water up by wick action from the battery jars. Copper sulfate crystals placed in the water prevented algae growth which would otherwise impede the movement of water up through the cheesecloth. The cheesecloth was replaced periodically as mineral deposits from the evaporating water reduced the efficiency of the cheesecloth wicks.

A 12-hour photoperiod was provided in the insect culture cabinet by a time switch which turned on a single 30-W cool white fluorescent lamp for 12 hours during the daylight period. Temperature and relative humidity were monitored by a mercury thermometer and a 6203-BB Humidial Co. relative-humidity-indicating card, both mounted in the cabinet.

Female rice weevils infest the grain by boring a hole in the wheat kernel and depositing an egg inside the kernel. The hole is then sealed with a gelatinous plug. The eggs hatch in 3 to 5 days and the young larvae feed inside the kernel, entering the pupal stage in about 3 weeks, and

emerging from the kernel as adults in 4 to 5 weeks. Under the culture

conditions used in this work, no emergence was noted 4 weeks after the

beginning of the infestation period, but, at the end of 5 weeks, heavy

emergence was noted. Peak emergence occurred about 5 weeks from the mid-

dle of the infestation period, and average adult ages were established on

this basis. One- to 3-week-old adults were used for the measurements to

determine the dielectric properties of the insects.

Average weight of individual adult rice weevils used for measurements

in the study, as determined from six different samplings of at least 100

insects from all cultures used, was 1.688 mg with a standard deviation of

0.049 mg. Moisture content of the insects (Sec. III, D, 1) averaged

48.95 percent (wet basis) with a standard deviation of 1.59 percent. In-

sect density as determined by air-comparison pycnometer measurements was

1.29 g/ml.

C. Preparation of Materials for Measurement

1. Wheat

Most electrical measurements for determination of dielectric proper-

ties were taken at the equilibrium moisture content for the wheat in the

laboratory. Some measurements were also desired on wheat of slightly

higher moisture content to observe the influence of moisture content on

the dielectric properties. For these measurements, a calculated amount

of distilled water was added to the wheat, and it was returned to a sealed

glass jar and stored in the laboratory at 76° F for at least 5 days before

being used. During this period it was mixed frequently and thoroughly by

rotating the jar in such a manner as to obtain complete mixing to improve the uniformity of moisture distribution. When ready for measurement, representative wheat samples were taken from the lot and poured into the respective sample holders, as will be described later for each measurement system.

2. Rice Weevils

When insects had reached the selected age for measurement, the culture jars were removed from the rearing cabinet, taken to the laboratory, and the adults were collected using an aspirator. The aspirator consisted of an 8-dram shell vial, 25-mm outside diameter and 95-mm deep, fitted with a two-hole No. 4 rubber stopper into which two pieces of 6-mm glass tubing, each with a right-angle bend, were inserted. A length of flexible rubber tubing was connected to one glass tube, and the other end of the rubber tubing was connected to a double-action rubber bulb to provide a means for drawing air through the tubing. A fine screen was fitted over the end of the glass tube inside the vial to prevent insects from being drawn into this tube. When the rubber bulb was operated to draw air, insects were then drawn into the vial through the other glass tube and retained in the vial.

When rice weevil population densities were very high in the culture jars, the jars could be agitated, and, in a few minutes, the weevils would climb to the top surface where they could be taken off the wheat with the aspirator. In order to collect a sufficient quantity of insects for most measurements, however, it was necessary to screen the insects from the wheat and separate them from the dust in the culture medium. A

Seedburo No. 10 F Official Grain Dockage Sieve (0.064 by 3/8-inch slots)

with a matching bottom pan served to separate the weevils and small par-

ticles from the wheat. The weevils and other material screened out were

then emptied into a 1-mm Ro-Tap sieve with bottom pan to remove the dust

and small particles. After waiting a few seconds, many of the weevils

would cling to the Ro-Tap sieve, so that it could be inverted over a grain

dockage bottom pan to dump out unwanted material. The weevils remaining

on the Ro-Tap sieve were then brushed into a clean bottom pan and col-

lected with the aspirator. Weevils dumped into the grain dockage bottom

pan along with unwanted material were permitted to crawl free of the

trash and were picked up with the aspirator as they did so. The few

light kernels and small amount of trash collected with the insects in

this way were removed with forceps after emptying the aspirator vial into

a beaker and anesthetizing the weevils with carbon dioxide to prevent

them from clinging to particles to be removed. Collection of weevils in

the quantities needed for some sample holders was a lengthy and tedious

procedure.

D. Moisture Content and Density Determinations

1. Moisture content

At the time when electrical measurements were taken for dielectric-

properties determination, moisture content measurements were also con-

ducted on all wheat and insect samples. All moisture contents are re-

ported on a wet basis. Standard oven moisture determinations were made

on all wheat samples by grinding triplicate samples and drying them in a

forced-air oven for 1 hr at 130° C in accordance with standard procedures (U. S. Department of Agriculture, 1959; Association of Official Agricultural Chemists, 1965).

Since no standard method was found for determining moisture content of adult rice weevils, approximately 1-ml samples (roughly 300 insects per sample) were used to obtain a drying curve at 105° C in the forced-air oven over a 24-hr period. The additional weight loss after 16 hr was less than 0.5 percent of that at 16 hr, so a 16-hr drying period was selected. For these determinations, empty standard aluminum moisture dishes were heated in the oven for at least 1 hr at 105° C and cooled in a desiccator with Drierite (calcium sulfate) before weighing. Triplicate samples of approximately 1 ml of adult rice weevils were weighed into the moisture dishes following anesthetization with carbon dioxide. Dishes were then placed in the oven with covers for about 10 min when covers were removed for the remainder of the 16-hr drying period. Dishes and contents were again cooled in the desiccator before weighing. All weights were taken to the nearest 0.1 mg.

2. Bulk density

As part of the description of the wheat lot used for the study, the test weight of the wheat was determined in accordance with standard procedures (U. S. Department of Agriculture, 1953) using a Fairbanks-Morse Code 11192 Weight-Per-Bushel Apparatus. Bulk densities of grain and insect samples in the sample holders for all of the different dielectric-properties measurement systems were also obtained at the time of electrical measurement. Because of differences in sample-holder dimensions

and cross sections, the bulk densities of samples poured naturally into the various sample holders differed from one another. For this reason, dielectric-properties measurements were usually obtained for at least two different sample densities in order that a common density might be used for comparison of dielectric properties measured on the different systems.

3. Air-comparison pycnometer density determinations

In order to more fully describe the materials being used in the study, and because the kernel density for the wheat and the individual insect density for the rice weevils might be useful in interpreting dielectric-properties data of the bulk materials, a method was sought for obtaining this information. Some consideration was given to use of a density-gradient column (Peters and Katz, 1962), but the time and trouble required to set up this system and the uncertainty of solubility of rice weevil cuticular waxes, etc., in the liquids to be used in the column rendered this procedure less attractive than the method chosen. Availability of a Beckman Model 930 Air-Comparison Pycnometer was the main factor in the decision to use this instrument.

The air-comparison pycnometer consists of two cylindrical chambers, each with an airtight-fitting piston, an interconnecting line with a shutoff valve between the two chambers and a differential pressure indicator connected to the two chambers. A sample of unknown volume can be placed in the sample chamber, and the piston movement in this chamber is mechanically coupled to a calibrated counter with the scale reading directly in cubic centimeters. The pistons of the sample chamber and the reference chamber operate independently.

To measure the volume of an unknown sample, the valve between the two chambers is opened and the reference chamber piston is backed clear out against a stop. The sample chamber piston is backed out also to a calibrated starting point on the scale, and the sample cup, which forms part of the sample chamber, is locked in place empty. The coupling valve is then closed, sealing off the air passage between the two chambers, and the two pistons are advanced into the chambers together so as to keep the differential pressure indication on scale. When the reference piston hits its stop, the sample chamber piston is adjusted to give a zero indication on the differential pressure indicator. If properly adjusted, the counter scale reading is zero. If not, a zero correction can be noted from the scale reading. The valve can then be opened and both pistons moved back out to their starting points already described. The sample cup is removed, the sample inserted, and the cup is locked back in place. The valve is then closed and the two pistons are advanced into the chambers together as described for the zero check. This time, when the reference piston hits its stop and the sample chamber piston is adjusted for zero pressure difference, the volume of the sample is indicated on the volume scale counter. The zero correction, if any, is then added or subtracted from the counter reading to give the proper volume.

Steel balls of known volume are provided with the instrument for calibration checks. On checking out the instrument, consistent errors were found in running calibration checks, and it was necessary to completely recalibrate the instrument following instructions in the manual before any data were obtained on insect or grain samples.

The measurement procedure described starts with the sample at atmospheric pressure, and the measurement is completed with a pressure of 2 atmospheres in the chambers. By following a different procedure, it is also possible to begin the measurement at 1 atmosphere, reduce the pressure to 1/2 atmosphere by drawing the pistons out to the starting points of the other procedure, and end the measurements at 1 atmosphere with the pistons at the same locations of the final settings using the 1- to 2-atmosphere method described. For elastic samples, which may compress or expand with the changes in pressure, the 1- to 1/2- to 1-atmosphere method might be expected to provide the most reliable measurement. Expansion at 1/2 atmosphere introduces errors, too, and for a sample which might expand more at 1/2 atmosphere than it will compress upon return to atmospheric pressure, there would be additional errors. Both procedures were used in measurements on grain and insect samples for comparison of resulting volume determinations. Densities were calculated from known weights of samples and their volumes as measured with the air-comparison pycnometer. Measurements on each of several samples of both insects and grain were repeated many times to obtain reliable averages.

E. Electrical Measurement Procedures

1. General methods

Instruments, equipment, principles of measurements, and methods of calculation are described in appropriate sections of Chapter II for each of the eight different measurement systems for determining dielectric properties. Procedures for the measurements on grain and insects for each

system are detailed here in the following sections. A few general comments are appropriate since some procedures were common to all methods used for all measurement systems.

For measurements on wheat, efforts were made to select samples for measurement which were representative of the lot. Since the lower frequency sample holders require the most wheat, measurements for a complete sequence, 250 Hz to 12.2 GHz, generally started with the audiofrequency impedance bridge and progressed on up through the frequency range with the other systems. For wheat in equilibrium with laboratory conditions, a representative subsample was selected from the initial sample as smaller samples were required in going from one measurement system to another. For samples not at the equilibrium moisture content, all wheat not being used for the sample measurement was kept in tightly sealed jars. A representative sample of the proper quantity was drawn for each measurement system as it was needed. Weights of samples were obtained using an analytical balance at the time of electrical measurement, except for the impedance bridge samples which exceeded the capacity of the balance. These samples were weighed with 1-g accuracy on a laboratory scale. Sample weights and volumes, as determined from sample-holder cross-sectional areas and sample-height measurements or sample-holder volumes, provided the information for calculating densities of samples in the sample holders.

Electrical measurements were generally taken for at least two sample densities in order to enable comparison of dielectric properties measured on different systems at a common density. One sample density was normally

that obtained by slowly pouring the wheat into the sample holder and carefully leveling where necessary. The other densities were obtained by settling the wheat in the sample holder, by tapping sample-holder bases on a solid surface, or by tamping them slightly with the sample-height gages for the various systems.

The same procedures were employed for the rice weevils, except that, in this case, securing sufficient volumes of insects was so time-consuming that measurements requiring the smaller samples (the higher frequencies) were normally taken first. Additional insects were then added as collected until enough were available for the system with the next larger sample holder. For some measurements, it was necessary to add insects of a different age range in order to obtain sufficient numbers for the largest sample holders. Comparison of dielectric properties on the two age groups did not reveal any real differences.

Anesthetization of the weevils with carbon dioxide was necessary to control them for some handling operations and to keep them quiet in the sample holders during measurement. A 5-lb. CO_2 cylinder equipped with a pressure regulator, low-pressure shutoff valve, and a length of plastic or rubber tubing served as a conveniently movable CO_2 source for this purpose (Fig. 3-1). In order to obtain uniform bulk densities for the insects in the sample holders, they were completely anesthetized before pouring them into the sample holders. Since they would begin to revive as soon as they obtained some oxygen, it was necessary to keep a low flow of CO_2 into the sample holders when possible during the measurement procedures. As the insects revived, the volume of the bulk sample swelled
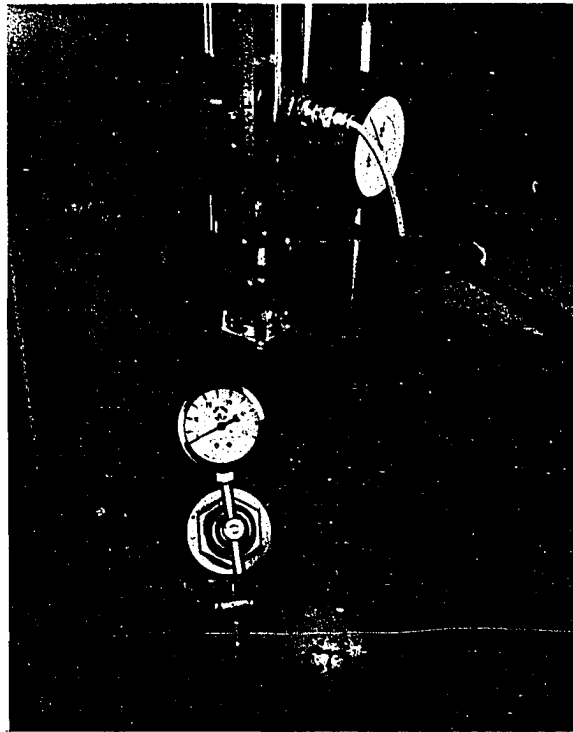
Fig. 3-1. Carbon dioxide cylinder, pressure regulator, and arrangement employed for maintaining rice weevil anesthetization during measurement

noticeably, and this sort of activity could usually be detected on the measuring instruments. Carbon dioxide anesthetization did not appear to be harmful to the insects as used. They were permitted to revive during any extended periods between measurements. Insects used during a day-long sequence of measurements with frequent anesthetization and revival cycles did not appear to suffer abnormal mortality when returned to the culture jars in normal population densities. Some of these insects were success-fully used to establish new cultures without any obvious problem.

Neither should anesthetization of the insects be expected to have any measurable influence on their dielectric properties. The dielectric

constants of air and carbon dioxide are both very nearly unity; so an exchange of these two gases would not be detected. It also seems doubtful that anesthetization should produce any temporary chemical changes which would be detectable by dielectric measurements.

2. Audiofrequency impedance bridge measurements

This system is described in Sec. II, B. When ready for measurement, 1-liter samples of wheat were introduced into the sample holder as described in Sec. II, B, 4, and the sample height was measured and recorded on the data form developed for these measurements (Fig. 10-1, Appendix B). The sample holder was then placed on the platform making connections to the bridge (Fig. 2-2). The frequency to be used was set on the audiofrequency oscillator, with the aid of the electronic frequency counter, and recorded on the data form. The bridge was then balanced using both the series and parallel bridge circuits separately, and the resulting dissipation-factor and capacitance readings, D_s and C_s, and D_p and C_p, were also recorded on the data form. The same procedures were used at each frequency where measurements were needed. Situations can be encountered where a bridge balance cannot be achieved with one or the other of the parallel or series circuits. In this case, zeros were entered for the D and C values for that particular circuit on the data form.

Calculations (Eqs. 2-4, 5, 6, and 7) were performed using the Wang 700B programmable calculator, and resulting values for the dielectric properties were entered on the data form. Sample density in the sample holder was calculated from sample height, sample-holder cross-sectional area, and sample weight data, and was also recorded on the data form.

Measurement procedures were simplified because the empty sample-holder readings remain constant at a given frequency and could, therefore, be supplied by the calculator program as explained in Sec. II, B, 2.

Measurements on rice weevils were obtained with the same procedures used for wheat, but it was necessary to use smaller samples. It was also necessary to keep the insects anesthetized during the measurement. This was accomplished by blocking the annular opening at the top of the sample holder with a cardboard ring cut to fit and flooding the sample holder with CO_2. The blocking ring and tube for the CO_2 were then removed briefly while the bridge was balanced for the measurements.

3. Q-Meter measurements

This system is described in Sec. II, C. About 100-ml samples were poured into the Q-Meter sample holder from a beaker and leveled with a circular motion of the sample holder while holding it in an upright position. Final leveling was accomplished by inserting the sample-height gage and rotating it slightly with very light pressure on the surface of the sample. Sample height was then read from the height-gage scale and recorded on the data form (Fig. 10-2, Appendix B). The appropriate coil for the set frequency was connected to the Q-Meter "Coil" terminals, and the sample holder, with its variable, air capacitor set to zero, was plugged into the "Condenser" terminals. Resonance was then obtained by varying the main tuning condenser dial until the Q-Meter voltmeter registered a maximum. The $+C$ and $-C$ values were then obtained by varying the vernier condenser until the Q-Meter voltmeter registered the selected V value as explained in Sec. II, C, 1. These values were all recorded on

the data form along with frequency. The vernier condenser was carefully reset to resonance. Next, the sample was poured out of the sample holder and the sample holder plugged back into the Q-Meter terminals. Resonance was then restored by adjustment of the variable, air capacitor of the sample holder and its scale reading recorded as C_x. The $+C$ and $-C$ values for the corresponding V_m and V readings for air were then obtained and recorded on the data form.

This same procedure was repeated at each frequency for which data were required. In using the Q-Meter, care is necessary to avoid possible burnout of the thermocouple meter used to measure oscillator output. The output level should be adjusted to minimum whenever changing oscillator ranges, and the output-level meter must be watched when adjusting the frequency dial. The output level is also adjusted to maintain the maximum readings possible for V_m, both for the sample readings and the air readings, when taking the measurements.

Calculations of dielectric properties were then performed with the Wang 700B programmable calculator by simply entering the measurement data in sequence from the data form and recording the results on the same form. Sample densities in the sample holder were calculated from sample height, sample-holder cross-sectional area, and sample weight, and these were also recorded on the form.

4. RX-Meter measurements

This measurement system is described in Sec. II, D. In using the RX Meter, the oscillator is tuned by setting the range switch and oscillator dial scale to the desired frequency. The C_p dial is set at zero and the

R_p scale at infinity. A 50-ohm coaxial termination was used on the "un-known" connection to the bridge to insure an unbalanced condition, and the detector was then tuned for a maximum indication on the null indicating meter. The termination was then removed and the bridge was adjusted for balance. Samples were then poured into the sample holder for the meas-urements. In the case of wheat, it was poured into the sample holder un-til it overflowed, and the excess was removed with a strike-off stick to provide a smooth surface even with the top of the conductors. The sample holder cap was then screwed on and the sample holder connected to the RX Meter. Rebalancing the bridge with the R_p and C_p controls then gave the parallel-equivalent capacitance and resistance readings needed. These were recorded on the data sheet (Fig. 10-1, Appendix B) along with fre-quency and sample-holder central conductor identification. Two different central conductors were used depending upon the frequency range (Sec. II, D).

Filling the sample holder with rice weevils required more patience. The insects were well anesthetized when poured from the beaker into the sample holder, but those on the top began to revive very quickly. There-fore, it was necessary to administer CO_2 almost continually, and the method used was to seal the top of the sample holder with a cupped hand, while holding the rubber tube from the CO_2 pressure regulator between the thumb and base of the forefinger in such a way as to keep CO_2 flowing into the sample holder. For final filling, a few insects were added at a time and the anesthetization continued until the sample holder was properly filled. Screwing the cap on quickly sealed the CO_2 in the sample holder

well enough that the insects remained quiet until the cap was removed again.

Only the frequency and parallel-equivalent capacitance and resistance readings are needed for input data to calculate the dielectric properties when the central conductor is identified. These calculations were performed also using a Wang 700B program. The sample height need not be recorded on the data form for these measurements because the sample-holding portion of the sample holder is completely filled. The sample-height column is provided on the data form, because it is possible to use the sample holder without the terminating cap for a direct substitution measurement for determination of dielectric properties at the low end of the RX-Meter frequency range. This method was not used in this study. Sample densities in the sample holder were calculated from sample weights and the volume of the sample holder.

5. Admittance-Meter measurements

This system is described in Sec. II, E. The frequency for the measurement was selected by the setting of the dial of the signal oscillator. The susceptance standard for the Admittance Meter was also set at the same frequency. With the Admittance Meter unbalanced, the local oscillator was set at a frequency 30 MHz below the signal oscillator to provide the 30-MHz IF frequency for the tuned detector and was adjusted to provide a peak on the detector panel meter. A short-circuit termination was then placed at the end of the line where the sample holder was to be connected, and, with the conductance, susceptance, and multiplier arms of the Admittance Meter set at 0, 0, and 1, respectively, the adjustable trombone line was

adjusted for a null indication on the detector. This procedure adjusts the line length so that it is an integral number of half-wavelengths long, and the admittance connected to the end of the line will be reflected back to the point of measurement in the Admittance Meter. The short-circuit termination was then removed and the sample holder, filled with the sample, was connected to the end of the line. After readjusting the conductance, susceptance, and multiplier arms of the Admittance Meter for a null indication, the admittance of the sample holder was indicated by the readings from the conductance, susceptance, and multiplier scales. These values were recorded along with frequency on the data form for Admittance-Meter measurements (Fig. 10-1, Appendix B). The dielectric properties were then calculated using a Wang 700B program and the results entered on the data form. Sample densities in the sample holder were calculated from sample weight and sample-holder volume.

The same procedures were used in filling the Admittance-Meter sample holder that were employed with the RX-Meter sample holder (Sec. III, E, 4).

6. Slotted-line measurements

This system is described in Sec. II, F. The frequency for the measurement was selected by tuning the SLRD signal generator anode and cathode circuits together for the proper indication on the anode frequency scale. The cathode tuning circuit was then uncoupled by rotating the tuning knob lock ring and adjusting the cathode circuit itself for the proper grid-current meter reading to indicate proper mode of oscillation. With the slotted-line probe set somewhere other than at a voltage minimum, the probe detector was tuned for a maximum indication on the UBK VSWR

indicator. Then, with the empty sample holder connected to the end of the slotted line, the probe was moved to a voltage minimum and the output attenuator of the signal generator set at the proper level to give a – 6-dB reading on the expanded scale at the minimum on the UBK indicator when set on the next to the most sensitive range. The probe was then moved slightly on both sides of the minimum to obtain slotted-line scale readings when the UBK indicator registered 0 dB. This corresponded to a 3-dB change in power level, and the difference in the two slotted-line scale readings gives the node width at the double-power points. The scale readings on each side of the air node were recorded along with frequency on the data form (Fig. 10-3, Appendix B). Similar node readings were taken and recorded for the next air node a half-wavelength away from the first to use for purposes of accurate frequency determination.

The sample holder was then removed and the sample poured in. The sample-height gage was used to level the surface of the sample and to measure the sample height, which was also recorded on the data form. The sample holder was then connected back on the slotted line, and the voltage minimum was again located. The sensitivity of the UBK indicator had to be decreased to locate the null accurately when lossy samples such as grain and insects were used. The double-power point readings were then obtained for the sample node and recorded on the data form. Three-dB power levels were normally used for both air and sample readings, but the programs used for calculations accommodate any dB level which may be necessary. The dB levels used for both air and sample nodes were recorded on the data form.

For lossy samples, it was sometimes necessary to increase the output

attenuation of the signal generator in order to use a sensitivity range on the UBK indicator which could be depended upon to preserve the square-law response of the detector, because the voltage of the sample node was so much greater than that of the air node. Frequency stability of the signal generator was checked under such conditions and found to be entirely satisfactory, i.e., no detectable change in frequency occurred when the output attenuator setting was changed for the purpose just described. Slight detuning of the probe detector circuit was sometimes used to accomplish the same thing when convenient.

Input data directly from the data form was then used in calculating the dielectric properties with a Wang 700B program or cards were punched for the IBM 360 computer program when data printout was desired. Sample densities in the sample holder were calculated from sample weight, sample height, and cross-sectional area of the sample holder.

7. Non-slotted-line measurements

This system is described in Sec. II, G. The frequency for the measurement was selected by setting the desired frequency on the scale of the SLRC power signal generator and tuning the cathode circuit for a proper grid-current meter indication. Because the non-slotted line provides a current standing-wave indication rather than a voltage standing-wave indication, one searches for peak readings rather than minimum readings in locating the nodes. When a peak is noted, the harmonic filter of the non-slotted line is adjusted for a maximum indication with final adjustment made somewhere off the node location. Air- and sample-node readings are taken in a similar way to those measured with the slotted line, except

that the node widths are measured at power levels 3 dB down from the peak rather than 3 dB up from the minimum. For this reason, higher sensitivity settings of the UBK are necessary for the sample-node than for the air-node readings. Therefore, when the sample holder is empty, the output attenuator of the signal generator is adjusted to provide a 0-dB reading with the UBK indicator set on one of the less sensitive ranges which still provides a reliable square-law response for the detector. When the sample is placed in the sample holder, a more sensitive setting of the UBK indicator is required to observe the peak indication.

Except for the differences noted, procedures for using the non-slotted-line system are similar to those described for the slotted-line measurements. A dial gage reading to 0.001 mm is furnished for determining node widths and half-wavelengths if necessary on the non-slotted line. Since the dial gage has a range of 10 mm, wavelength determinations require the use of gage blocks with the dial gage. Another scale on the non-slotted line permits reading to 0.05-mm accuracy using a vernier. This scale was normally good enough for grain and insect sample measurements, but the dial gage was used for air-node width determinations.

A short-circuit termination was used directly on the non-slotted line in some measurements to observe adjacent nodes for frequency determinations. With lossy samples, it was sometimes necessary to increase the output from the signal generator to provide a peak indication of sufficient amplitude to observe it with the most sensitive range of the UBK indicator. The changes in output attenuator settings necessary in these

cases did not result in any detectable shift in output frequency of the signal generator.

8. Microwave Dielectrometer measurements

This system is described in Sec. II, H. The detailed setup procedure outlined in the manual for this equipment was followed in preparation for the measurements on grain and insect samples. Once adjusted, the instrument remained very stable. For operation at 8.5 GHz, the waveguide was used as a cylindrical guide operating in the TE_{11} mode. At 1 and 3 GHz, a central conductor is employed for coaxial mode operation. The switch on the dielectrometer which permits selection of any of the three klystrons was set to the desired frequency. The empty sample holder was then installed on the end of the slotted section, and the tuning plunger, which carries the loop coupling power into the waveguide, was adjusted to resonate the guide. This was indicated by a peak meter reading when monitoring the waveguide power level or observing the probe amplifier output on the panel meter.

The probe was tuned for a maximum meter indication while set at some location other than a voltage minimum. Observing the probe output, the voltage minimum was then easily located by moving the probe carriage. Three-dB node widths were then measured for the empty waveguide and recorded (Fig. 10-3, Appendix B). Adjacent air nodes were normally measured for purposes of calculating frequency at 3 and 8.5 GHz. Since two nodes could not be observed for the lower frequency, 1 GHz, the location of the short-circuit termination with respect to the scale zero was obtained by measurements at 3 GHz and a correction applied to the scale

reading for accurate determination of a half-wavelength for the 1-GHz nominal frequency.

The sample was poured into the sample holder and leveled, using the sample-height gage made for use with the dielectrometer. Sample height was read and recorded. The sample holder with the sample was then reconnected to the waveguide and the tuning plunger again used to resonate the guide. The sample 3-dB points were then determined and recorded. The dB levels at which the air and sample nodes were measured were entered on the data forms. Three-dB levels were normally used, but other levels could be used if necessary.

Upon supplying an estimate for the dielectric constant of the material, data from the data form could then be used either with the Wang 700B program or the IBM 360 computer program for calculation of the dielectric properties. Sample densities were again determined from sample weight, sample height, and sample-holder cross-sectional area, and recorded on the data forms along with the other results.

In using the dielectrometer in the coaxial mode, care had to be taken to remember to retract the probe before inserting the sample holder; otherwise, the central conductor could strike and bend the probe as the central conductor was inserted into the guide. A practice was adopted of retracting the probe as soon as the measurement was completed.

For measurements on rice weevils, a low flow rate of CO_2 was maintained through the bottom of the slot in the slotted section to keep the waveguide full of CO_2 to insure that the weevils remained anesthetized during measurement. For measurements on the empty guide, the same

procedure was followed because a shift in the null was detectable when air in the waveguide was replaced by CO_2.

9. X-band measurements

This system is described in Sec. II, I, 4. In putting the system into operation, the klystron power supply was turned on to the standby position supplying filament voltage to the klystron and starting the cooling fan in the klystron tube mount. After a few minutes, the beam voltage was applied to the klystron and the klystron current indication checked to see if it was normal. The desired frequency of operation was obtained by setting the micrometer scale of the klystron according to a calibration curve or notes made previously concerning the relationship between klystron frequency and scale readings. The klystron can be operated with many different beam and reflector voltages which also influence the frequency. Therefore, a beam voltage which provided good output at all frequencies planned for use was set on the power supply (530 V), and wooden wedges were used to lock the beam voltage adjustment knob at this position. The reflector voltage control on the power supply was then set for the best peak output as observed on the power meter, and the frequency of operation was checked using the frequency meter. Usually, some adjustment of the klystron tuning micrometer and reflector voltage was necessary to arrive at the desired frequency or peak output.

Frequencies for the measurements on grain and insects were selected where the klystron had good output power. With reflex klystrons, several modes of operation are observed as the reflector voltage is adjusted through a given range. Normally, the highest output power was available

from the mode obtained with the greatest reflector voltage (absolute value), so this was the reflector voltage used. Checks with an oscilloscope showed that adjusting the reflector voltage for a peak did provide proper modulation of the klystron output.

Calibration of the cavity-type frequency meter was checked as explained in Sec. II, I, 4, a. This frequency meter was set at the desired point to monitor the klystron operating frequency. As measurements on insect and grain samples proceeded, any drift in frequency could be corrected by minor adjustment of the reflector voltage to hold the power meter indication at the bottom of the dip registered as a result of resonant absorption by the frequency meter. Klystron stability was generally so good that no reflector voltage adjustment was necessary.

With the empty sample holder connected to the end of the slotted section, a voltage minimum was located by moving the probe carriage until the VSWR indicator registered a minimum reading. With the precision attenuator set at 0 dB, the signal level was set using the level-set attenuator or the slide-screw tuner so that the voltage minimum indication could be adjusted to midrange on the VSWR meter with the sensitivity range set on the next to the most sensitive range. With the probe carefully set at the voltage minimum, the gain controls of the VSWR meter were then adjusted for a meter indication at any convenient reference mark near midscale. The precision attenuator was then set for 6 dB, or some other level when appropriately noted, and the probe carriage was adjusted to one side of the minimum and then to the other to restore the VSWR meter indication to the same reference mark on its scale. The dial-gage readings for these two

probe positions were recorded on the data form (Fig. 10-3, Appendix B) along with the frequency.

The waveguide shorting switch was then closed, the precision attenuator setting returned to zero, and the sample holder removed. The grain or insect sample to be measured was poured into the sample holder, and it was shaken sideways slightly to level the sample. The rectangular plunger was then inserted, light pressure exerted to insure a plane top surface for the sample perpendicular to the waveguide walls, and the sample height was read from the scale on the plunger and recorded on the data form in mm. After connecting the sample holder to the slotted section again, the sensitivity of the VSWR meter was reduced and the voltage null located by movement of the probe carriage. The precision attenuator was then set for the dB level at which the sample-node width was to be determined. This was usually the 6- or 3-dB level, but occasionally a sample would provide such a well-matched termination that less than 3-dB differences were observed between voltage maxima and minima. The dial-gage readings for the sample node were then taken using the same procedure as for the air-node readings, and these were recorded on the data form. The dB levels employed for both air-node and sample-node measurements were also recorded on the data form, and, with an estimate for the dielectric constant, this completed the necessary data for the calculation.

The dB scale of the VSWR meter could be employed as an alternate means for measuring the dB levels above the minimum rather than inserting attenuation with the precision attenuator. This would be permissible on the higher sensitivity ranges of the VSWR where the crystal detector

follows the square-law-response curve, but, for low sensitivity ranges, the characteristics of the detector depart from the square-law response. The VSWR-meter scale calibration can be checked easily with the precision attenuator in the circuit, but for this work the possibilities of errors were deemed less likely using the precision attenuator as described.

Calculation of dielectric properties was then performed using either a Wang 700B program or the IBM 360 computer program, and results were entered on the data form along with sample density results.

10. Selection of frequencies

With equipment providing nearly continuous coverage of the frequency range from 250 Hz to 12.4 GHz, some thought had to be given to a selection of frequencies at which data on wheat and rice weevils were to be taken. Examination of a logarithmic scale which would be needed to display the whole frequency range graphically was helpful. Review of each measurement system and the reliability of measurement data obtained throughout its frequency range provided additional guidelines in the selection of frequencies to be used. Where the measurement system had overlapping ranges, measurements at a common frequency were scheduled as a means of checking agreement between the two systems. For the RX-Meter system, frequencies were chosen which provided values for the dielectric constant of Rexolite 1422 within about 2 percent of the correct value. For the Admittance-Meter system, the chosen frequencies yielded dielectric-constant values within less than 4 percent of the correct value for Rexolite 1422. All of the other systems have better accuracy than these two. The region below 1 GHz was avoided in using the Rohde & Schwarz LMD Slotted Line because of

the problem described in Sec. II, F, 3.

The frequencies selected for the measurements using the eight different systems are identified in Table 3-1. While not indicated in the

Table 3-1. Dielectric-properties measurement systems, frequency ranges, and frequencies selected for frequency-dependence study of wheat and rice weevils

Measurement system	Frequency range	Frequencies selected
Audiofrequency impedance bridge	0.25 - 20 kHz	0.25, 1, 5, 20 kHz
Q-Meter	0.05 - 50 MHz	0.05, 0.2, 1, 5, 20, 50 MHz
RX-Meter	50 - 250 MHz	50, 100, 200 MHz
Admittance-Meter	200 - 500 MHz	200, 300, 440 MHz
Slotted-line	0.3 - 2.75 GHz	1 GHz
Non-slotted-line	2.3 - 6.3 GHz	2.4, 5.5 GHz
Microwave dielectrometer	1, 3, 8.5 GHz	1, 3, 8.5 GHz
X-band	8.2 - 12.4 GHz	8.4, 10.1, 11.0, 12.2 GHz

table, RX-Meter measurements were made at 100 MHz using both central conductors in the sample holder. Twenty-seven different measurements were made at 22 different frequencies, considering 8.4 and 8.5 GHz the same frequency. When measurements were taken at two different sample densities, 54 measurements were necessary to obtain the data for each sample.

F. Density - Dielectric-Properties Relationships

Because the dielectric properties of materials are dependent upon the density, some exploration of the nature of this dependence seemed necessary in order to properly relate the dielectric properties of samples which might be measured at different densities using the different measurement systems. This study was conducted with the X-band system using the straight-section sample holder and plunger described in Sec. II, I, 4, b and pictured in Fig. 2-26. Measurements were made on both whole-kernel wheat and ground wheat samples. Samples were finely ground using a Labconco Heavy-Duty Laboratory Mill.

Samples were poured into the sample holder, leveled in the usual manner, and the sample holder and plunger assembly placed in a Carver Model C Laboratory Press for compression. Samples were measured which had been subjected to forces ranging from 0 to 1,300 lb. in the press in order to obtain a range of sample densities for both ground and whole-kernel samples. Sample heights were obtained by measuring the over-all length of the sample holder and plunger assembly using a dial caliper with 0.05-mm scale divisions and subtracting the appropriate length (60.03 mm). Dial indications were read to 0.01 mm, though sample lengths were not determined with this degree of accuracy.

Similar measurements were made on adult rice weevils taking data following a series of compressions while maintaining the insects in an anesthetized state. The weevils used for this particular set of measurements were of mixed ages ranging from 0 to 11 weeks after emergence. Hand pressure was sufficient to cover much of the density range, but the press was

employed to obtain higher compressions. The measurements were stopped

when fluids from the insects were forced out around the plunger at about

300-lb. force. Because of the spongy nature of the mass of rice weevils,

sample lengths were measured using the scale scribed on the plunger.

There was considerably greater uncertainty in sample length determinations

for the insect samples than for the wheat samples. After each compression

a few minutes was allowed to elapse before taking the measurement to allow

the sample length to stabilize.

IV. RESULTS

A. Influence of Sample Density on Dielectric Properties

Results of dielectric-constant measurements at 9.367 GHz on ground

and whole-kernel samples of Scout 66 hard red winter wheat at 11.3-percent

moisture and a few different sample densities are shown in Fig. 4-1. Data
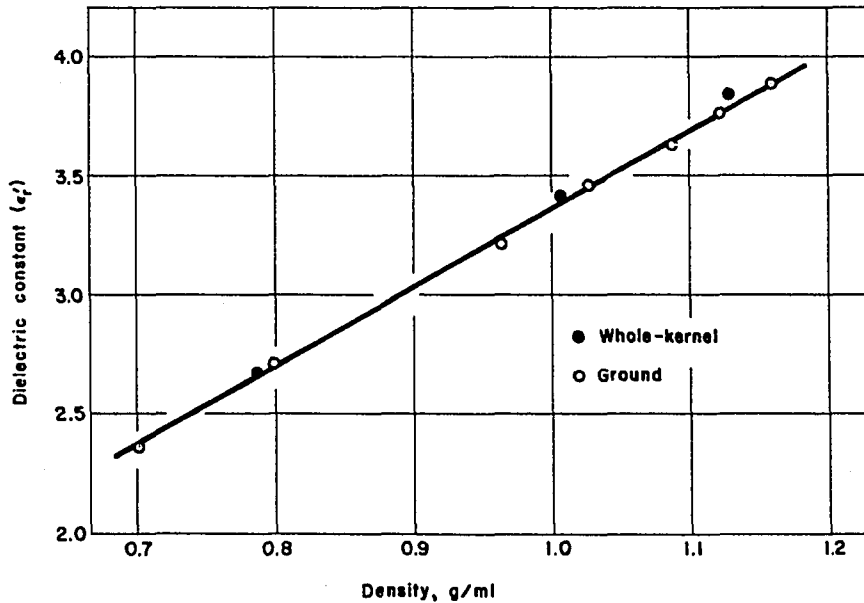
Fig. 4-1. Variation of dielectric constant with density for
ground and whole-kernel samples of 1970 Scout 66 hard
red winter wheat of 11.3-percent moisture measured at
9.367 GHz and 76° F

for the whole-kernel and ground wheat samples agree reasonably well, and

the relationship between the dielectric constant and sample density ap-

pears to be linear. The difference in homogeneity of the sample under

these two conditions did not appear to be a very important factor influ-

encing the dielectric properties.

Taking measurements on whole-kernel samples of the same wheat 1 week later at a larger number of sample densities resulted in the data summarized in Table 4-1. As before, the dielectric constant increased with

Table 4-1. Dielectric properties of a bulk sample of 11.3-percent moisture 1970 Scout 66 hard red winter wheat measured at indicated compressions and densities at 9.367 GHz and 76° F

Compression (lb.)	Sample length (mm)	Bulk density (g/ml)	Dielectric constant ε'_r	Loss tangent tan δ	Loss factor ε''_r
0	31.75	0.798	2.685	0.093	0.250
100	30.77	0.823	2.751	0.094	0.258
200	30.39	0.833	2.788	0.097	0.270
300	29.62	0.855	2.850	0.095	0.272
400	28.67	0.883	2.913	0.089	0.260
500	27.59	0.918	3.006	0.083	0.249
600	26.38	0.960	3.166	0.090	0.283
700	25.20	1.005	3.329	0.126	0.418
800	24.37	1.039	3.439	0.130	0.448
900	23.73	1.067	3.526	0.135	0.475
1000	23.08	1.097	3.631	0.136	0.495
1100	22.62	1.120	3.707	0.138	0.513
1200	22.44	1.128	3.706	0.140	0.519
1300	21.80	1.162	3.866	0.136	0.526

sample density in a nearly linear fashion. The loss tangent and dielectric loss factor, however, appear to increase, then show a slight decrease as sample density increases, and, finally, continue the increasing trend with increasing sample density. The explanation for this would require further measurements to verify the phenomenon and is beyond the scope of the problem at hand.

The data on dielectric constants from Table 4-1 are shown plotted against density in Fig. 4-2. This closer examination of the data reveals
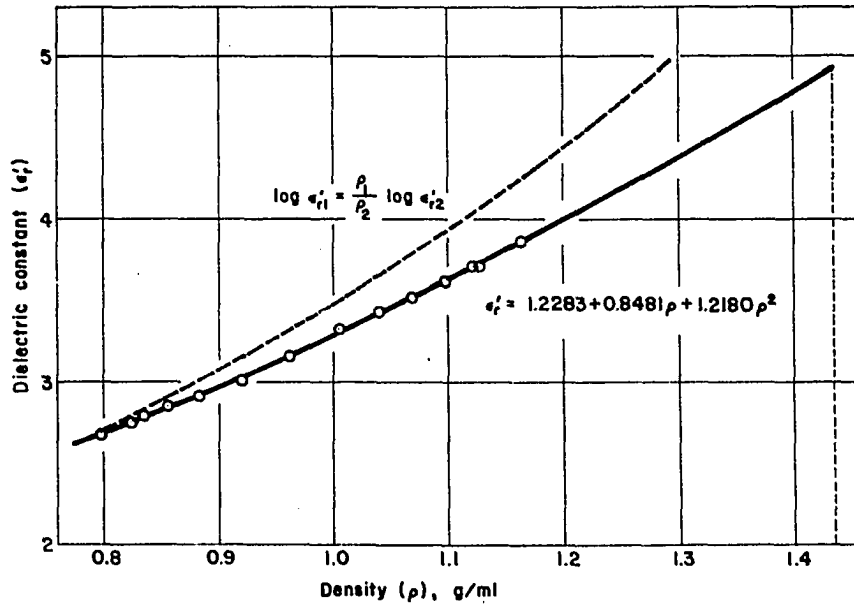
Fig. 4-2. Relationship between dielectric constant and density
for whole-kernel sample of Scout 66 hard red winter
wheat of 11.3-percent moisture content measured at
9.367 GHz and 76° F

a departure from true linearity. A second-order curve of the form

$y = a_0 + a_1 x + a_2 x^2$ fitted to the experimental data by minimizing the

function $\sum_{i=1}^{n} (y_i - a_0 - a_1 x_i - a_2 x_i^2)^2$ is shown extended to lower and higher

densities for purposes to be taken up later in Sec. V, B. The dashed

curve will also be discussed there. Similar data taken at 10.218 GHz for

rice weevils are shown in Fig. 4-3. Loss-tangent data for the rice wee-

vils showed no definite trend for this density range, but fluctuated some-

what randomly between 0.12 and 0.28.

This study of the influence of sample density and the dielectric prop-

erties was conducted partly to identify the degree of difficulty which

might be encountered in relating to each other dielectric properties of
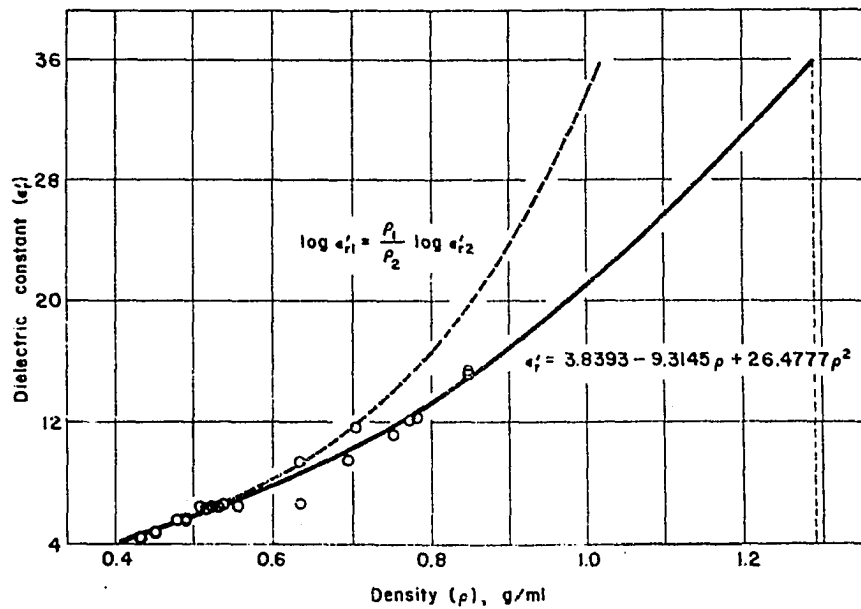
Fig. 4-3. Relationship between dielectric constant and density for bulk sample of mixed-age adult rice weevils measured at 10.218 GHz and 76° F

samples measured at different densities in the different sample holders of the various systems needed for the frequency-dependence study. For the narrow range of sample densities encountered in using different sample holders, these observations justify linear interpolation and extrapolation, if necessary, to obtain common densities for comparison of data taken with the different measuring systems.

B. Frequency Dependence of the Dielectric Properties

Disregarding a number of preliminary measurements on grain and insect samples on all systems, three complete sets of measurements at all selected frequencies were obtained on the wheat at 10.6-percent moisture, and six sets of measurements were obtained on rice weevils. The results

of these measurements were analyzed separately for the wheat and insects.

First, the range of sample densities was reviewed for all of the measurement sets and a general mean density was selected (0.79 g/ml for wheat and 0.49 g/ml for rice weevils). Linear interpolation was then employed to transform dielectric-constant and loss-tangent data obtained on each of the eight systems to the common sample density. Where sample densities for particular measurements did not span a range which included the selected density value, extrapolation was required. In a few instances, such extrapolation did not appear to be reliable, and these sets of data were excluded. All valid observations, then, for each frequency were employed in a calculation of the mean values for the dielectric constant and loss factor, and the corresponding standard deviations and coefficients of variation. The results of these analyses are presented in Tables 4-2 and 4-3. Values for the corresponding dielectric loss factors and conductivities were also calculated (Eqs. 2-6 and 2-7) and included in these tables.

Variability of resulting measurements is indicated by the magnitude of the coefficient of variation, which is expressed as standard deviation in percent of the mean. These values could be improved by greater numbers of measurements and with greater care in obtaining sample densities near a common value. A rather consistent relationship, however, is noted between frequency and the dielectric properties of the bulk wheat and the bulk rice weevils. This is illustrated in Figs. 4-4 and 4-5, where the mean dielectric constant and loss factor are plotted against frequency over the complete range of measurements. Where measurements were obtained at a common frequency with different measurement systems, the values were

Table 4-2. Mean dielectric properties of 1970 Scout 66 hard red winter wheat (0.79-g/ml bulk density) at 10.6-percent moisture and 76° F at selected frequencies in the range from 250 Hz to 12.2 GHz

Frequency	Dielectric constant ε'_r	c.v. (%)	Loss tangent tan δ	c.v. (%)	Loss factor ε''_r	Conductivity σ
0.25 kHz	7.83	1	0.312	1	2.44	0.34 nmho/cm
1.0	6.27	1	0.263	2	1.65	0.92
5.0	5.36	0	0.157	3	0.84	2.34
20.0	4.99	0	0.092	2	0.46	5.11
0.05 MHz	4.68	4	0.045	10	0.21	0.006 μmho/cm
0.20	4.53	2	0.057	5	0.26	0.029
1.0	4.33	2	0.060	3	0.26	0.145
5.0	4.14	1	0.083	4	0.34	0.956
20.0	3.90	1	0.106	0	0.41	4.60
50.0	3.81	1	0.137	4	0.52	14.53
50	3.91	17	0.097	3	0.38	10.56
100	3.39	1	0.104	1	0.35	19.63
100	3.38	1	0.107	4	0.36	20.13
200	3.08	1	0.122	17	0.38	41.84
200	3.07	2	0.071	24	0.22	24.27
300	3.09	1	0.097	24	0.30	50.06
440	3.09	0	0.130	8	0.40	98.40
1.0 GHz	2.78	1	0.110	10	0.31	0.17 mmho/cm
2.4	2.63	1	0.113	21	0.30	0.40
5.5	2.46	2	0.112	15	0.28	0.85
1.0	2.74	0	0.121	0	0.33	0.18
3.0	2.61	0	0.097	0	0.25	0.42
8.5	2.61	0	0.079	0	0.21	0.98
8.4	2.59	2	0.091	9	0.24	1.10
10.1	2.55	2	0.093	6	0.24	1.33
11.0	2.58	0	0.108	1	0.28	1.70
12.2	2.56	1	0.091	8	0.23	1.58

Table 4-3. Mean dielectric properties of 1- to 3-week-old adult rice weevils (0.49-g/ml bulk density) at 76° F at selected frequencies in the range from 250 Hz to 12.2 GHz

Frequency	Dielectric constant ε'_r	c.v. (%)	Loss tangent tan δ	c.v. (%)	Loss factor ε''_r	Conductivity σ
0.25 kHz	14.80	6	0.056	14	0.83	0.12 nmho/cm
1.0	14.54	5	0.046	9	0.67	0.37
5.0	14.24	4	0.034	10	0.48	1.35
20.0	13.98	2	0.027	5	0.38	4.20
0.05 MHz	12.16	1	0.028	35	0.34	0.01 μmho/cm
0.20	11.71	5	0.050	10	0.59	0.06
1.0	11.56	5	0.118	9	1.36	0.76
5.0	9.68	6	0.223	4	2.16	6.0
20.0	7.63	7	0.266	3	2.03	22.6
50.0	6.49	5	0.323	6	2.10	58.3
50	7.08	5	0.322	1	2.28	63.5
100	6.09	6	0.308	3	1.88	104.4
100	6.16	0	0.330	4	2.03	113.2
200	5.06	2	0.256	7	1.30	144.2
200	5.20	2	0.211	5	1.10	122.2
300	5.15	4	0.208	5	1.07	179.0
440	5.38	2	0.171	3	0.92	225.4
1.0 GHz	4.04	1	0.102	15	0.41	0.23 mmho/cm
2.4	3.82	2	0.079	5	0.30	0.41
5.5	3.68	6	0.124	10	0.46	1.40
1.0	4.32	4	0.099	2	0.43	0.24
3.0	4.16	4	0.092	4	0.38	0.64
8.5	4.54	4	0.159	12	0.72	3.40
8.4	4.22	16	0.112	25	0.47	2.20
10.1	4.19	9	0.106	25	0.44	2.50
11.0	4.17	4	0.098	8	0.41	2.50
12.2	4.05	3	0.085	25	0.34	2.30
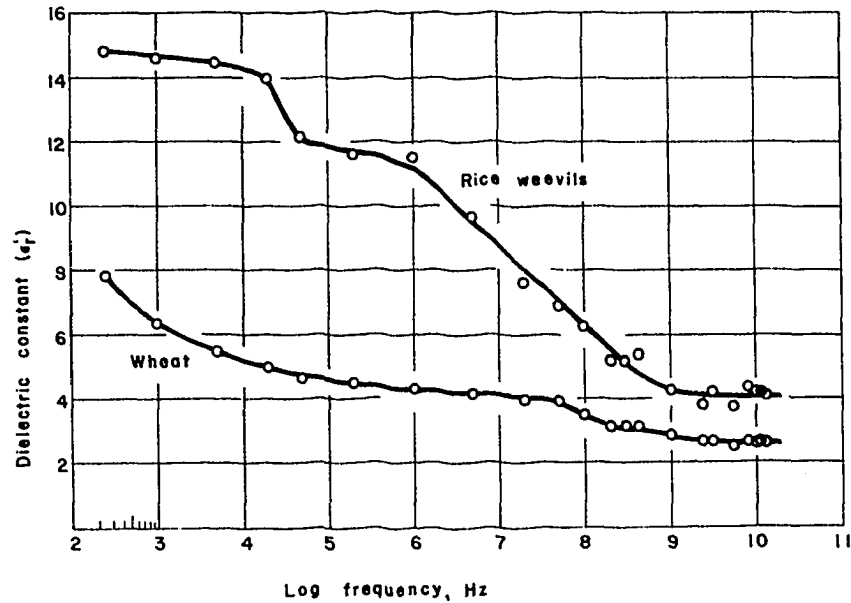
Fig. 4-4. Comparison of the frequency dependence of the dielectric constants of bulk samples of 1970 Scout 66 hard red winter wheat (10.6-percent moisture, 76° F, and 0.79-g/ml density) and 1- to 3-week-old adult rice weevils (49-percent moisture, 76° F, and 0.49-g/ml density)
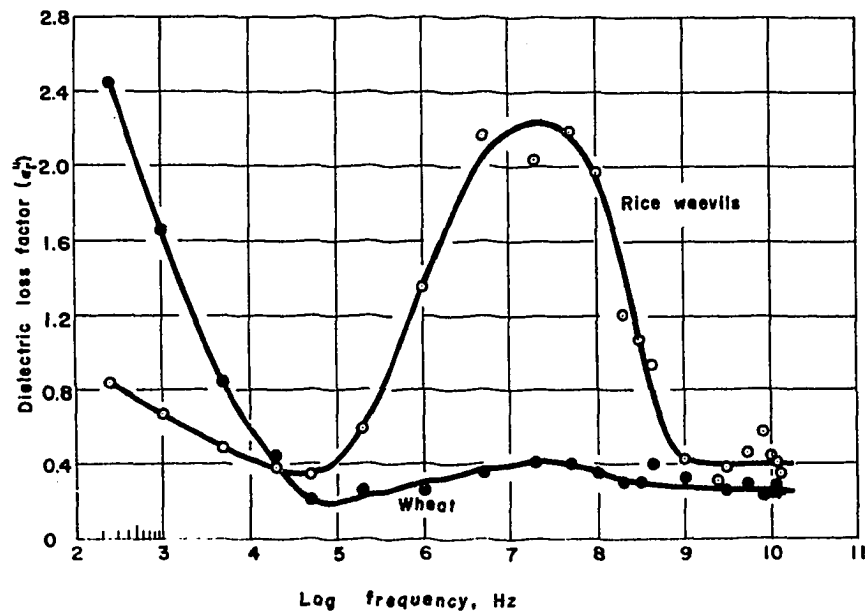
Fig. 4-5. Comparison of the frequency dependence of the dielectric loss factor of bulk samples of 1970 Scout 66 hard red winter wheat (10.6-percent moisture, 76° F, and 0.79-g/ml density) and 1- to 3-week-old adult rice weevils (49-percent moisture, 76° F, and 0.49-g/ml density)

averaged for purposes of plotting these curves.

As expected, the dielectric constant of both insects and grain decreases with increasing frequency (Fig. 4-4). The loss tangent and, consequently, the loss factor (Fig. 4-5), however, both show greater fluctuation with frequency. Starting at the lower frequencies, the loss factor falls somewhat with increasing frequency, then rises to a peak somewhere in the region between 5 and 100 MHz, and again falls off as frequency continues to increase. While the loss-factor curve for wheat at this moisture content (10.6 percent) is relatively flat in the frequency region of interest, there is a sharp rise in the loss factor of the rice weevils, and the evidence for differential absorption of energy by the insects is illustrated rather clearly in Fig. 4-5.

As noted in Secs. I, B, 2, and I, B, 3, e, the insect-to-grain dielectric-constant ratio, as well as the loss-factor ratio, influences the degree of differential heating which may result when infested grain is exposed to high-frequency electric fields. The power dissipation in the materials, $P \propto f E^2 \epsilon_r''$ (Eq. 1-9), depends directly upon the loss factor and the square of the electric field intensity. Eq. 1-11, which expresses the relationship between the field intensity in the wheat and that in the rice weevils, based upon the model of a sphere in an infinite medium, can be rewritten

$$E_i/E_g = 3/[2 + (\epsilon_{ri}/\epsilon_{rg})] \qquad [4\text{-}1]$$

where subscripts 1 and 2 have been replaced by i and g for reference to the insects and grain, and the equation has been rearranged for more convenient expression of insect-to-grain ratios for the factors being

considered. Since the magnitude of $\epsilon_r = \epsilon_r' - j\epsilon_r''$ is within about 5 per-
cent of the value of ϵ_r', even for the insects in the region of highest
loss, the dielectric constants may be used in place of the complex permit-
tivities in Eq. 4-1 for purposes of the following discussion.

Based on the assumptions already outlined, the influence of frequency
on the selective or differential heating of rice weevils in wheat can now
be evaluated using Eqs. 1-9 and 4-1 and values for ϵ_r' and ϵ_r'' from the
curves of Figs. 4-4 and 4-5. An index of the relative power dissipation
in the insects compared to the grain can be calculated as the ratio of
power dissipation in the insects to that dissipated in the grain. This
index, or ratio of power absorption, is defined here as
$R_p = (E_i/E_g)^2(\epsilon_{ri}''/\epsilon_{rg}'')$, and the calculation of its value for several se-
lected frequencies is summarized in Table 4-4. Examination of values in
the table shows that the loss-factor ratio is the dominant factor

Table 4-4. Calculation of the power dissipation ratio, R_p, for adult
rice weevils in wheat at selected frequencies[p]

Frequency (Hz)	$\epsilon_{ri}'/\epsilon_{rg}'$	E_i/E_g	$(E_i/E_g)^2$	$\epsilon_{ri}''/\epsilon_{rg}''$	R_p
10^3	2.32	0.69	0.48	0.41	0.20
10^4	2.75	0.63	0.40	0.70	0.28
10^5	2.57	0.66	0.43	2.10	0.91
10^6	2.63	0.65	0.42	4.53	1.90
10^7	2.15	0.72	0.52	5.59	2.93
10^8	1.77	0.80	0.63	5.60	3.54
10^9	1.50	0.86	0.73	1.56	1.15
10^{10}	1.60	0.83	0.69	1.60	1.11

influencing the ratio of power dissipation in this case. The dielectric-constant ratio does not change as much with frequency. Therefore, the field-intensity ratio does not change very much and has little influence compared to the loss-factor ratio.

R_p values listed in Table 4-4 show that the frequency range between 10 and 100 MHz offers the best opportunity for selectively heating the rice weevils. In fact, for the case of rice weevils in wheat, the plot of loss factors vs. frequency can be used to identify the most promising frequency range for differential heating. The peak of the loss-factor curve for rice weevils (Fig. 4-5) falls in the range between 5 and 100 MHz.

Measurements throughout the 250-Hz to 12.2-GHz range on wheat conditioned to 12.4-percent moisture gave somewhat higher dielectric-constant values and somewhat higher values for the loss factor at frequencies below 1 MHz than those observed for wheat at 10.6-percent moisture. At all frequencies above 1 MHz, however, the loss factor had very nearly the same value as did the wheat at 10.6-percent moisture. This means that the conditions for selective heating of the rice weevils is not appreciably changed by an increase in wheat moisture content from 10.6 percent to 12.4 percent.

C. Wheat-Kernel and Rice-Weevil Densities

Air-comparison pycnometer determinations for density of the wheat kernels gave very repeatable results. Measurements on four different samples at 10.5-percent moisture averaged 1.434 g/ml with a coefficient of variation of less than 1 percent. Volume measurements with the

air-comparison pycnometer using the 1- to 2-atmosphere and the 1- to 1/2- to 1-atmosphere modes gave the same results, and both methods were represented in the average result obtained.

These results are consistent with air-comparison pycnometer average density determinations ranging between 1.414 and 1.436 reported by Mattern (1965) for five hard red winter wheat varieties grown in Nebraska in 1964. Measurements reported by Thompson and Isaacs (1967) using the same method resulted in density values for soft wheat between 1.342 and 1.424.

Greater variability was encountered in measurements on rice weevils, so a larger number of observations were taken. Averages of 25 measurements using the 1- to 2-atmosphere mode and 1- to 1/2- to 1-atmosphere mode yielded densities of 1.225 and 1.353 g/ml, respectively, with coefficients of variation of 6 percent for each. Since the rice weevils might be expected to compress somewhat under 2 atmospheres of pressure, a higher density value was expected to be obtained when using the 1- to 2-atmosphere mode. The opposite result was obtained, however. One explanation is that the weevils may react to pressure changes in such a way that they expand slightly when subjected to increased pressure and/or contract somewhat when exposed to less than atmospheric pressure. Results obtained using the two different modes were averaged giving a rice weevil density value of 1.29 g/ml.

V. DISCUSSION

A. Suitability of the Model

Modeling the insects in wheat as spheres in an infinite homogeneous medium may seem oversimplified, and it must be admitted that this model, in certain aspects, does not represent the actual situation. Without simplification, however, the problem is simply not amenable to mathematical analysis. A model treating the insects as ellipsoids of revolution in a homogeneous medium would be somewhat more satisfactory with regard to the shape of the insects, but such a model is orientation-sensitive. When one takes into account the random orientation of the insects, the spherical model appears to be as satisfactory a choice as any.

Perhaps the greatest shortcoming of the model is the lack of homogeneity in either medium. One can think in terms of effective dielectric properties for an inhomogeneous medium which are related to an average electric field in the medium (Taylor, 1965, 1966). In the case of grain, this permits one to consider the bulk grain as having dielectric properties which are a sort of effective average (in a nonlinear sense) of the dielectric properties of the kernels and the interstitial air space. One can then also consider, for a bulk quantity of rice weevils, effective dielectric properties which take into account not only the insect, but also its share of the surrounding air space. When speaking of the dielectric properties of the insects, one is then implying an effective dielectric constant or loss factor for the insect and its associated air envelope.

Taking these factors into account, it appears logically sound to

measure the dielectric properties of the bulk wheat and bulk insects and make comparisons of the sort described (Sec. IV, B). Comparison of the dielectric properties of the insects and wheat over the frequency range should provide a valid basis on which to draw conclusions with regard to the relative energy absorption of the insects and grain.

B. Dielectric Properties of Wheat Kernels and Rice Weevils

While knowledge of the dielectric properties of the wheat kernel and the insect proper are not required for the principal conclusions of the frequency-dependence study, it is interesting to consider the relationship between the bulk dielectric properties and those of the kernel or the insect. Some information was obtained in the conduct of this research which may be useful in estimating those properties of the individual kernel or insect.

The air-comparison pycnometer measurements which provide information on the volume occupied by the kernels and the insects were used to calculate the kernel and insect densities. Thus, the fractional volume occupied by the wheat kernels or the insects and that occupied by the air are available. A relationship between the dielectric constant of a mixture and the dielectric properties of its constituents is given by Kay (1961):

$$\varepsilon_r' = (\varepsilon_r')_a^{v_a} \, (\varepsilon_r')_b^{v_b} \qquad\qquad [5\text{-}1]$$

where subscripts a and b refer to the two constituents, and v represents the volume fraction occupied by each. Eq. 5-1, known as the Lichtenecker mixture formula (Lichtenecker, 1926; American Society for Testing and

Materials, 1969), is equivalent to the following relation between density and dielectric constant also given by Kay (1961) where one of the constituents is air:

$$\log \varepsilon'_{r1} = (\rho_1/\rho_2) \log \varepsilon'_{r2} \qquad [5\text{-}2]$$

where subscripts 1 and 2 represent different densities.

Shackelford (1970) confirmed the validity of Eq. 5-2, using finely powdered slip-cast fused silica, Rexolite, and Panelite G-10, by measuring dielectric properties of pellets of different densities formed by a series of compressions in a waveguide cell. Dielectric properties of finely ground insect exoskeleton were also shown to follow this relationship.

Data for the dielectric-constant vs. density relationships presented in Figs. 4-2 and 4-3 were examined in relation to Eq. 5-2. They were not found to follow this relationship, which is expressed by the dashed curves for $\rho_2 = 0.79$ in Fig. 4-2 and $\rho_2 = 0.49$ in Fig. 4-3. As explained in Sec. IV, A, the solid curves in these figures are second-order polynomial regression curves fitted to the data. Extending these curves to the densities measured for the wheat kernels (1.434 g/ml) in Fig. 4-2 and for the rice weevils (1.29 g/ml) in Fig. 4-3 results in a dielectric constant for the wheat kernels of 4.95 and a dielectric constant for the rice weevils of 35.89.

It is interesting to compare these values with the result of applying Eq. 5-1. Taking a unit volume of bulk wheat, the bulk density $\rho = m$ may be substituted in the relation for kernel density $\rho_k = m/v_k$, where m is the mass of the kernels in a unit volume of bulk wheat, and v_k is the volume fraction occupied by the kernels. The result shows that $v_k = \rho/\rho_k$.

For a bulk density of 0.79 g/ml and a kernel density of 1.434 g/ml,

v_k = 0.5509. Taking $\varepsilon_r' = 1$ for air, and $\varepsilon_r' = 2.66$ for bulk wheat at 0.79-g/ml density, Eq. 5-1 gives 5.91 for the dielectric constant of the wheat kernels. This compares to 4.95 resulting from extrapolation of the more reliable curve fitting the data.

Similar calculations using Eq. 5-1 for rice weevils with a bulk dielectric constant of 5.7 at bulk density 0.49 g/ml results in a dielectric constant of 97.7 for the insect of 1.29-g/ml density. This is too high, of course. The value of 35.89 obtained using the curve fitted to the data should be more reliable. This value does not seem too unreasonable considering that the insect moisture content is about 50 percent. A dielectric-constant range of 14.3 to 18.4 was reported by Hamid *et al.* (1968) for confused flour beetles at 10.02 GHz, but, from the description of sample size, it must be assumed that this was a bulk insect sample. Dielectric constants of 40 to 42 are listed by Schwan (1957) for muscular body tissue at 8.5 GHz, so perhaps $\varepsilon_r' = 36$ may be reasonable for the rice weevils at 10.2 GHz.

The dielectric loss factors corresponding to the dielectric-constant data presented in Figs. 4-2 and 4-3 were also subjected to curvilinear regression analyses. Results for the wheat and rice weevils are summarized in Tables 5-1 and 5-2 along with information on the dielectric constants.

Table 5-1. Relationships between dielectric properties and density for 1970 Scout 66 hard red winter wheat at 11.3-percent moisture, 76° F, and 9.367 GHz

Property	Regression equation	Density, ρ (g/ml)	
		0.79 (Bulk)	1.434 (Kernel)
ϵ'_r	$\epsilon'_r = 1.2283 + 0.8481\rho + 1.2180\rho^2$	2.66	5.91
ϵ''_r	$\epsilon''_r = 0.8603 - 1.9346\rho + 1.4473\rho^2$	0.24	1.06

Table 5-2. Relationships between dielectric properties and density for adult rice weevils at 76° F and 10.218 GHz

Property	Regression equation	Density, ρ (g/ml)	
		0.49 (Bulk)	1.29 (Weevil)
ϵ'_r	$\epsilon'_r = 3.8393 - 9.3145\rho + 26.4777\rho^2$	5.63	35.89
ϵ''_r	$\epsilon''_r = 2.7231 - 9.8189\rho + 12.8145\rho^2$	0.99	11.38

C. Frequency Dependence of the Dielectric Properties

The nature of the frequency dependence of the dielectric constant and the dielectric loss factor for both bulk wheat and bulk rice weevils is quite clearly illustrated in Figs. 4-4 and 4-5. In the region between 10^5 and 10^9 Hz, curves are characteristic of the Debye-type disperson associated with polar molecules (Debye, 1929). Discussions of anomalous dispersion, the decreasing of the dielectric constant with increasing frequency, and the dielectric theories of Debye, Onsager, Cole, Kirkwood, Fröhlich,

and others are found in many references, including Böttcher (1952), von Hippel (1954a), and Hill *et al.* (1969). Basically, all of these formulations recognize a contribution to the dielectric constant of materials containing molecules with dipole moments through the polarization resulting from the orientation of the dipoles with the applied electric field. Two lesser contributions to the polarizability arise from electronic polarization, the displacement of electrons of atoms with respect to the nucleus, and atomic polarization, the displacement of nuclei with respect to one another. These two types of polarization are termed "distortion" or "deformation" polarization.

As frequency increases from low values, the polar molecules can follow the changes in direction of the electric field up to a point, and, as frequency continues to increase, the dipole motion can no longer keep up with the changing field. As a result, the dielectric constant decreases with increasing frequency in this region and energy is absorbed as a result of the phase lag between the dipole rotation and the field. At higher frequencies, the dielectric constant again levels off at the so-called optical value, the square of the index of refraction, and the loss factor again drops to a low value. The relationship between the dielectric constant and loss factor is illustrated in Fig. 5-1. Debye (1929) developed the mathematical formulation which can be expressed as

$$\varepsilon_r = \varepsilon'_{r\infty} + (\varepsilon'_{rs} - \varepsilon'_{r\infty})/(1 + j\omega\tau) \qquad [5\text{-}3]$$

Separating this into its real and imaginary components yields

$$\varepsilon_r' = \varepsilon_{r\infty}' + (\varepsilon_{rs}' - \varepsilon_{r\infty}')/(1 + \omega^2\tau^2)$$

$$\varepsilon_r'' = (\varepsilon_{rs}' - \varepsilon_{r\infty}')\omega\tau/(1 + \omega^2\tau^2)$$

[5-4]
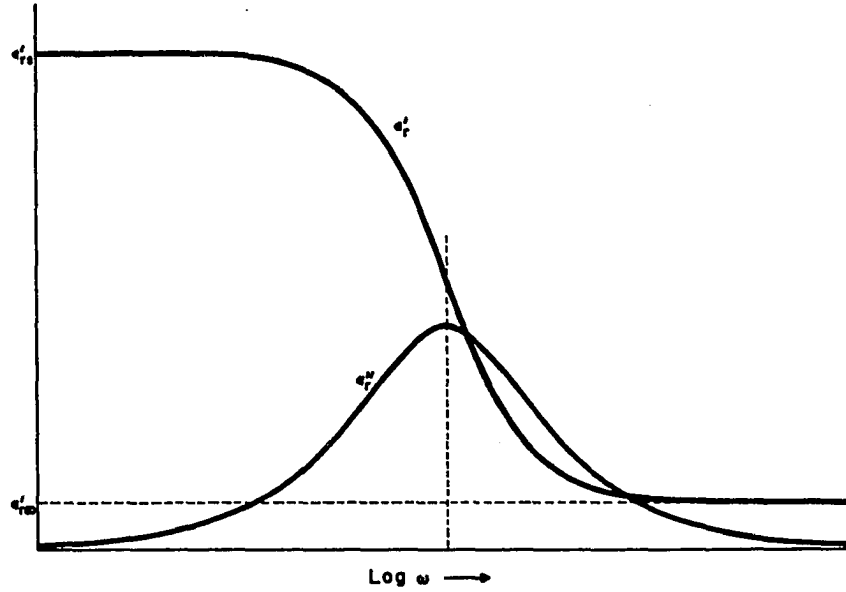
Fig. 5-1. Dispersion and absorption curves for a polar material following the Debye relaxation process

where ε_{rs}' is the static or d-c value of the dielectric constant, $\varepsilon_{r\infty}'$ is the infinite-frequency or optical value, and τ is the relaxation time, the period associated with the time for the dipoles to revert to random orientation. The loss factor, ε_r'', peaks where $\omega = 2\pi f = 1/\tau$, and, at this frequency (the relaxation frequency), ε_r'' has the value $(\varepsilon_{rs}' - \varepsilon_{r\infty}')/2$ and ε_r' has the value $(\varepsilon_{rs}' + \varepsilon_{r\infty}')/2$. Because the loss decreases to zero at the frequency extremes, $\varepsilon_{rs}' = \varepsilon_{rs}$ and $\varepsilon_{r\infty}' = \varepsilon_{r\infty}$. Therefore, Eqs. 5-3 and 5-4 are frequently seen without the prime marks on ε_{rs} and $\varepsilon_{r\infty}$.

The similarity of the relationship between ε_r' and ε_r'' in Fig. 5-1 to that of ε_r' and ε_r'' in Figs. 4-4 and 4-5 is obvious and indicative that the

Debye dispersion phenomenon is predominant in the dispersion and absorption noted for the dielectric properties of rice weevils and wheat in the frequency range above 100 kHz.

The dispersion of some pure liquids closely follows the Debye equations, Eqs. 5-4 (Buckley and Maryott, 1958), but where there is a distribution of relaxation times in materials, a modification by Cole and Cole (1941) more satisfactorily describes the dispersion. It was noted by Cole and Cole (1941) that plotting ε_r' and ε_r'' in the complex plane (Argand diagram), in accordance with the Debye relation, results in a semicircle (Fig. 5-2). Eqs. 5-4 are parametric equations of a circle, and combining
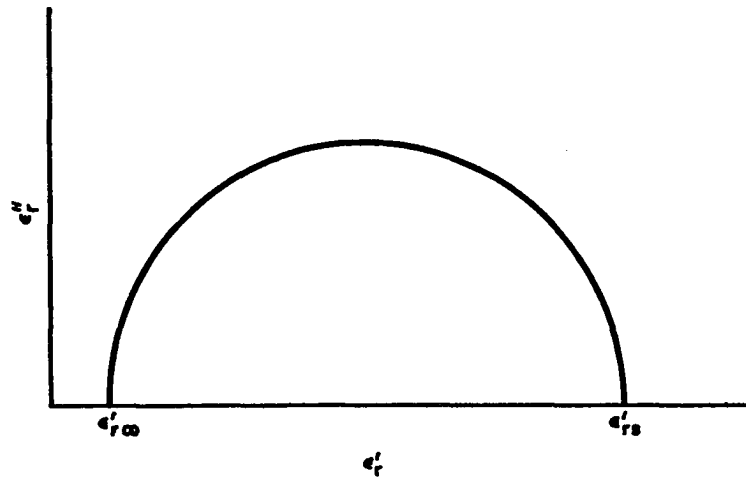
Fig. 5-2. The Cole-Cole plot for the Debye relation

the two equations and eliminating $\omega\tau$ provides the following Cole-Cole relation:

$$\left(\varepsilon_r' - \frac{\varepsilon_{rs}' + \varepsilon_{r\infty}'}{2}\right)^2 + (\varepsilon_r'')^2 = \left(\frac{\varepsilon_{rs}' - \varepsilon_{r\infty}'}{2}\right)^2 \qquad [5\text{-}5]$$

This describes a circle of radius $(\varepsilon_{rs}' - \varepsilon_{r\infty}')/2$ with center on the ε_r' axis

at $(\varepsilon'_{rs} + \varepsilon'_{r\infty})/2$, 0. The modified equation presented by Cole and Cole (1941)

$$\varepsilon_r = \varepsilon'_{r\infty} + \frac{\varepsilon'_{rs} - \varepsilon'_{r\infty}}{1 + (j\omega\tau)^{1-\alpha}} \qquad [5\text{-}6]$$

results in a Cole-Cole plot which is an arc of a circle with the center below the $\varepsilon''_r = 0$ axis (Fig. 5-3). The empirical relaxation-time distribution parameter α takes on values between 0 and 1, and is an index of the
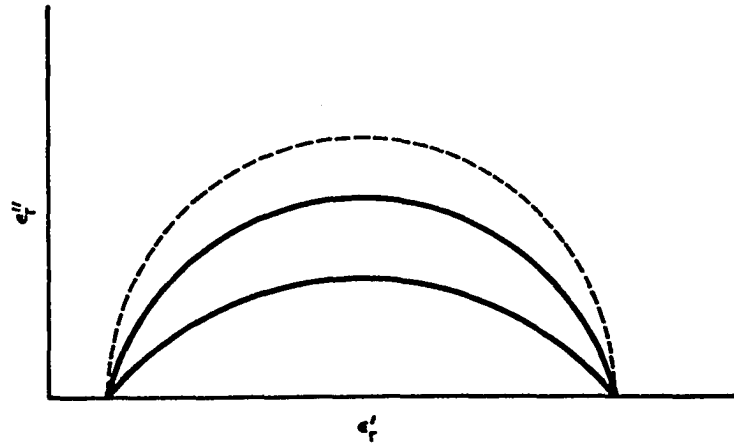
Fig. 5-3. Cole-Cole circular arcs

spread in the relaxation times. Several other models have been developed to explain the behavior of certain types of materials. One known as the Cole-Davidson representation results in a skewed arc (Fig. 5-4) rather than the symmetrical Cole-Cole circular arc (Davidson and Cole, 1951). The Cole-Davidson representation is mathematically defined as

$$\varepsilon'_r = \varepsilon'_{r\infty} + \frac{\varepsilon'_{rs} - \varepsilon'_{r\infty}}{(1 + j\omega\tau)^\beta} \qquad [5\text{-}7]$$

where β is restricted to values between 0 and 1. For $\beta = 1$ the arc is the Debye semicircle, but for values of $\beta < 1$ the arc is skewed to the right,
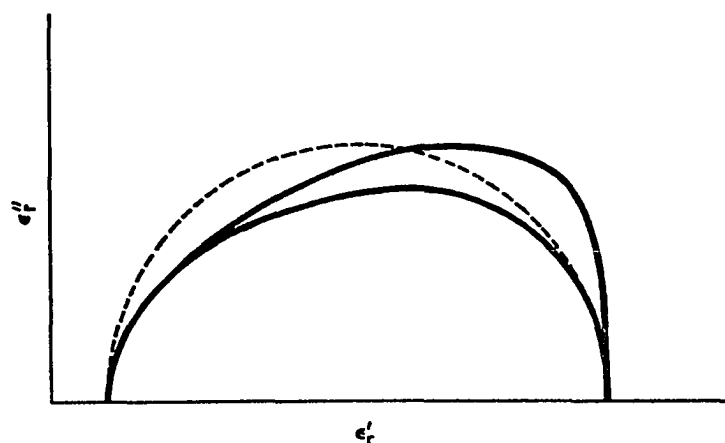
Fig. 5-4. Cole-Davidson skewed arcs

i.e., the value of ϵ_r'' peaks to the right of the center line for the Cole-Cole arc. The Cole-Davidson representation is useful for materials exhibiting a nonsymmetrical distribution of relaxation times with polarization processes of decreasing importance extending into the higher frequency region.

Dielectric properties of materials are also temperature-dependent. In polar materials the relaxation time decreases with increasing temperature, and examination of Eq. 5-3 reveals that the dielectric constant will, therefore, increase with temperature in the region of dispersion or dielectric loss. In the absence of dielectric loss, the dielectric constant for such materials decreases with increasing temperature (Böttcher, 1952).

The Cole-Cole relation (Eq. 5-6) has been found to describe reasonably well the frequency dependence of some biological substances (Schwan, 1957; de Loor and Meijboom, 1966; Grant, 1969). Henson and Hassler (1965) employed this model in a study of the dielectric properties of tobacco

leaves. While it does not appear that one should necessarily expect the

frequency dependence of such chemically complex substances as wheat and

insects to follow a simple model such as the Cole-Cole representation,

Eq. 5-6, it is interesting to plot values measured for rice weevils and

wheat in the complex ϵ_r' - ϵ_r'' plane. These Cole-Cole plots are shown in

Figs. 5-5 and 5-6. Data for frequencies above 100 kHz approximate a cir-

cular arc, but the absorption processes for these substances have not been

well enough classified to insist that they should fall in such an arc.
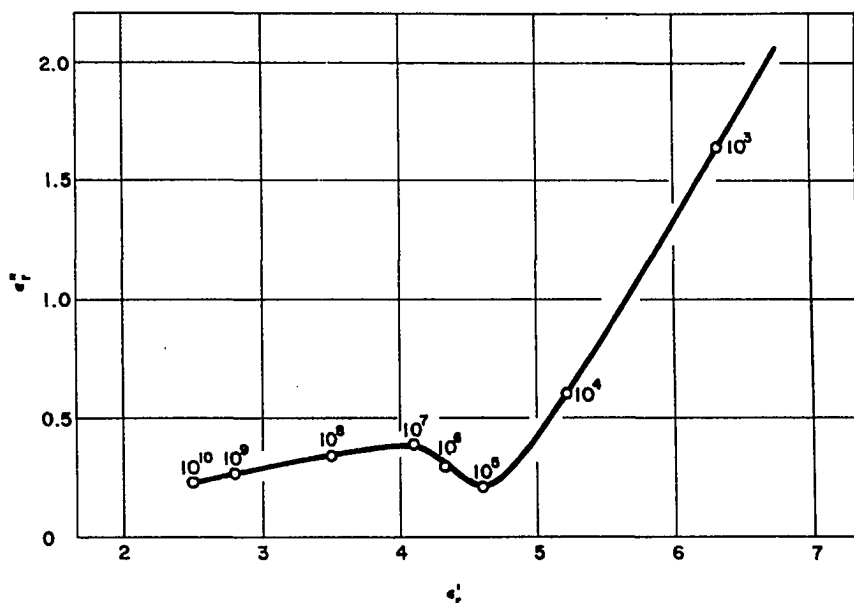
Fig. 5-5. Cole-Cole plot for Scout 66 hard red winter wheat at 76° F

The rise in curves for ϵ_r' and ϵ_r'' at frequencies below 100 kHz, Figs.

4-4, 4-5, 5-5, and 5-6, is most likely due to the influence of the d-c

conductivity and interfacial polarization processes encountered in non-

homogenous materials (Davies, 1969). Electrode polarization is another

factor which might account for the indicated frequency dependence at
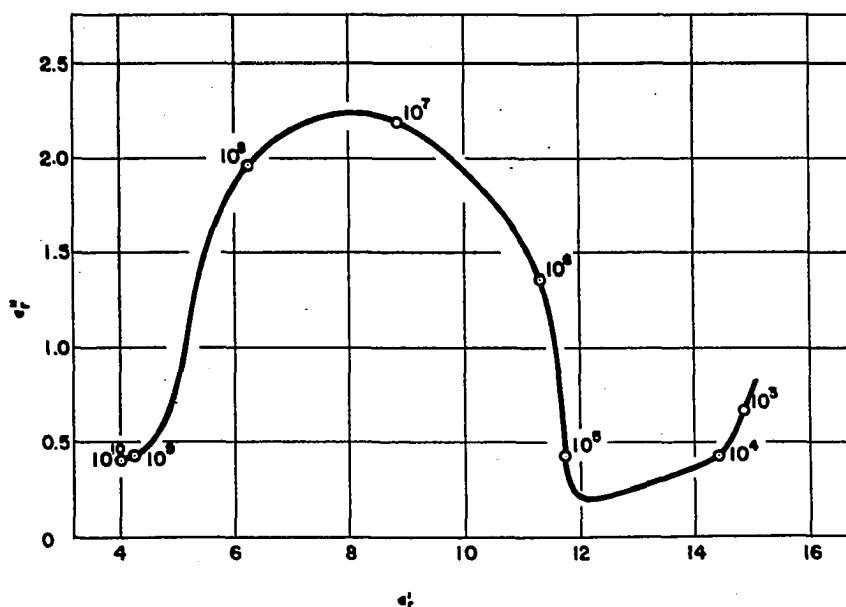
Fig. 5-6.   Cole-Cole plot for adult rice weevils at 76° F

audiofrequencies (Schwan, 1966). The peak in the loss-factor curve, be-

tween 5 and 100 MHz, "is almost certainly due to water—in its various

'bound' conditions within the specimens" (Mansel Davies, personal communi-

cation. The Edward Davies Chemical Laboratory, University College of

Wales, Aberystwyth. 1971). The relaxation region for bound forms of

water is also identified by de Loor (1968) as the region between 10^6 and

10^9 Hz. Curves for dielectric constants of blood, muscle tissue, and bac-

terial suspensions are presented by Schwan (1957). The low-frequency

characteristics of these curves are very similar to the curves obtained

for dielectric constants of wheat and rice weevils (Fig. 4-4). The con-

tinuing rise in the dielectric constant at low frequencies was attributed

by Schwan (1957) to a wide spectrum of relaxation times.

Another absorption process is likely to be present in wheat and rice

weevils. The Maxwell-Wagner absorption, which results from polarizations at interfacial boundaries, occurs in nonhomogeneous materials and is frequently seen in biological materials (Davies, 1969; Schwan, 1957, 1959). Frequency dependence of the Maxwell-Wagner absorption is similar in nature to that of the Debye dipolar absorption (Davies, 1969), but occurs at lower frequencies (de Loor and Meijboom, 1966; de Loor, 1968).

Since the bulk samples of wheat and rice weevils are granular material, i.e., particles of one substance surrounded by another substance, air, a Maxwell-Wagner effect could possibly account for the dispersion at radiofrequencies (Herman P. Schwan, personal communication. Department of Biomedical Electronic Engineering, The Moore School of Electrical Engineering, University of Pennsylvania, Philadelphia. 1971). Whether the dispersion in the 10^5- to 10^9-Hz region results principally from Debye or Maxwell-Wagner absorption processes remains to be resolved.

Dielectric-constant values obtained for rice weevils indicate a lower frequency dispersion in the 10- to 100-kHz region, but no accompanying peak in the loss-factor curve was observed in this region. Possibly Maxwell-Wagner effects could account for this dispersion if a dispersion does truly exist in the 10- to 100-kHz region.

D. Suggestions for Further Study

The frequency dependence of the dielectric properties of wheat and rice weevils of the descriptions used is reasonably well defined by the curves shown in Figs. 4-4 and 4-5 for the temperature of 76° F. Dielectric properties of materials, however, are also temperature-dependent.

Because the temperature of both the insects and the grain change considerably in the RF dielectric heating process when used as an insect control treatment, it would be useful to explore the temperature dependence of the dielectric constant and loss factor of insects and grain through the temperature range involved in such a treatment. While it is likely that the temperature coefficient of dielectric properties of insects and wheat will have the same sign, their relative magnitudes could well influence the degree of differential dielectric heating to be expected as the temperatures of the two materials increase during exposure. Temperature coefficients may be either positive or negative, and in some biological materials the sign is frequency-dependent (Schwan, 1957). Indications were obtained in some experimental RF insect control work with rice weevils in wheat that the differential heating effect diminished with increasing temperature (Nelson and Whitney, 1960). Determination of the temperature dependence of dielectric loss and the influence of temperature on the dielectric constant in the frequency range between about 5 and 100 MHz should be helpful in explaining these effects.

Further study and identification of the absorption processes in insects and grain would also be of interest. The study of absorption processes would probably be aided by information arising from the temperature-dependence study just discussed.

Because the rice weevil is only one species of many which infest grain, frequency- and temperature-dependence data on dielectric properties of other species and developmental stages within species would provide helpful information concerning the interspecies and interstage

variation in properties needed for an over-all assessment of RF insect control possibilities. The nature of the absorption and the general frequency ranges of interest should be expected to be similar for all insects, but differences in magnitudes of the dielectric constants and loss factors of different species and different host grains may influence the degree of differential heating to be expected.

With regard to the further exploration of dielectric properties in the 5- to 100-MHz range, improvements can be made in the instrumentation employed for the measurements. The Q-Meter is a useful instrument, but improved accuracy could be achieved by using a supplemental voltmeter with more sensitive ranges and greater accuracy. The accuracy of loss measurements could also be improved with some work on sample-holder design and improved calibration of the variable capacitor built into the sample holder. It then might be employed for more accurate determination of the width of the voltage-vs.-capacitance resonance peak. Higher resolution of such capacitance changes would also provide more accurate measurement of the dielectric constant.

Finally, one must not forget the possibility of physiological effects which might be achieved without the necessity of thermal damage to biological systems. Confirmation of any lethal effects or discovery of mechanisms of lethal action of a nonthermal nature are worth looking for, and, if found to exist, could materially change the entire picture for controlling insects with RF energy.

VI. SUMMARY AND CONCLUSIONS

A. Summary

The need for new insect control methods to supplement present chemical methods is discussed, and the potential for electromagnetic methods is considered briefly. The literature on insect control studies using radiofrequency (RF) electric fields is reviewed in some detail. A theoretical basis for differential absorption of energy from high-frequency electric fields by insects in infested grain is presented beginning with Maxwell's equations and defining the a-c constitutive parameters of materials with emphasis on the dielectric properties and interpretation of dielectric loss in materials. The influence of various entomological and physical factors is considered, the need to improve the efficiency of RF treatment for insect control application is recognized, and the problem of determining the frequency dependence of the dielectric properties of wheat and the rice weevil is formulated.

Methods and techniques for determining the dielectric properties of materials are reviewed, and eight different instrument systems selected or developed for measurement of the dielectric properties of insects and grain at frequencies from 250 Hz to 12.4 GHz are described in some detail. Verification of the reliability of measurements obtained on all systems is also related in considerable detail.

Basic principles and mathematical relationships were verified for calculation of dielectric properties of materials from slotted-section measurements taken with samples in contact with a short-circuit

termination of coaxial, cylindrical, or rectangular waveguides. A general

computer program with a number of unique features was developed for the

complex computations. The program takes into account corrections for the

influence of the slot in the slotted section on the measurements associ-

ated with the guide wavelength in rectangular and cylindrical waveguides.

It takes into account the fact that measurements are conducted with air

in the waveguide rather than vacuum. The proper corrections are made for

wall losses in the waveguide, and the computations are valid for high-loss

as well as low-loss materials. Convenience features include automatic

selection of proper calculations for coaxial, cylindrical, or rectangular

waveguides, provision for node-width measurements at any measurable dB

level, use of any combination of measurable air and sample nodes, print-

out of three possible sets of dielectric properties resulting from adja-

cent solutions to the transcendental equation, and a summary table of

dielectric properties for each set of samples. A complete treatment of

the principles and measurement considerations and a description of the

computer program are included in an appendix.

The wheat and rice weevils selected for the study are described.

Methods of sample preparation and measurement of moisture content, bulk

density, and particle density for both insects and grain are fully de-

scribed. The special methods employed for each of the eight different

electrical measurement systems in obtaining the data on insect and wheat

samples are discussed, and bases are given for the selection of 22 dif-

ferent frequencies at which measurements were taken.

Results are presented, in tabular and graphical form, on density –

dielectric-properties relationships for wheat and insect samples throughout a wide density range. They serve to justify linear interpolation through small density ranges for dielectric-properties data obtained on the different measurement systems at somewhat different sample densities.

Summaries of the dielectric properties at the 22 different frequencies are tabulated for 1- to 3-week-old adult rice weevils and for wheat at 10.6-percent moisture. Mean values are presented for the dielectric constant, dielectric loss factor, loss tangent, and conductivity, along with the coefficients of variation observed at each frequency in the interpolated dielectric-constant and loss-tangent data for the replicated measurements. Curves are presented showing the frequency dependence of the dielectric constant and the loss factor for the 250-Hz to 12.2-GHz range. From these data on the dielectric properties of wheat and rice weevils, insect-to-grain ratios are calculated for the loss factor and also for the field intensity, based on a spherical model of the insect in a homogeneous dielectric with the properties of bulk wheat. A ratio of power dissipation in the insect to that dissipated in the grain is then calculated, which serves as an index to identify the most promising frequencies for differential heating of the rice weevils in wheat when exposed to the electric fields.

Data on the densities of wheat kernels and individual insects as determined from air-comparison pycnometer measurements are also presented.

Questions which might be raised concerning the suitability of the spherical model for the insect in a homogeneous medium are discussed, and the advantages and shortcomings of the model are pointed out. The concept

of effective dielectric properties for inhomogeneous media is described and an argument advanced for the validity of energy-absorption comparisons based on dielectric properties of bulk rice weevils and bulk wheat.

Estimates of the dielectric properties of wheat kernels and insects proper are obtained by extrapolation of curves plotted from measurements on bulk samples of wheat and rice weevils compressed to a series of different densities. Values are compared to those calculated from the same data using empirical relationships derived from data on more nearly homogeneous materials.

The dispersion and absorption curves obtained for wheat and rice weevils are examined in the light of classical models developed to explain dispersion and absorption phenomena in dielectrics. Representations considered include the Debye, Cole-Cole, Cole-Davidson, and Maxwell-Wagner relations for describing the frequency-dependent behavior of compounds.

Suggestions for further study include the temperature-dependent nature of the dielectric properties of grain and insects, identification of the absorption processes, measurements on other insect species, improvement of measurement methods in the 5- to 100-MHz range, and continued search for nonthermal biological effects which might be useful in insect control.

B. Conclusions

The following conclusions are drawn from these studies:

1. The short-circuited waveguide method serves very well for the determination of dielectric properties of high-loss materials such as grain

and insects, provided that a suitable computer program is used for the calculations.

2. The dielectric constant and loss factor for bulk wheat and bulk rice weevils vary almost linearly with density over narrow ranges, and empirical data were closely matched by a second-order polynomial regression curve over a wide density range. Empirical relations developed earlier for more nearly homogeneous materials did not accurately describe the variation of dielectric properties of wheat and rice weevils with density.

3. The dielectric constant and loss factor at 10 GHz and 76° F for hard red winter wheat kernels are estimated to be 5.9 and 1.1, respectively, compared to 2.7 and 0.2 for bulk wheat. Corresponding values for mixed-age adult rice weevils at the same frequency and temperature are estimated to be 36 and 11 for the insects proper, compared to 5.6 and 1.0 for bulk insects.

4. Analysis of differential heating between insects and grain, based on the model of a sphere in another homogeneous medium, showed that the loss-factor ratio is the dominant factor affecting differential absorption of energy in a high-frequency electric field. The ratio of the electric field intensity in the two materials plays a much less important role.

5. Measurements of the dielectric properties of wheat at 10.6- to 12.4-percent moisture and of 1- to 3-week-old adult rice weevils, both at 76° F, throughout the frequency range from 250 Hz to 12.2 GHz clearly show that the frequency range between about 5 and 100 MHz offers by

far the best potential for selectively heating the insects through dielectric absorption.

6. The peak in the absorption curves for rice weevils and wheat in the 5- to 100-MHz range and the associated dispersion of the dielectric constant suggest rather strongly the prevalence of a Debye polar absorption process, though the Maxwell-Wagner absorption process is also believed to be present.

VII. REFERENCES CITED

Altschuler, H. M.
    1963   Dielectric constant. Ch. IX, pp. 495-548. *In* Handbook of
        microwave measurements, M. Sucher and J. Fox, eds., Polytechnic
        Institute of Brooklyn. Polytechnic Press, Brooklyn, N.Y.

American Association of Cereal Chemists
    1962   American Association of Cereal Chemists approved methods. 7th
        ed. American Association of Cereal Chemists, St. Paul, Minn.

American ENKA Corporation, Brand-Rex Division
    1971   Rexolite microwave dielectric rod and sheet stock. Tech. Bull.
        S-266A. American ENKA Corp., Brand-Rex Div., Willimantic, Conn.

American Society for Testing and Materials
    1969   Standard methods of test for dielectric constant and dissipa-
        tion factor of expanded cellular plastics used for electrical
        insulation. ASTM Designation: D1673-61 (Reapproved 1967). 1969
        Book of ASTM Standards, Part 29, 218-224. ASTM, Philadelphia,
        Pa.

Association of Official Agricultural Chemists
    1965   Official methods of analysis of the Association of Official
        Agricultural Chemists. Tenth ed., Secs. 13.004 and 13.059.
        AOAC, Washington, D.C.

Baker, Vernon H., Dennis E. Wiant, and Oscar Taboada
    1956   Some effects of microwaves on certain insects which infest wheat
        and flour. J. Econ. Entomol. 49: 33-37.

Böttcher, C. J. F.
    1952   Theory of electric polarisation. Elsevier Publishing Co., New
        York.

Boulanger, R. J., W. M. Boerner, and M. A. K. Hamid
    1969   Comparison of microwave and dielectric heating systems for the
        control of moisture content and insect infestations of grain.
        J. Microwave Power 4: 194-208.

Brady, M. Michael
    1970   Tables of constants for ISM waveguides. J. Microwave Power 5:
        175-182.

Buckley, Floyd, and Arthur A. Maryott
    1958   Tables of dielectric dispersion data for pure liquids and dilute
        solutions. U. S. National Bureau of Standards Circ. 589.

Bussey, H. E.
    1967   Measurement of RF properties of materials--a survey. Proc. IEEE
            55: 1046-1053.

Bussey, H. E., and J. L. Dalke
    1967   Radio frequency properties of materials, Topic 11. Unpublished
            lecture notes, electromagnetic measurements and standards.
            Radio Standards Laboratory, National Bureau of Standards, U. S.
            Dept. of Commerce, Washington, D.C.

Bussey, H. E., and J. E. Gray
    1962   Measurement and standardization of dielectric samples. IRE
            Trans. Instrumentation I-11: 162-165.

Carpenter, Russell L., and Elliot M. Livstone
    1971   Evidence for nonthermal effects of microwave radiation: ab-
            normal development of irradiated insect pupae. IEEE Trans. of
            Microwave Theory and Techniques MTT-19: 173-178.

Cole, Kenneth S., and Robert H. Cole
    1941   Dispersion and absorption in dielectrics. I. Alternating cur-
            rent characteristics. J. Chem. Phys. 9: 341-351.

Corcoran, P. T., S. O. Nelson, L. E. Stetson, and C. W. Schlaphoff
    1970   Determining dielectric properties of grain and seed in the
            audiofrequency range. Trans. ASAE 13: 348-351.

Dakin, T. W., and C. N. Works
    1947   Microwave dielectric measurements. J. Appl. Phys. 18: 789-796.

Davidson, D. W., and R. H. Cole
    1951   Dielectric relaxation in glycerol, propylene glycol, and n-
            propanol. J. Chem. Phys. 19: 1484-1490.

Davies, Mansel
    1969   Dielectric dispersion and absorption and some related studies
            in condensed phases. Ch. 5, pp. 280-461. *In* Dielectric prop-
            erties and molecular behaviour, Nora E. Hill, Worth E. Vaughan,
            A. H. Price, and Mansel Davies. Van Nostrand Reinhold Company,
            New York.

Debye, P.
    1929   Polar molecules. The Chemical Catalog Co., New York.

de Loor, G. P.
    1968   Dielectric properties of heterogeneous mixtures containing
            water. J. Microwave Power 3: 67-73.

de Loor, G. P., and F. W. Meijboom
    1966   The dielectric constant of foods and other materials with high water contents at microwave frequencies. J. Food Tech. 1: 313-322.

Eichacker, R.
    1958   A material-characteristics test assembly for determining the electromagnetic material constants of solid and liquid media at frequencies between 30 and 7000 MC and temperatures between -60 and +240° C. Rohde & Schwarz-Mitteilungen No. 11: 185-205.

Eichacker, R.
    1961   Materials testing by standing-wave detectors. Rohde & Schwarz-Mitteilungen No. 15: 15-27.

Field, Robert F.
    1954   Dielectric measuring techniques, A. Permittivity, 1. Lumped circuits. Ch. II, pp. 47-62. *In* Dielectric materials and applications, Arthur R. von Hippel, ed. John Wiley and Sons, Inc., New York.

Franceschetti, G.
    1967   A complete analysis of the reflection and transmission methods for measuring the complex permeability and permittivity of materials at microwaves. Alta Frequenza 36: 757-764.

Franceschetti, G., and S. Silleni
    1964   Measurement techniques and experimental data on mixture-type artificial dielectrics. Alta Frequenza 33: 733-745.

General Radio Company
    1965   Operating instructions, Type 1608-A impedance bridge. General Radio Company, West Concord, Mass.

Giordano, Anthony B.
    1963   Measurement of standing wave ratio. Ch. II, pp. 73-133. *In* Handbook of microwave measurements, M. Sucher and J. Fox, eds., Polytechnic Institute of Brooklyn. Polytechnic Press, Brooklyn, N.Y.

Grant, Edward H.
    1969   The study of biological molecules by dielectric methods. Ch. 9, pp. 297-325. *In* Solid state biophysics, McGraw Hill advanced physics monograph series, S. J. Wyard, ed. McGraw-Hill Book Company, New York.

Hamid, M. A. K., and R. J. Boulanger
    1969   A new method for the control of moisture and insect infestations of grain by microwave power. J. Microwave Power 4: 11-18.

Hamid, M. A. K., C. S. Kashyap, and R. Van Cauwenberghe
    1968   Control of grain insects by microwave power. J. Microwave Power
            3: 126-135.

Harrington, Roger F.
    1961   Time-harmonic electromagnetic fields. McGraw-Hill Book Company,
            New York.

Hartshorn, L., and W. H. Ward
    1936   The measurement of permittivity and power factor of dielectrics
            at frequencies from 10^4 to 10^8 C.P.S. J. Inst. Electrical Eng.
            79: 597-609.

Henson, W. H., Jr., and F. J. Hassler
    1965   Certain dielectric and physical properties of intact tobacco
            leaves. Trans. ASAE 8: 524-527, 529.

Hill, Nora E., Worth E. Vaughan, A. H. Price, and Mansel Davies
    1969   Dielectric properties and molecular behaviour. Van Nostrand
            Reinhold Company, New York.

Jorgensen, J. L.
    1966   A method for determining the dielectric properties of grain and
            seed in the 50- to 250-MHz range. Unpublished M.S. thesis, Uni-
            versity of Nebraska Library, Lincoln, Nebr.

Jorgensen, J. L., A. R. Edison, S. O. Nelson, and L. E. Stetson
    1970   A bridge method for dielectric measurements of grain and seed
            in the 50- to 250-MHz range. Trans. ASAE 13: 18-20, 24.

Kadoum, Ahmed M.
    1969   Effect of radiofrequency electric field treatment on protein
            metabolism in yellow mealworm larvae. J. Econ. Entomol. 62:
            220-223.

Kadoum, A. M., H. J. Ball, and S. O. Nelson
    1967   Morphological abnormalities resulting from radiofrequency treat-
            ment of larvae of *Tenebrio molitor*. Ann. Entomol. Soc. Amer.
            60: 889-892.

Kay, Alan F.
    1961   Radomes and absorbers. Ch. 32, pp. 32-1 to 32-40. *In* Antenna
            engineering handbook, Henry Jasik, ed., McGraw-Hill Book Com-
            pany, Inc., New York.

Lebrun, André
    1955   IX. Spectres hertziens de molécules d'alcools normaux à longue
            chaîne. Cahiers de Physique 60: 11-14.

Lichtenecker, Karl
   1926   Die Dielektrizitätskonstante natürlicher und künstlicher Misch-
          körper. Physik. Zeitschr. 27: 115-158, 833-837.

Marcuvitz, N.
   1951   Waveguide handbook. MIT Radiation Laboratory Series, Vol. 10,
          McGraw-Hill Book Company, Inc., New York.

Maryott, Arthur A., and Edgar R. Smith
   1951   Table of dielectric constants of pure liquids. U. S. National
          Bureau of Standards Circ. 514.

Mattern, Paul J.
   1965   Sedimentation test modification study, final report, Great
          Plains wheat project EU-R-44. Unpublished report, Dept. of
          Agronomy, University of Nebraska, Lincoln, Nebr.

Nelson, S. O.
   1952   A method for determining the dielectric properties of grain.
          Unpublished M.S. thesis, University of Nebraska Library, Lin-
          coln, Nebr.

Nelson, S. O.
   1965   Dielectric properties of grain and seed in the 1 to 50 MC range.
          Trans. ASAE 8: 38-48.

Nelson, S. O.
   1966   Electromagnetic and sonic energy for insect control. Trans.
          ASAE 9: 398-403, 405.

Nelson, S. O., and B. H. Kantack
   1966   Stored-grain insect control studies with radio-frequency energy.
          J. Econ. Entomol. 59: 588-594.

Nelson, S. O., and J. L. Seubert
   1966   Electromagnetic and sonic energy for pest control. Scientific
          aspects of pest control. Natl. Acad. Sci.-Natl. Res. Council
          Publication No. 1402: 135-166.

Nelson, S. O., L. H. Soderholm, and F. D. Yung
   1953   Determining the dielectric properties of grain. Agr. Eng. 34:
          608-610.

Nelson, S. O., L. E. Stetson, and J. J. Rhine
   1966   Factors influencing effectiveness of radio-frequency electric
          fields for stored-grain insect control. Trans. ASAE 9: 809-815.

Nelson, S. O., and W. K. Whitney
   1960   Radio-frequency electric fields for stored grain insect control.
          Trans. ASAE 3: 133-137, 144.

Nelson, Stuart O.
    1967   Electromagnetic energy. Ch. 3, pp. 89-145. *In* Pest control--
            biological, physical, and selected chemical methods, Wendell W.
            Kilgore and Richard L. Doutt, eds. Academic Press, New York.

Peters, Wendell R., and Katz, Robert
    1962   Using a density gradient column to determine wheat density.
            Cereal Chem. 39: 487-494.

Purcell, E. M.
    1948   Measurements of standing waves. Ch. 8. *In* Techniques of micro-
            wave measurements, Carol G. Montgomery, ed., Vol. 11, MIT Radia-
            tion Laboratory Series. McGraw-Hill Book Company, Inc., New
            York.

Rai, Patte Shivarama
    1970   An investigation of the morphological and reproductive changes
            induced by exposure of the yellow mealworm, *Tenebrio molitor* L.,
            to radiofrequency energy. Unpublished Ph.D. thesis, University
            of Nebraska Library, Lincoln, Nebr.

Rai, P. S., H. J. Ball, S. O. Nelson, and L. E. Stetson
    1971   Morphological changes in adult *Tenebrio molitor* (Coleoptera:
            Tenebrionidae) resulting from radiofrequency or heat treatment
            of larvae or pupae. Ann. Entomol. Soc. Amer. 64: 1116-1121.

Redheffer, R. M.
    1948   The measurement of dielectric constants. Ch. 10. *In* Techniques
            of microwave measurements, Carol G. Montgomery, ed., Vol. 11,
            MIT Radiation Laboratory Series. McGraw-Hill Book Company,
            Inc., New York.

Roberts, S., and A. von Hippel
    1946   A new method for measuring dielectric constant and loss in the
            range of centimeter waves. J. Appl. Phys. 17: 610-616.

Rohde & Schwarz
    1962   Die kurzinformation. 3+4, Rohde & Schwarz, München, Western
            Germany.

Schwan, Herman P.
    1963   Determination of biological impedances. Ch. 6, pp. 323-407. *In*
            Physical techniques in biological research, Vol. 6, W. L. Nas-
            tuk, ed. Academic Press, Inc., New York.

Schwan, Herman P.
    1957   Electrical properties of tissue and cell suspensions. Pp. 147-
            209. *In* Advances in biological and medical physics, Vol. V,
            John H. Lawrence and Cornelius A. Tobias, eds. Academic Press,
            Inc., New York.

Schwan, H. P.
    1966   Alternating current electrode polarization.   Biophysik 3: 181-
            201.

Schwan, H. P.
    1959   Alternating current spectroscopy of biological substances.
            Proc. IRE 47: 1841-1855.

Shackelford, R. G.
    1970   Studies to determine the electromagnetic spectrum effect on
            arthropods. Georgia Inst. Tech. Eng. Exp. Sta. Final report,
            project A-985.

Smith, Ernest K., Jr., and Stanley Weintraub
    1953   The constants in the equation for atmospheric refractive index
            at radio frequencies. Proc. IRE 41: 1035-1037.

Stetson, L. E., and S. O. Nelson
    1970   A method for determining dielectric properties of grain and seed
            in the 200- to 500-MHz range. Trans. ASAE 13: 491-495.

Taylor, Leonard S.
    1965   Dielectric properties of mixtures. IEEE Trans. on Antennas and
            Propagation AP-13: 943-947.

Taylor, Leonard S.
    1966   Dielectrics loaded with anisotropic materials. IEEE Trans. on
            Antennas and Propagation AP-14: 669-670.

Thomas, A. Morris
    1952   Pest control by high-frequency electric fields--critical resume.
            British Electric and Allied Industries Research Assn. Tech. Rpt.
            W/T23 (Leatherhead, Surrey, England).

Thompson, R. A., and G. W. Isaacs
    1967   Porosity determinations of grains and seeds with an air-
            comparison pycnometer. Trans. ASAE 10: 693-696.

U. S. Department of Agriculture
    1953   The test weight per bushel of grain: methods of use and cali-
            bration of the apparatus. Grain Branch, Production and Market-
            ing Adm. Circ. No. 921.

U. S. Department of Agriculture
    1959   Methods for determining moisture content as specified in the
            official grain standards of the United States and in the United
            States standards for beans, peas, lentils and rice. U. S. D. A.,
            Agricultural Marketing Service, Service and Regulatory Announce-
            ments No. 147, Revised.

U. S. Department of Agriculture
    1970   Official grain standards of the United States, revised. Con-
           sumer and Marketing Service, Grain Division, U. S. D. A., Wash-
           ington, D.C.

Vaughan, Worth E.
    1969   Experimental methods. Ch. 2, pp. 108-190. *In* Dielectric prop-
           erties and molecular behaviour, Nora E. Hill, Worth E. Vaughan,
           A. H. Price, and Mansel Davies. Van Nostrand Reinhold Company,
           New York.

von Hippel, A.
    1954a Dielectrics and waves. John Wiley and Sons, Inc., New York.

von Hippel, Arthur R., editor
    1954b Dielectric materials and applications. John Wiley and Sons,
           Inc., New York.

Wangsgard, A. P., and T. Hazen
    1946   The Q-Meter for dielectric measurements on polyethylene and
           other plastics at frequencies up to 50 megacycles. Trans. Elec-
           trochem. Soc. 90: 361-375.

Westphal, William B.
    1954   Dielectric measuring techniques, A. Permittivity, 2. Distri-
           buted circuits. Ch. II, pp. 63-122. *In* Dielectric materials
           and applications, Arthur R. von Hippel, ed. John Wiley and
           Sons, Inc., New York.

Whitney, W. K., S. O. Nelson, and H. H. Walkden
    1961   Effects of high-frequency electric fields on certain species of
           stored-grain insects. U. S. D. A., Market Quality Research Div.,
           Agricultural Marketing Service, Marketing Research Report No.
           455.

Wilson, I. G., C. W. Schramm, and J. P. Kinzer
    1946   High Q resonant cavities for microwave testing. The Bell System
           Tech. J. 25: 408-413.

VIII. ACKNOWLEDGMENTS

Massachusetts Institute of Technology.

Appreciation is expressed to the Entomology Department, University of Nebraska, for making available facilities for rearing the insect cultures and to the University of Nebraska, where the research was conducted, for peripheral support of the work.

The author is grateful to Iowa State University for the opportunity to study there and for the granting of permission to complete the research off campus.

Gratitude is particularly expressed to the Agricultural Research Service, U. S. Department of Agriculture, for the opportunity offered and support provided while pursuing these studies. The encouragement of Drs. T. E. Hienton and L. B. Altman in initiating the program is gratefully acknowledged.

Finally, sincere appreciation is expressed to Mrs. R. W. Hadfield for particular attention to detail and patience in use of special symbols and type in typing the dissertation.

IX. APPENDIX A:
SHORT-CIRCUITED WAVEGUIDE METHOD
FOR DETERMINING DIELECTRIC PROPERTIES

A. General Description

Using a slotted-line or slotted-waveguide section, it is possible to

obtain information from which dielectric properties may be calculated.

One method originally reported by Roberts and von Hippel (1946), expanded

upon by Dakin and Works (1947), and refined by Westphal (1954) has been

used successfully for a wide variety of dielectric measurements (von

Hippel, 1954b). It employs a short-circuited line or waveguide with the

dielectric sample filling the line for a given length, d, at the shorted

end (Fig. 9-1). The dielectric properties can be determined from slotted-

line measurements of the voltage minimum location and voltage standing-
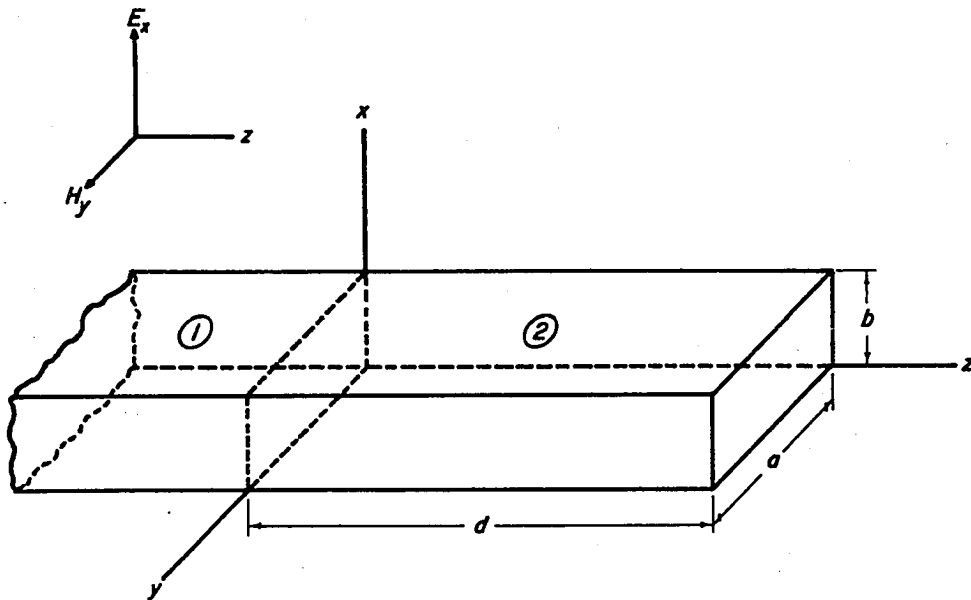
Fig. 9-1. Short-circuited rectangular waveguide with dielectric
sample of length d at the shorted end

wave ratio (VSWR) with the waveguide or line empty and then noting the shift of the minimum and the change in the VSWR when the sample is placed in the line. Since the theory for a coaxial transmission line turns out to be a special case of the waveguide situation, the development of the underlying theory for the method begins here with the more general case of the waveguide.

B. Theoretical Development

A wave propagating in a waveguide in the $+z$ direction is reflected either totally or in part upon striking the surface of a different medium unless there is a perfect impedance match (Fig. 9-1). The incident and reflected waves combine to form standing waves whose phasor field components are independent of time, but vary with position along the z-axis. The transverse electric and magnetic field components of the standing wave may be represented in terms of components of incident and reflected traveling waves. For standing waves in medium 1, the air space,

$$E_{x1}(z) = E_{x1i} \, e^{-\gamma_1 z} + E_{x1r} \, e^{\gamma_1 z} \qquad [9\text{-}1a]$$

$$H_{y1}(z) = H_{y1i} \, e^{-\gamma_1 z} + H_{y1r} \, e^{\gamma_1 z} = \frac{E_{x1i}}{Z_1} \, e^{-\gamma_1 z} + \frac{E_{x1r}}{Z_1} \, e^{\gamma_1 z} \qquad [9\text{-}1b]$$

where γ_1 is the complex propagation constant for medium 1, and where Z_1 is the characteristic wave impedance of medium 1.

Considering the complex reflection coefficient Γ, which has the same magnitude but opposite signs for E and H, Eqs. 9-1a and 9-1b may be written

$$E_{x1}(z) = E_{x1i}(e^{-\gamma_1 z} + \Gamma e^{\gamma_1 z}) \qquad [9\text{-}2a]$$

$$H_{y1}(z) = \frac{E_{x1i}}{Z_1}(e^{-\gamma_1 z} - \Gamma e^{\gamma_1 z}) \qquad [9\text{-}2b]$$

At the air-dielectric boundary, $z = 0$, the wave impedance

$$Z(0) = \frac{E(0)}{H(0)} = Z_1\frac{1 + \Gamma_{12}(0)}{1 - \Gamma_{12}(0)}$$. The reflection coefficient may be expressed

as $\Gamma(z) = \Gamma(0)e^{-2\gamma z}$, but for the mathematical manipulations which follow,

it is convenient to express the reflection coefficient at the air-

dielectric boundary as $\Gamma_{12}(0) = e^{-2u}$, where $u = \rho + j\psi$. Here ρ is related

to the magnitude of the reflection coefficient and 2ψ is its phase angle.

Then

$$Z(0) = Z_1\frac{1 + e^{-2u}}{1 - e^{-2u}} = Z_1 \coth u \qquad [9\text{-}3]$$

An expression for the VSWR may be obtained by examining Eq. 9-2a.

The complex propagation constant, $\gamma = \alpha + j\beta$, has a real component, α,

called the attenuation constant, and an imaginary component, β, the phase

constant. Since attenuation in air is negligibly small, γ is purely imag-

inary in medium 1. Therefore, $e^{-\gamma_1 z}$ and $e^{\gamma_1 z}$ have absolute values of

unity, and the ratio of the maximum value of E_{x1} to the minimum value will

be $\frac{E_{max}}{E_{min}} = \frac{1 + |\Gamma_{12}|}{1 - |\Gamma_{12}|}$. Since $\Gamma_{12} = e^{-2u} = e^{-2\rho} e^{-j2\psi}$, $|\Gamma_{12}| = e^{-2\rho}$, and

$$\frac{E_{max}}{E_{min}} = \frac{1 + e^{-2\rho}}{1 - e^{-2\rho}} = \coth \rho,$$ the inverse VSWR will be

$$\frac{E_{min}}{E_{max}} = \tanh \rho \qquad [9\text{-}4]$$

The first standing-wave voltage minimum at a distance z_o in front of the dielectric (medium 2) surface (Fig. 9-2) will occur where the incident
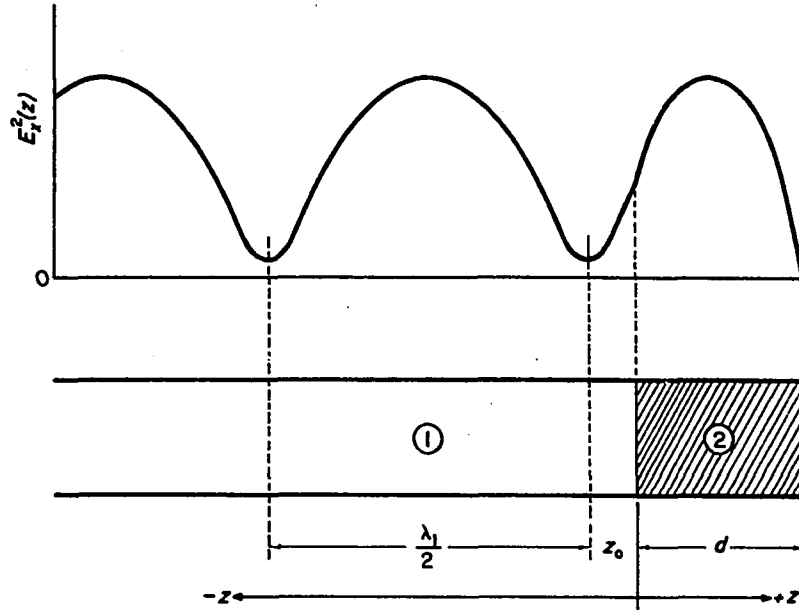
Fig. 9-2. Relationship of voltage standing-wave pattern to shorted waveguide with dielectric sample

and reflected traveling E waves are π radians out of phase. Since the reflection coefficient has a phase angle of -2ψ, the required phase relationship between the incident and reflected waves for a voltage minimum will be $-\beta_1 z_o = (2\psi + \beta_1 z_o) \pm \pi$. A more detailed explanation of this phase relationship is given by von Hippel (1954a, 1954b). Simplifying this expression and noting that the phase constant, $\beta_1 = \frac{2\pi}{\lambda_1}$, the following equation results:

$$\psi = \pm \frac{\pi}{2} - \frac{2\pi z_o}{\lambda_1}$$

[9-5]

Expanding Eq. 9-3,

$$Z(0) = Z_1 \coth(\rho + j\psi) = Z_1 \frac{\cosh(\rho + j\psi)}{\sinh(\rho + j\psi)} = Z_1 \frac{\cosh \rho \cos \psi + j \sinh \rho \sin \psi}{\sinh \rho \cos \psi + j \cosh \rho \sin \psi}.$$

Upon dividing through the numerator and denominator of the second term on the right-hand side by $\sinh \rho \cos \psi$, and multiplying both by $-j \tanh \rho \cot \psi$,

$$Z(0) = Z_1 \frac{\tanh \rho - j \cot \psi}{1 - j \tanh \rho \cot \psi} \qquad [9-6]$$

Since $\cot (\frac{\pi}{2} \pm \theta) = \mp \tan \theta$, it follows from Eq. 9-5 that $\cot \psi = \tan \frac{2\pi z_0}{\lambda_1}$.

Substituting this and Eq. 9-4 into Eq. 9-6 yields an expression for $Z(0)$ in terms of Z_1 and measurable quantities:

$$Z(0) = Z_1 \frac{\dfrac{E_{min}}{E_{max}} - j \tan \dfrac{2\pi z_0}{\lambda_1}}{1 - j \dfrac{E_{min}}{E_{max}} \tan \dfrac{2\pi z_0}{\lambda_1}} \qquad [9-7]$$

For the transverse components of standing waves in medium 2, one may write

$$E_{x2}(z) = E_{x2i}(e^{-\gamma_2 z} + \Gamma_{2s} e^{\gamma_2 z}) \qquad [9-8a]$$

$$H_{y2}(z) = \frac{E_{x2i}}{Z_2}(e^{-\gamma_2 z} - \Gamma_{2s} e^{\gamma_2 z}) \qquad [9-8b]$$

Since the waveguide is terminated in a short-circuit at $z = d$, however, the electric field must vanish there. $E_{x2}(d) = 0 = E_{x2i} e^{-\gamma_2 d} + E_{x2r} e^{\gamma_2 d}$. $\frac{E_{x2r}}{E_{x2i}} = \Gamma_{2s} = -\frac{e^{-\gamma_2 d}}{e^{\gamma_2 d}} = -e^{-2\gamma_2 d}$. Substituting this expression for Γ_{2s} into Eqs. 9-8a and 9-8b gives an expression for $Z(z)$ in terms of the propagation constant in the dielectric (medium 2),

$$Z(z) = \frac{E_{x2}(z)}{H_{y2}(z)} = Z_2 \frac{e^{-\gamma_2 z} - e^{-2\gamma_2 d} e^{\gamma_2 z}}{e^{-\gamma_2 z} + e^{-2\gamma_2 d} e^{\gamma_2 z}} \cdot \quad \text{Thus,}$$

$$Z(0) = Z_2 \frac{1 - e^{-2\gamma_2 d}}{1 + e^{-2\gamma_2 d}} = Z_2 \tanh \gamma_2 d \qquad [9\text{-}9]$$

The characteristic wave impedances for TEM or TE waves in the two media are $Z_1 = \dfrac{j\omega\mu_1}{\gamma_1}$ and $Z_2 = \dfrac{j\omega\mu_2}{\gamma_2}$, where μ is the magnetic permeability.

Thus, $\dfrac{Z_1 \gamma_1}{\mu_1} = \dfrac{Z_2 \gamma_2}{\mu_2}$. Equating Eqs. 9-7 and 9-9, substituting $\dfrac{\gamma_2 \mu_1}{\gamma_1 \mu_2}$ for $\dfrac{Z_1}{Z_2}$,

and dividing through by d yields $\dfrac{\tanh \gamma_2 d}{\gamma_2 d} = \dfrac{\mu_1}{\mu_2 \, \gamma_1 d} \dfrac{\dfrac{E_{min}}{E_{max}} - j \tan \dfrac{2\pi z_o}{\lambda_1}}{1 - j \dfrac{E_{min}}{E_{max}} \tan \dfrac{2\pi z_o}{\lambda_1}}$.

Since the attenuation in medium 1, the air space, is negligibly small, $\gamma_1 = j\beta_1 = j \dfrac{2\pi}{\lambda_1}$, and, since the permeability of air and the dielectric materials to be considered are both μ_o, the permeability of free space, this expression simplifies to

$$\frac{\tanh \gamma_2 d}{\gamma_2 d} = - \frac{j\lambda_1}{2\pi d} \frac{\dfrac{E_{min}}{E_{max}} - j \tan \dfrac{2\pi z_o}{\lambda_1}}{1 - j \dfrac{E_{min}}{E_{max}} \tan \dfrac{2\pi z_o}{\lambda_1}} \qquad [9\text{-}10]$$

Values for all terms on the right-hand side of the equation may be obtained by measurement and the whole term calculated as $Ce^{j\zeta}$. Letting $\gamma_2 d$ be represented by $Te^{j\tau}$, the complex transcendental equation, $\dfrac{\tanh Te^{j\tau}}{Te^{j\tau}} = Ce^{j\zeta}$, may be solved for $Te^{j\tau}$ by reference to charts of the function

(Westphal, 1954.) or, in special cases, by a series approximation (Roberts and von Hippel, 1946). A computer program, which will be described later, has been developed to provide solutions for $\gamma_2 d$.

Since, for nonmagnetic dielectrics,

$$\gamma' = j \, \omega \, \sqrt{\varepsilon \, \mu_o} \qquad [9\text{-}11]$$

where γ' is the intrinsic propagation constant (unbounded medium), this relationship provides a means for obtaining ε_2 from γ_2, the characteristic propagation constant of medium 2, if γ_2 can be expressed in terms of γ_2', the intrinsic propagation constant of medium 2,

$$\varepsilon_2 = -\frac{\gamma_2'^2}{\omega^2 \, \mu_o} \qquad [9\text{-}12]$$

The required expression may be derived from the fundamental relationship resulting from the requirement that Maxwell's equations be satisfied for z-directed wave propagation in a waveguide:

$$k_c^2 = \gamma^2 + \omega^2 \, \varepsilon \, \mu_o \qquad [9\text{-}13]$$

where k_c^2 is the coefficient of the electric field phasor in the Helmholz equation, $\nabla^2 E + k_c^2 E = 0$. (In the rectangular-waveguide case, $k_c^2 = \left[\frac{m\pi}{a}\right]^2 + \left[\frac{n\pi}{b}\right]^2$, where a and b are waveguide dimensions and m and n are the mode integers.) It can also be shown that $k_c = \frac{2\pi}{\lambda_c}$, where λ_c is the cutoff wavelength of the waveguide. The guide propagation constant,

$\gamma = \alpha + j\beta = \sqrt{k_c^2 - \omega^2 \, \varepsilon \, \mu_o}$, is either real or imaginary, depending upon the value of the angular frequency, ω. If it is real, the wave will be attenuated, but, if it is imaginary, the wave will propagate in the guide.

The cutoff frequency is, therefore, $f_c = \dfrac{k_c}{2\pi \sqrt{\varepsilon\,\mu_o}}$, for, at this frequency, the radicand in the expression for γ vanishes. Since the velocity of propagation is $v = \dfrac{1}{\sqrt{\varepsilon\,\mu_o}}$, and $\lambda f = v$, it follows that $k_c = \dfrac{2\pi}{\lambda_c}$. Eq. 9-13 may, therefore, be written $\gamma^2 = \left(\dfrac{2\pi}{\lambda_c}\right)^2 - \omega^2\,\varepsilon\,\mu_o$, or, using Eq. 9-11,

$\gamma^2 = \left(\dfrac{2\pi}{\lambda_c}\right)^2 + \gamma'^2$. We may then write for media 1 and 2[1]

$$\gamma_1{}^2 = \left(\frac{2\pi}{\lambda_c}\right)^2 - \omega^2\,\varepsilon_o\,\mu_o \qquad\qquad [9\text{-}14a]$$

and

$$\gamma_2{}^2 = \left(\frac{2\pi}{\lambda_c}\right)^2 + \gamma_2'^2 \qquad\qquad [9\text{-}14b]$$

Substituting $\gamma_2'^2$ and $\omega^2\,\mu_o$ from Eqs. 9-14a and 9-14b into Eq. 9-12,

$\varepsilon_2 = \varepsilon_o \dfrac{\left(\dfrac{2\pi}{\lambda_c}\right)^2 - \gamma_2{}^2}{\left(\dfrac{2\pi}{\lambda_c}\right)^2 - \gamma_1{}^2}$, and, since medium 1 is lossless, $\gamma_1 = j\beta = j\,\dfrac{2\pi}{\lambda_1}$, and

$\varepsilon_2 = \varepsilon_o \dfrac{\left(\dfrac{1}{\lambda_c}\right)^2 - \left(\dfrac{\gamma_2}{2\pi}\right)^2}{\left(\dfrac{1}{\lambda_c}\right)^2 + \left(\dfrac{1}{\lambda_1}\right)^2}$. The relative permittivity and loss factor,

$\varepsilon_r' = \dfrac{\varepsilon'}{\varepsilon_o}$ and $\varepsilon_r'' = \dfrac{\varepsilon''}{\varepsilon_o}$, may then be calculated from

$$\frac{\varepsilon_2}{\varepsilon_o} = \varepsilon_r' - j\,\varepsilon_r'' = \frac{\left(\dfrac{\lambda_1}{\lambda_c}\right)^2 - \left(\dfrac{\gamma_2\,\lambda_1}{2\pi}\right)^2}{1 + \left(\dfrac{\lambda_1}{\lambda_c}\right)^2} = \frac{\left(\dfrac{\lambda_1}{\lambda_c}\right)^2 - \left(\dfrac{\gamma_2 d\,\lambda_1}{2\pi d}\right)^2}{1 + \left(\dfrac{\lambda_1}{\lambda_c}\right)^2} \qquad [9\text{-}15]$$

---

[1] See von Hippel (1954a), Ch. I, p. 77, noting difference in prime notation.

Noting that the relationship between guide wavelength λ_1 and free space wavelength λ_o is

$$\lambda_1 = \frac{\lambda_o}{\sqrt{1 - \left(\frac{\lambda_o}{\lambda_c}\right)^2}} \qquad [9\text{-}16]$$

Eq. 9-15 becomes

$$\epsilon_r' - j\,\epsilon_r'' = \left[\frac{\lambda_o}{\lambda_c}\right]^2 - \left[\frac{\gamma_2 d\,\lambda_o}{2\pi d}\right]^2 \qquad [9\text{-}17]$$

The loss tangent and conductivity are then easily obtained as $\tan\delta = \dfrac{\epsilon_r''}{\epsilon_r'}$ and $\sigma = \omega\,\epsilon_o\,\epsilon_r''$ (Eqs. 1-6 and 1-8).

For a coaxial line, $\lambda_c = \infty$, $\lambda_1 = \lambda_o$, and, since, in lossless media, $\lambda_1 = j\,\dfrac{2\pi}{\gamma_1}$, Eq. 9-15 reduces to

$$\epsilon_r' - j\,\epsilon_r'' = -\left[\frac{\gamma_2 d\,\lambda_1}{2\pi d}\right]^2 = -\left[\frac{\gamma_2\,\lambda_1}{2\pi}\right]^2 = -\left[\frac{\gamma_2\,\lambda_o}{2\pi}\right]^2 = \left[\frac{\gamma_2}{\gamma_1}\right]^2 \qquad [9\text{-}18]$$

Because solving Eq. 9-10 for $\gamma_2 d$ is a laborious process, Dakin and Works (1947) reported a simplification which is valid when $\tan\delta < 0.1$. Since these simplified relations are useful and are employed as preliminary steps in the computer program to be explained later, these equations are considered here. The simplified equations are obtained by expanding the left-hand side of Eq. 9-10, rationalizing both sides, and separating and equating the real and imaginary parts. Performing these operations on the right-hand side yields:

$$\frac{\tanh \gamma_2 d}{\gamma_2 d} = \frac{-\lambda_1 \tan \frac{2\pi z_0}{\lambda_1} \left(1 - \frac{E_{min}^2}{E_{max}^2}\right) - j\, \lambda_1 \frac{E_{min}}{E_{max}} \left(1 + \tan^2 \frac{2\pi z_0}{\lambda_1}\right)}{2\pi d \left(1 + \frac{E_{min}^2}{E_{max}^2} \tan^2 \frac{2\pi z_0}{\lambda_1}\right)} \qquad [9\text{-}19]$$

Considering the left-hand side,

$$\frac{\tanh \gamma_2 d}{\gamma_2 d} = \frac{\tanh (\alpha_2 d + j\beta_2 d)}{\alpha_2 d + j\beta_2 d} = \frac{(\sinh 2\alpha_2 d + j \sin 2\beta_2 d)\,(\alpha_2 d - j\beta_2 d)}{(\cosh 2\alpha_2 d + \cos 2\beta_2 d)\,(\alpha_2^2\, d^2 + \beta_2^2\, d^2)} =$$

$$\frac{\alpha_2 d \sinh 2\alpha_2 d + \beta_2 d \sin 2\beta_2 d + j\,(\alpha_2 d \sin 2\beta_2 d - \beta_2 d \sinh 2\alpha_2 d)}{(\cosh 2\alpha_2 d + \cos 2\beta_2 d)\,(\alpha_2^2\, d^2 + \beta_2^2\, d^2)} \qquad [9\text{-}20]$$

Using the double-angle trigonometric and hyperbolic trigonometric identi-

ties, this becomes $\dfrac{\alpha_2 d\ 2\sinh \alpha_2 d \cosh \alpha_2 d + \beta_2 d\ 2\sin \beta_2 d \cos \beta_2 d}{1 + 2\sinh^2 \alpha_2 d + 1 - 2\sin^2 \beta_2 d}\ +$

$\dfrac{j(\alpha_2 d\ 2\sin \beta_2 d \cos \beta_2 d - \beta_2 d\ 2\sinh \alpha_2 d \cosh \alpha_2 d)}{1 + 2\sinh^2 \alpha_2 d + 1 - 2\sin^2 \beta_2 d}$. Dividing through by

$2\cos^2 \beta_2 d \cosh^2 \alpha_2 d$, rearranging and combining terms, and noting that

$\sec^2 \beta_2 d = 1 + \tan^2 \beta_2 d$ and $\text{sech}^2 \alpha_2 d = 1 - \tanh^2 \alpha_2 d$, yields the equations

for real and imaginary parts presented by Dakin and Works (1947)[2/]:

$$\frac{\beta_2 d \tan \beta_2 d\ (1 - \tanh^2 \alpha_2 d) + \alpha_2 d\ (1 + \tan^2 \beta_2 d) \tanh \alpha_2 d}{(1 + \tanh^2 \alpha_2 d \tan^2 \beta_2 d)\,(\alpha_2^2\, d^2 + \beta_2^2\, d^2)} =$$

$$\frac{-\lambda_1 \tan \frac{2\pi z_0}{\lambda_1} \left(1 - \frac{E_{min}^2}{E_{max}^2}\right)}{2\pi d \left(1 + \frac{E_{min}^2}{E_{max}^2} \tan^2 \frac{2\pi z_0}{\lambda_1}\right)} \qquad [9\text{-}21]$$

[2/] In the published paper, the exponent was omitted from the $\tan^2 \beta_2 d$ term in the numerator of the real-parts equation.

$$\frac{\alpha_2 d \tan \beta_2 d - \alpha_2 d \tanh^2\alpha_2 d \tan \beta_2 d - \beta_2 d \tanh \alpha_2 d - \beta_2 d \tanh \alpha_2 d \tan^2\beta_2 d}{(1 + \tanh^2 \alpha_2 d \tan^2 \beta_2 d)(\alpha_2^2 d^2 + \beta_2^2 d^2)} =$$

$$\frac{-\lambda_1 \dfrac{E_{min}}{E_{max}} \left(1 + \tan^2 \dfrac{2\pi z_o}{\lambda_1} \right)}{2\pi d \left(1 + \dfrac{E_{min}^2}{E_{max}^2} \tan^2 \dfrac{2\pi z_o}{\lambda_1} \right)} \qquad [9\text{-}22]$$

In the case of a low-loss dielectric where α and $\dfrac{E_{min}}{E_{max}}$ are very small, using the approximation $\tanh \alpha_2 d \simeq \alpha_2 d$ and neglecting $(\alpha_2 d)^2$ and $\tanh^2 \alpha_2 d$ terms, Eqs. 9-21 and 9-22 reduce to:

$$\frac{\tan \beta_2 d}{\beta_2 d} = \frac{-\lambda_1 \tan \dfrac{2\pi z_o}{\lambda_1}}{2\pi d} \qquad [9\text{-}23]$$

$$\alpha_2 d = \frac{(\beta_2 d)^2 \lambda_1}{2\pi d} \frac{E_{min}}{E_{max}} \frac{\left(1 + \tan^2 \dfrac{2\pi z_o}{\lambda_1} \right)}{\beta_2 d (1 + \tan^2 \beta_2 d) - \tan \beta_2 d} \qquad [9\text{-}24]$$

Here $\beta_2 d$ may be obtained easily from tables of the function $\dfrac{\tan x}{x}$ after calculating the right-hand side of Eq. 9-23 from measurements data. The relative permittivity may be obtained from Eq. 9-15 or 9-17 by substituting $j\beta_2$ for γ_2 since the loss is negligible,

$$\varepsilon_r' = \frac{\left(\dfrac{\lambda_1}{\lambda_c} \right)^2 + \left(\dfrac{\beta_2 d \, \lambda_1}{2\pi d} \right)^2}{1 + \left(\dfrac{\lambda_1}{\lambda_c} \right)^2} = \frac{\dfrac{1}{\lambda_c^2} + \left(\dfrac{\beta_2 d}{2\pi d} \right)^2}{\dfrac{1}{\lambda_c^2} + \dfrac{1}{\lambda_1^2}} = \left(\dfrac{\lambda_o}{\lambda_c} \right)^2 + \left(\dfrac{\beta_2 d \, \lambda_o}{2\pi d} \right)^2 \qquad [9\text{-}25]$$

A useful expression for $\tan \delta$, the loss tangent or dissipation factor of the dielectric, may be obtained from Eq. 9-24. From Eq. 9-14b we may

write $(\alpha_2 + j\beta_2)^2 = \gamma_2^2 = \left(\dfrac{2\pi}{\lambda_c}\right)^2 + \gamma_2'^2 = \left(\dfrac{2\pi}{\lambda_c}\right)^2 + (j\omega\sqrt{\varepsilon_2\,\mu_o})^2 =$

$\left(\dfrac{2\pi}{\lambda_c}\right)^2 - \omega^2\,\mu_o\,\varepsilon_2' + j\omega^2\,\mu_o\,\varepsilon_2''$. Expanding the left-hand side and equating

imaginary parts yields the following expression for α_2: $\alpha_2 = \dfrac{\omega^2\,\mu_o\,\varepsilon_2''}{2\beta_2} =$

$\dfrac{\omega^2\,\mu_o\,\varepsilon_o\,\varepsilon_r''}{2\beta_2} = \dfrac{\omega^2\,\mu_o\,\varepsilon_o\,\varepsilon_r'\,\tan\delta}{2\beta_2}$. Substituting this expression for α_2

into Eq. 9-24 and making the substitution, $\dfrac{E_{min}}{E_{max}} = \dfrac{\pi\Delta z}{\lambda_1}$, which will be

justified later (Eq. 9-38),

$$\tan\delta = \frac{\beta_2^2\,\Delta z}{\omega^2\,\mu_o\,\varepsilon_o\,\varepsilon_r'\,d}\left[\frac{\beta_2 d\left(1 + \tan^2\dfrac{2\pi z_o}{\lambda_1}\right)}{\beta_2 d\,(1 + \tan^2\beta_2 d) - \tan\beta_2 d}\right].$$ Since $\omega = 2\pi f$,

$\dfrac{1}{\sqrt{\varepsilon_o\,\mu_o}} = c$, and $\dfrac{c}{f} = \lambda_o$, the coefficient of the bracketed term on the

right-hand side simplifies to $\dfrac{\beta_2^2\,\lambda_o^2}{(2\pi)^2\,\varepsilon_r'}\cdot\dfrac{\Delta z}{d}$. Substituting an expression

from Eq. 9-25 for β_2 and simplifying gives

$$\tan\delta = \frac{\Delta z}{d}\,\lambda_o^2\left(\frac{1}{\lambda_c^2} + \frac{1}{\lambda_1^2} - \frac{1}{\lambda_c^2\,\varepsilon_r'}\right)\left[\frac{\beta_2 d\left(1 + \tan^2\dfrac{2\pi z_o}{\lambda_1}\right)}{\beta_2 d\,(1 + \tan^2\beta_2 d) - \tan\beta_2 d}\right].$$

Using the relationship of Eq. 9-16, we may write

$$\lambda_o^2 = \lambda_1^2\left[1 - \left(\frac{\lambda_o}{\lambda_c}\right)^2\right] = \frac{\lambda_1^2\,\lambda_c^2 - \lambda_1^2\,\lambda_o^2}{\lambda_c^2}.$$ Solving for λ_o^2 gives

$$\lambda_o^2 = \frac{\lambda_1^2\,\lambda_c^2}{\lambda_1^2 + \lambda_c^2} = \frac{1}{\dfrac{1}{\lambda_c^2} + \dfrac{1}{\lambda_1^2}}.$$ Substituting this last expression for λ_o^2

gives the equation for $\tan\delta$ in the form originally presented by Dakin and

Works (1947),

$$\tan \delta = \frac{\Delta z}{d} \left[\frac{\left(\frac{1}{\lambda_c^2} + \frac{1}{\lambda_1^2} \right) - \frac{1}{\lambda_c^2 \, \varepsilon_r'}}{\frac{1}{\lambda_c^2} + \frac{1}{\lambda_1^2}} \right] \left[\frac{\beta_2 d \left(1 + \tan^2 \frac{2\pi z_o}{\lambda_1} \right)}{\beta_2 d \, (1 + \tan^2 \beta_2 d) - \tan \beta_2 d} \right] \qquad [9\text{-}26]$$

It was verified by numerical calculation that the approximations resulting in Eqs. 9-23, 9-25, and 9-26 result in errors in calculated values of ε_r' and $\tan \delta$ not greater than about $\pm$ 1 percent for dielectrics with loss tangents of 0.1 or less (Dakin and Works, 1947).

For coaxial lines, Eqs. 9-25 and 9-26 reduce to

$$\varepsilon_r' = \left(\frac{\beta_2 d \, \lambda_1}{2\pi d} \right)^2 = \left(\frac{\beta_2 \, \lambda_1}{2\pi} \right)^2 = \left(\frac{\beta_2}{\beta_1} \right)^2 \qquad [9\text{-}27]$$

and

$$\tan \delta = \frac{\Delta z}{d} \left[\frac{\beta_2 d \left(1 + \tan^2 \frac{2\pi z_o}{\lambda_1} \right)}{\beta_2 d \, (1 + \tan^2 \beta_2 d) - \tan \beta_2 d} \right] = \frac{\Delta z}{d} \left[\frac{1 + \tan^2 \frac{2\pi z_o}{\lambda_1}}{1 + \tan^2 \beta_2 d - \frac{\tan \beta_2 d}{\beta_2 d}} \right]$$

$$[9\text{-}28]$$

In practice, the empty shorted-line or waveguide section is not truly lossless. The value of $\tan \delta$ calculated from Eq. 9-26 for a dielectric sample, therefore, includes not only losses of the dielectric, but also losses in the waveguide walls or line conductors. Following Dakin and Works (1947), this calculated value of $\tan \delta$ may be corrected by sub-tracting a loss tangent term for the empty waveguide which results because of wall losses.

Considering Eq. 9-26, ε_r' will be unity for the empty waveguide, β_2 will be $\beta_1 = \frac{2\pi}{\lambda_1}$, z_o will be zero, and d will be the distance from the

measured voltage minimum to the short-circuit termination. Since d will, therefore, be an integral number of half-wavelengths in the guide, $\beta_2 d$ will be an integral multiple of π, so $\tan \beta_2 d = 0$. Thus, Eq. 9-26 for the empty waveguide reduces to

$$\tan \delta_w = \frac{\Delta z}{d} \frac{1}{1 + \left(\frac{\lambda_1}{\lambda_c}\right)^2} = \frac{\Delta z}{d} \left[1 - \left(\frac{\lambda_o}{\lambda_c}\right)^2\right] \qquad [9\text{-}29]$$

Since the low-loss characteristics of the empty waveguide meet the restrictions imposed for validity of Eqs. 9-25 and 9-26, Eq. 9-29 can be used for correcting loss tangents resulting from Eq. 9-15, where $\varepsilon_r' - j\,\varepsilon_r'' = \varepsilon_r'\,(1 - j\,\tan \delta)$.

C. Measurement and Calculation Considerations

Next, consider the quasi-mechanical means for obtaining the necessary measurements from which to calculate ε_r', ε_r'', and $\tan \delta$. For grain and insect samples, the dielectric may be too lossy to permit the use of Eqs. 9-25 and 9-26. The more general situation must be employed whereby the proper value for $\gamma_2 d$ is extracted from Eq. 9-10 and the dielectric properties from Eq. 9-15. Examination of Eq. 9-10 reveals the need for numerical values of λ_1, d, z_o, and $\frac{E_{min}}{E_{max}}$, the inverse voltage standing-wave ratio. The sample length, d, is obtained by direct physical measurement.

The guide wavelength is best calculated as $\lambda_1 = \dfrac{\lambda_o}{\sqrt{1 - \left(\dfrac{f_c}{f}\right)^2}}$ from the

known frequency of the source if it can be measured accurately enough. It

can also be measured directly with the slotted section and corrected, if necessary, for the influence of the slot on the propagation constant in accordance with the following relation (Purcell, 1948; Marcuvitz, 1951)[3/] between measured guide wavelength λ_{gm} and true guide wavelength λ_g in a nonslotted section of the same waveguide.

$$\lambda_{gm} = \lambda_g \left(1 + \frac{w^2 \lambda_g^2}{8\pi \, b \, a^3} \right)$$ [9-30]

where w is the width of the slot, a is the inside width of the guide, and b is the inside height ($b < a$).

This same relationship has also been derived by Bussey (personal communication. National Bureau of Standards, U. S. Department of Commerce. Boulder, Colo. 1971) employing the Boltzman-Ehrenfest (energy) principle for a wave propagating in the TE_{10} mode in rectangular waveguide. He has also derived the corresponding relationship which takes into account the slot in a cylindrical waveguide for the TE_{11} mode:

$$\lambda_{gm} = \lambda_g \left[1 + \frac{(w \, \lambda_g \, \tau)^2}{8(a\pi)^4 \, (\tau^2 - 1)} \right]$$ [9-31]

a is the radius here only.

where τ is the first root providing a zero value for the first derivative of the first-order Bessel function of the first kind and has the value 1.84118 (Wilson et al., 1946).

In the theoretical development, z_0 was defined as the distance between the surface of the dielectric sample and the first voltage minimum

---

[3/]For a derivation, see Marcuvitz (1951), Sec. 8-5, p. 397, First Edition.

outside the dielectric (Fig. 9-3). By inspection of Fig. 9-3 we may write

$n_a \dfrac{\lambda_1}{2} = z_a - z_s + n_s \dfrac{\lambda_1}{2} + z_0 + d$, where z_a is the location of the measured

voltage node with respect to $z = 0$ at the short circuit for the air-filled

guide, z_s is the z-value for the voltage node when the sample is inserted,

and n_a and n_s are integers. We then have
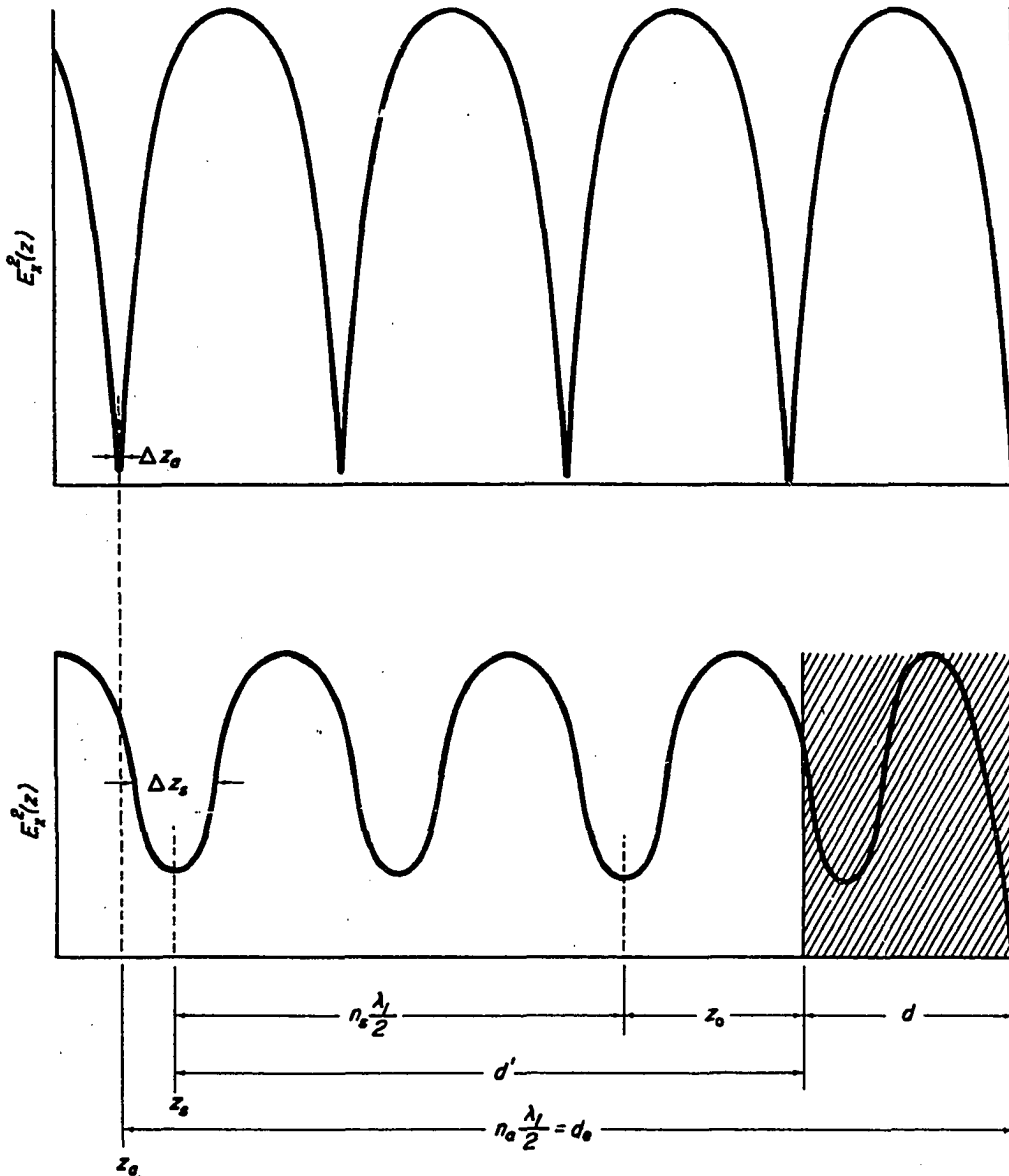
Fig. 9-3. Voltage standing-wave pattern relationships in empty wave-
guide and in waveguide with dielectric sample in place

$$z_o = (n_a - n_s) \frac{\lambda_1}{2} - [d + (z_a - z_s)] \qquad [9\text{-}32]$$

The fact that n_a and n_s may not be known exactly is of no consequence, because $n_a - n_s = n'$ is an integer, and n' will be the smallest integer value which provides a positive value for z_o as long as z_s is always measured as the first node encountered in moving toward the sample from z_a.

The final quantity to be measured is then $\frac{E_{min}}{E_{max}}$. The voltage standing-wave ratio $\frac{E_{max}}{E_{min}}$ is very high for the empty guide, and it will also be large even for samples with substantial loss. Therefore, it cannot be determined accurately by the usual direct measurement of E_{min} and E_{max}, because the square-law response of the crystal detector or bolometer will not span the necessary range. The ratio may be obtained indirectly by measurement in the vicinity of the minimum, where the perturbation of fields by the probe is less troublesome anyway, using the method reported by Roberts and von Hippel (1946), which is now in common use. The customary approximation is $\frac{E_{max}}{E_{min}} = \frac{\lambda_1}{\pi \Delta z}$, where Δz is the width of the voltage node (distance between points of twice-minimum value observed on each side of the minimum) 3 dB above the minimum (frequently referred to as the twice-minimum-power method). This relation gives values within 1 percent when $\left(\frac{E_{max}}{E_{min}}\right) > 133$ (Redheffer, 1948). Since this approximation may not be valid for high-loss dielectric samples, the exact expression, to be derived in the following paragraph following a procedure outlined by Giordano (1963), must be employed.

Eq. 9-2a expresses the electric field intensity of the standing wave as a function of z, the propagation constant, the reflection coefficient,

and the electric field phasor for the incident traveling wave. For an

air-filled line or waveguide, the attenuation constant is essentially

zero, and we may write $E_x(z) = E_{xi}(e^{-j\beta z} + \Gamma e^{j\beta z})$. Since Γ is the complex

reflection coefficient, $\Gamma = |\Gamma| e^{-j2\psi}$, $E_x(z) = E_{xi}\left[e^{-j\beta z} + |\Gamma| e^{j(\beta z - 2\psi)}\right]$.

Multiplying by the conjugate to obtain the square of the absolute value

of $E_x(z)$ we have $E_x(z)E_x^*(z) = |E_x(z)|^2 =$

$$|E_{xi}|^2 \left[1 + |\Gamma| [e^{-j2(\beta z - \psi)} + e^{j2(\beta z - \psi)}] + |\Gamma|^2\right], \text{ so}$$

$$|E_x(z)|^2 = |E_{xi}|^2 [1 + 2|\Gamma| \cos 2(\beta z - \psi) + |\Gamma|^2] \qquad [9\text{-}33]$$

The magnitude of $E_x(z)$ will be minimum ($z = z_n$, Fig. 9-4) when

$\cos 2(\beta z - \psi) = -1$. Then

$$|E_x(z_n)|^2 = |E_{xi}|^2 (1 - |\Gamma|)^2 \qquad [9\text{-}34]$$
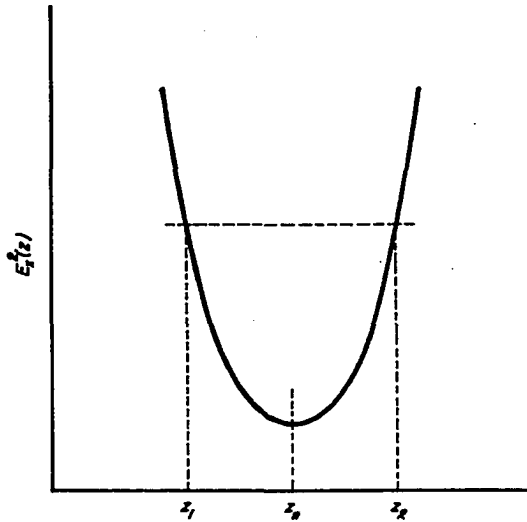
Fig. 9-4. Region of voltage standing-wave minimum

For this condition $2(\beta z_n - \psi) = (2m - 1)\pi$, where z_n denotes the node posi-

tion and m is an integer to provide an odd multiple of π. Thus,

$\psi = \beta z_n - (2m - 1)\pi/2$. At some point z_2 above the minimum, $|E_x(z_2)|^2 =$

$|E_{xi}|^2 [1 + 2|\Gamma| \cos 2(\beta z_2 - \psi) + |\Gamma|^2]$. Since $\beta z_2 - \psi =$

$\beta z_2 - (\beta z_n - \frac{2m - 1}{2} \pi) = \beta(z_2 - z_n) + \frac{2m - 1}{2} \pi$, and, since $z_2 - z_n = \frac{\Delta z}{2}$,

$2(\beta z_2 - \psi)$ becomes $\beta \Delta z + (2m - 1)\pi$ and

$$|E_x(z_2)|^2 = |E_{xi}|^2 [1 - 2|\Gamma| \cos (\beta \Delta z) + |\Gamma|^2] \qquad [9\text{-}35]$$

Taking the ratio of Eq. 9-35 to Eq. 9-34, we have

$\left(\frac{E(z)}{E_{min}}\right)^2 = \frac{|E_x(z_2)|^2}{|E_x(z_n)|^2} = \frac{1 - 2|\Gamma| \cos (\beta \Delta z) + |\Gamma|^2}{(1 - |\Gamma|^2)}$. Substituting the rela-

tionship $|\Gamma| = \frac{VSWR - 1}{VSWR + 1}$ yields

$\left(\frac{E(z)}{E_{min}}\right)^2 = \frac{(VSWR)^2 (1 - \cos \beta \Delta z) + (1 + \cos \beta \Delta z)}{2}$. Substituting $\beta = \frac{2\pi}{\lambda_g}$ and

noting that $1 - \cos \frac{2\pi \Delta z}{\lambda_g} = 2 \sin^2 \frac{\pi \Delta z}{\lambda_g}$ and $1 + \cos \frac{2\pi \Delta z}{\lambda_g} = 2 \cos^2 \frac{\pi \Delta z}{\lambda_g}$ yields

$$VSWR = \frac{\sqrt{\left(\frac{E(z)}{E_{min}}\right)^2 - \cos^2 \frac{\pi \Delta z}{\lambda_g}}}{\sin \frac{\pi \Delta z}{\lambda_g}} \qquad [9\text{-}36]$$

If the twice-minimum-power points are selected for the measurement of z_1

and z_2, $\left(\frac{E(z)}{E_{min}}\right)^2 = 2$, and Eq. 9-36 simplifies to

$$\frac{E_{max}}{E_{min}} = VSWR = \frac{\sqrt{2 - \cos^2 \frac{\pi \Delta z}{\lambda_g}}}{\sin \frac{\pi \Delta z}{\lambda_g}} = \frac{\sqrt{1 + \sin^2 \frac{\pi \Delta z}{\lambda_g}}}{\sin \frac{\pi \Delta z}{\lambda_g}} = \sqrt{1 + \csc^2 \frac{\pi \Delta z}{\lambda_g}} \qquad [9\text{-}37]$$

When the value of $\frac{\pi \Delta z}{\lambda_g}$ is small, the approximation $\theta \simeq \sin \theta$ may be used,

and, neglecting second-order small terms, we have

$$\frac{E_{max}}{E_{min}} = \frac{\lambda_g}{\pi \Delta z} \qquad\qquad [9\text{-}38]$$

In some cases, e.g., for very high standing-wave ratios and short wavelengths, greater accuracy may be achieved by measuring probe displacement between points of greater than twice-minimum power. Eq. 9-36 may be written

$$\frac{E_{max}}{E_{min}} = \sqrt{\frac{\left[\frac{E(z)}{E_{min}}\right]^2 - \left[1 - \sin^2 \frac{\pi \Delta z}{\lambda_g}\right]}{\sin^2 \frac{\pi \Delta z}{\lambda_g}}} = \sqrt{1 + \csc^2 \frac{\pi \Delta z}{\lambda_g} \left[\left[\frac{E(z)}{E_{min}}\right]^2 - 1\right]}$$

$$[9\text{-}39]$$

When $\frac{\pi \Delta z}{\lambda_g}$ is small enough to justify the approximation $\sin \frac{\pi \Delta z}{\lambda_g} \simeq \frac{\pi \Delta z}{\lambda_g}$,

$$\frac{E_{max}}{E_{min}} \simeq \sqrt{\left[\frac{E(z)}{E_{min}}\right]^2 \left[\frac{\lambda_g}{\pi \Delta z}\right]^2 - \left[\frac{\lambda_g}{\pi \Delta z}\right]^2 + 1} = \frac{\lambda_g}{\pi \Delta z} \sqrt{\left[\frac{E(z)}{E_{min}}\right]^2 - 1 + \left(\frac{\pi \Delta z}{\lambda_g}\right)^2}, \text{ and,}$$

since $\frac{\pi \Delta z}{\lambda_g}$ is much less than unity,

$$\frac{E_{max}}{E_{min}} \simeq \frac{\lambda_g}{\pi \Delta z} \sqrt{\left[\frac{E(z)}{E_{min}}\right]^2 - 1} \qquad\qquad [9\text{-}40]$$

Eqs. 9-39 and 9-40 are particularly useful when the detector crystal current can be measured and when it follows the square-law response. Then $\frac{I(z)}{I_{min}}$ can be substituted in Eqs. 9-39 and 9-40 for $\left[\frac{E(z)}{E_{min}}\right]^2$.

Thus, Eq. 9-36 or 9-37 provide a means for calculating the inverse standing-wave ratio needed in Eq. 9-10 from measurements taken in the vicinity of the voltage minimum where it is possible to remain within the square-law-response range of the detector.

The measurement of $\frac{E_{min}}{E_{max}}$ with the waveguide empty and its measurement with the sample in place provide the means for determining loss characteristics of the dielectric sample. As mentioned previously, the loss determination based on these two measurements alone will include losses in the waveguide, and, for very low-loss dielectrics, the resulting tan δ will be too large. Dakin and Works (1947) developed a correction for the wall losses in the waveguide (Eq. 9-29), which is subtracted from the calculated tan δ of the sample to provide a proper tan δ value. Westphal (1954) presents a correction procedure which appears to be more precise, since it takes into account differences in the wall losses which occur with and without the sample present in the guide.

The value $\frac{E_{min}}{E_{max}}$ measured with the empty waveguide reflects the waveguide losses which exist between the short-circuit termination and the probe position at the voltage minimum when measuring $\frac{E_{min}}{E_{max}}$. The Δz_a (Fig. 9-3) is larger than it would be for a lossless guide. In fact, since E_{min}^2 would be zero in a truly lossless guide, Δz at twice minimum would also be zero. The Δz_s measured with the dielectric sample in place includes a contribution due to the waveguide losses. Since the wall losses in the region of the guide surrounding the sample of length d are not the same with the sample in place as they are with the guide empty, the procedure outlined by Westphal (1954) should be used. The value of Δz_s measured may be corrected for losses occurring in the guide between the dielectric sample and the probe as follows:

$$(\Delta z_s)_{corrected} = (\Delta z_s)_{measured} - \frac{d'}{d_e} \Delta z_a \qquad [9\text{-}41]$$

The value $(\Delta z_s)_{corrected}$ is then used in Eq. 9-26 for the calculation of

tan δ or for determining $\frac{E_{min}}{E_{max}}$ for use in Eq. 9-10 if the general equations

for lossy materials are employed.

Correction for wall losses in the region of the guide surrounding the

sample is then taken into account by subtracting a term tan δ_{ws} from the

value for tan δ obtained from Eqs. 9-26 or 9-15.

Eq. 9-29, based on approximations entirely valid for low-loss mate-

rials, provides a value for the loss tangent of the empty waveguide,

tan δ_w. The correction, tan δ_{ws}, to be subtracted from tan δ is provided

by the following expression given by Westphal (1954):

$$\frac{\tan \delta_{ws}}{\tan \delta_w} = \frac{\mu_o}{\mu} \frac{C_g + \left(\frac{\lambda_o}{\lambda_c}\right)^2 \frac{\mu_o \, \varepsilon_o}{\mu_2 \, \varepsilon_2}}{C_g + \left(\frac{\lambda_o}{\lambda_c}\right)^2} \qquad [9\text{-}42]$$

where μ_2 and ε_2 refer to the permeability and permittivity of the dielec-

tric sample. For rectangular waveguide, $C_g = \frac{a}{2b}$, where a and b are, re-

spectively, the large and small inside dimensions of the guide. For

cylindrical waveguide, $C_g = 0.42$, and for coaxial lines, $\frac{\tan \delta_{ws}}{\tan \delta_w} = \frac{\mu_o}{\mu_2}$.

For nonmagnetic materials, the term $\frac{\mu_o}{\mu_2}$ is unity.

Corrections for losses in the waveguide walls or line conductors are

only important for low-loss materials where the value of tan δ_w assumes

some significance compared to tan δ for the sample. Therefore, these cor-

rections are ordinarily used in conjunction with Eq. 9-26. On casual ex-

amination of Eq. 9-41, it may appear that $(\Delta z_s)_{measured}$ ought to be cor-

rected also for the contribution to Δz_a provided by wall losses in the

sample-filled portion of the waveguide, since $(\Delta z_s)_{corrected}$ is used for

the determination of $\dfrac{E_{min}}{E_{max}}$ used in Eq. 9-10. Further consideration re-

veals, however, that, for low-loss measurements, the Δz does not enter

into the determination of ϵ_r' (Eq. 9-25), and, if the sample loss is great

enough to provide an interaction of Δz in the determination of ϵ_r' (Eqs.

9-10 and 9-15), the contribution of guide wall losses in the region sur-

rounding the sample is negligibly small without question. Eqs. 9-41 and

9-42 thus provide the proper corrections necessary to obtain the true loss

tangent of the sample material.

In summary, the adopted calculation procedures are as follows:

For low-loss samples (tan δ < 0.1 for 1-percent accuracy), find the

value for $\beta_2 d$ using Eq. 9-23 after finding z_o from Eq. 9-32, and then cal-

culate ϵ_r' from Eq. 9-25. Since $\dfrac{\tan \beta_2 d}{\beta_2 d}$ is a transcendental function,

the proper solution for $\beta_2 d$ must be selected on the basis of an estimated

value for ϵ_r' or by taking measurements on two samples of different

lengths. Calculate tan δ using $(\Delta z_s)_{corrected}$ in Eq. 9-26 and subtract

from it tan δ_{ws} determined from Eq. 9-42 using tan δ_w as calculated from

Eq. 9-29 using Δz_a. Calculate $\epsilon_r'' = \epsilon_r' \tan \delta_{corrected}$, and conductivity

$\sigma = \omega \, \epsilon_r''$.

For lossy dielectric samples, find the value of $\gamma_2 d$ using $\dfrac{E_{min}}{E_{max}}$ based

on $(\Delta z_s)_{corrected}$ from Eq. 9-41 in Eq. 9-10. Again, the desired $\gamma_2 d$ value

must be selected from the multivalued solutions for the complex transcen-

dental function $\dfrac{\tanh \gamma_2 d}{\gamma_2 d}$ on the basis of an estimated ϵ_r' or from the

common resulting value for measurements on two different sample lengths.

Then calculate ϵ_r' and ϵ_r'' from Eq. 9-15. Corrections for guide losses are

most likely insignificant, but tan $\delta = \varepsilon_r''/\varepsilon_r'$ can be corrected using the

same procedure outlined for the low-loss case, and a corrected value for

ε_r'' calculated from the corrected value of tan δ.

Details of the necessary calculations are covered in the description

of the computer program which follows.

D. Computer Program Description for Short-Circuited Waveguide
   Calculations

1. Main program

Because of the laborious nature of calculations for the lossy dielec-

tric case and the anticipation of large numbers of such calculations, a

computer program was developed to handle these calculations. The program

was designed for the general case and accommodates input data taken from

measurements on coaxial lines, or cylindrical or rectangular waveguides.

It properly performs the necessary calculations for either low-loss or

high-loss dielectric samples and prints out the final values for ε_r', ε_r'',

tan δ, and σ.

Calculations were programmed for computation on an IBM 360 Model 65

computer using FORTRAN IV programming language. See Sec. IX, E for the

program listing. Input data are punched on three cards (Fig. 9-5). An

initial card indicates the number of data sets to be run (limit of 50).

A parameter card for each data set carries the number of samples for

the data set, 40-character sample description for the data set, waveguide

dimensions, a reference dimension, R, which corresponds to an approximate

distance between the slotted-line or slotted-section probe carriage scale

zero reference and the short-circuit termination, the width of the slot in

```
                    S A M P L E    D A T A    C A R D

   SAMID  | DATE |M.C.|TEMPF FREQ | ANODP | ANODM |SNODP |SNODM | DDIMS |ADB|SDB|EST|
    (A)   | (A)  |(A) |(A)  |      |       |       |      |      |       |   |   |DC |
```

```
                    P A R A M E T E R    C A R D
   JJ                    SAMPL              |HDIMW|VDIMW|RDIMW| SLOT |ALCALC|
                          (A)
```

```
                    I N I T I A L    C A R D
   LL
```

Fig. 9-5.   Three types of input data cards for computer program,
initial card, parameter card, and sample data card,
showing division of fields and automatic decimal point
locations

the slotted section for use in correcting slotted-section wavelength data,
and instructions for the detail of printout desired. For rectangular
waveguides, the horizontal and vertical dimensions, a and b $(a > b)$, are
entered on the card. If the diameter of a cylindrical waveguide is en-
tered in the "a-dimension" column only, the calculations are carried out
for the cylindrical-waveguide case. If nothing is punched for the a and b
dimensions, the calculation proceeds for the coaxial-line case.

The third card carries the individual sample data including sample
identification, date, moisture content, temperature, frequency, twice-
minimum-power-point readings [or readings taken at other power-ratio
levels for z_a and z_s, the air (empty-waveguide) and sample voltage nodes],
the sample length, d, the dB levels used for the node width readings if
other than 3-dB levels, and an estimate of the value of ϵ'_r, the dielectric
constant. All length measurements are in mm, and f is in GHz.

Provisions are made in the program for calculating frequency from adjacent node data taken on the slotted lines or slotted sections if this is more convenient or results in a more accurate frequency determination for any particular system. If frequency is to be determined in this way, an extra card is punched in accordance with the sample data card format and placed in front of the sample data cards for which this frequency applies. No entry is made in the frequency columns on this card, but data for the two adjacent air nodes are punched in the air-node and sample-node columns. No other entries are made on this card. The program then checks for the presence of data in the frequency and sample length columns, and, if none is found, the calculation of frequency from the guide-wavelength data is performed. The check for sample-length data is necessary since data cards immediately following this card have no frequency data punched either.

For coaxial lines, frequency is simply determined as $f = 299.6966/\lambda_g$, since $\lambda_o = \lambda_g$, and $\lambda_g/2$ is the distance between adjacent nodes in the air-filled line. The constant used here represents the velocity for electromagnetic propagation in unbounded air space. Using ϵ_r for air $= 1.00064$[4],

---

[4] The value of ϵ_r for air at $20°$ C and 760 mm Hg pressure with a dew-point temperature of $9°$ C (Brady, 1970). The equation for ϵ_r used by Brady (1970) was originally produced by Smith and Weintraub (1953), since $\epsilon_r = n^2$, where n is the index of refraction. Their equation was $n = \frac{77.6}{T}\left[p + 4810\,\frac{e}{T}\right]$, where T is the absolute temperature in degrees K, p is the total pressure in millibars, and e is the partial pressure of water vapor in millibars. The elevation at Lincoln, Nebraska, is about 1200 feet above sea level, and the corresponding mean atmospheric pressure is 730 mm Hg. Under these conditions at 40-percent relative humidity and $76°$ F, the equation gives $n^2 = \epsilon_r = 1.00061$. Since the difference between $\sqrt{1.00064}$ and $\sqrt{1.00061}$ is less than 2×10^{-5}, no correction for the 1200-ft difference in elevation or $8°$-F difference in temperature is justified in this study.

the velocity of light in air = $c/\sqrt{\epsilon_p}$ = 2.996966 x 10^8 m/sec, where c is

the velocity of light in vacuum (2.997925 x 10^8 m/sec). Use of the value

for velocity in air provides higher accuracy in the measurement results.

For either cylindrical or rectangular waveguide, the relationship

from Eq. 9-16, $\lambda_o = \lambda_g/\sqrt{1 + (\lambda_g/\lambda_c)^2}$, must be employed to find the free

space wavelength, λ_o. Before calculating λ_o, however, the proper value

for λ_g must be obtained from Eqs. 9-30 or 9-31, depending upon the type

of waveguide, which correct for the error in measured guide wavelength due

to the influence of the slot in the slotted section. Finding λ_g in Eq.

9-30 or Eq. 9-31 requires the solution to a cubic equation, so an itera-

tive solution using Newton's approximation,

$$x_{n+1} = x_n - f(x_n)/f'(x_n) \qquad [9\text{-}43]$$

is employed in the program. Once λ_o is found, f is calculated as

299.6966/λ_o in the same way as in the coaxial case.

Calculations then proceed, using f, whether entered directly on the

data card, or calculated as just explained using adjacent node measurement

data, as follows:

Wavelength in air, λ_o = 299.6966/f. Waveguide cutoff wavelength,

λ_c = $2a$ for rectangular guide or λ_c = 1.706293 D, where D represents diam-

eter of cylindrical guide. Guide wavelength, $\lambda_g = \lambda_1 = \lambda_o/\sqrt{1 - (\lambda_o/\lambda_c)^2}$.

Next, for the waveguide case, a correction factor for the influence of the

slot on z-dimension data taken on a slotted section is calculated using

Eq. 9-30 or Eq. 9-31. The air- and sample-node positions, z_a and z_s, with

reference to the slotted-line or slotted-section scale zero are calculated

by averaging the double-power-point readings (or readings taken at other

power-ratio levels), and Δz_a and Δz_s are obtained as the absolute value of their differences, so that the order of double-power-point entries for each node on the data cards is of no importance. Δz_a and Δz_s values are then corrected for the influence of the slotted-section slot. The node shift due to the sample, $z_a - z_s$, is then calculated and corrected for the influence of the slot. At this point in the program, d_e of Fig. 9-3, which is needed later for line and wall loss corrections, is estimated by adding the reference dimension R (the approximate distance from the slotted-line or slotted-section scale zero to the short circuit) to the z_a value referenced to the scale zero. Since d_e is an integral number of half-wavelengths in the guide, the precise value for d_e is found in the program by successively adding half-wavelengths until the difference between n $\lambda_g/2$ and the estimate for d_e is less than $\lambda_g/4$. With this determination of n, d_e is set equal to n $\lambda_g/2$.

Next, the provision for using other than 3-dB points (twice-minimum-power points) for the node-width measurement is considered. If no entry is punched in the dB-level columns of the data card, the program automatically inserts 3 dB. The usual procedure is to employ 3-dB levels to simplify calculations; however, better accuracy may be provided using levels greater than 3 dB for very high standing-wave ratios, and, in practice, some samples were found to provide such a good impedance match that 3-dB levels could not be used because E^2_{min} was less than 3 dB below E^2_{max}. Therefore, the calculations are programmed to provide for any possible dB level in measuring Δz_a and Δz_s. Since a greater dB level will always be possible for the air-node measurement, the program converts the Δz_a

value to the proper value for the dB level employed for the measurement of Δz_s if they are measured at different dB levels. Eq. 9-36 provides a value for the VSWR for any dB level or power ratio. The dB level is converted to power ratio, $P_r = (E(z)/E_{min})^2$, as follows for use in Eq. 9-36: dB = $10 \log_{10} P_r = (10 \ln P_r)/(\ln 10)$, so $P_r = e^{0.2302585(dB)}$. After finding the VSWR value from Eq. 9-36, the Δz_a value corresponding to the dB level at which Δz_s was measured is obtained by solving Eq. 9-36 for Δz_a with P_r for the sample dB level inserted for $(E(z)/E_{min})^2$.

Since Δz_s must be corrected for guide or line losses between the sample and the probe, the ratio d'/d_e (see Fig. 9-3) is calculated and used in Eq. 9-41 to provide the value of Δz_s corrected for these losses. The inverse standing-wave ratio with the sample in the guide is then calculated using Eq. 9-36.

Next, the program calculates z_o according to Eq. 9-32 by successively adding half-wavelengths to $-[d + (z_a - z_s)]$, if it is not already positive, until the result is positive. If a sample-node position is used which is farther away from the short circuit than the air-node position, $(z_a - z_s)$ will have a negative value, and if $|z_a - z_s|$ exceeds d, the quantity $-[d + (z_a - z_s)]$ will be positive. This value is then taken for z_o in the program. Even if a sample node should be selected which is more than $\lambda_g/2$ beyond the air node, the value obtained in this way for z_o will work all right in the program, since $\tan (2\pi z_o/\lambda_g)$ is equivalent to $\tan [2\pi(z_o + \lambda_g/2)/\lambda_g]$ as a consequence of the identity, $\tan (\theta + \pi) = \tan \theta$. Thus, any air node and any sample node, without reference to relative position or distance apart, will suffice for the measurement.

In order to use Eq. 9-10 for computation, the right-hand side must be rationalized and separated into its real and imaginary components as shown in Eq. 9-19. This may be rewritten

$$\frac{\tanh \gamma_2 d}{\gamma_2 d} = Ce^{j\zeta} = \frac{\lambda_g \tan U \, (\phi^2 - 1) - j \, \lambda_g \, \phi \, (1 + \tan^2 U)}{2\pi d \, (1 + \phi^2 \tan^2 U)} =$$

$$\frac{\lambda_g \, (A - jB)}{2\pi d \, (1 + \phi^2 \tan^2 U)} \qquad [9\text{-}44]$$

where ϕ represents the inverse standing-wave ratio and U represents $(2\pi z_0)/\lambda_g$. Calculation of C and ζ permits finding $\gamma_2 d = Te^{j\tau}$ from charts mentioned previously, though it is a tedious process. For computer solution, however, we hope to obtain close estimates for the components of $\gamma_2 d = \alpha_2 d + j\beta_2 d$ and adjust them until Eq. 9-10 or one of its equivalent forms, such as Eq. 9-44, is satisfied. For given values of $\alpha_2 d$ and $\beta_2 d$, Eq. 9-20 is used to calculate real and imaginary parts of $(\tanh \gamma_2 d)/\gamma_2 d$ in a subroutine called ACOMP.

An initial estimate of $\beta_2 d$ is obtained from Eq. 9-25, which is valid for the low-loss case, by solving for $\beta_2 d$ using the estimated value from the data input for ϵ_r'. In the program, if no value is entered on the parameter card for the estimated dielectric constant, a value of 2.5 is automatically taken. Provision is also made in the program to use the dielectric constant calculated for the previous sample as the estimated dielectric constant for the next sample in a series of similar samples if no estimated value is punched on the data card. Since, in the lossless case, $\alpha_2 = 0 = \zeta$, $(\tanh \gamma_2 d)/\gamma_2 d = Ce^{j\zeta}$ becomes, in accord with Eq. 9-23, $(\tan \beta_2 d)/\beta_2 d = C$. C is calculated as the magnitude of the right-hand

side of Eq. 9-44 because, for lossy dielectric samples, C will include a contribution due to the loss and will provide a better estimate for $\beta_2 d$ than might be obtained using Eq. 9-23.

On certain usually rare occasions, the sample may turn out to be very nearly an odd multiple quarter-guide-wavelength in the sample material. In this case, z_o is nearly a quarter-guide-wavelength, so tan $U =$ tan $(2\pi\, z_o/\lambda_g)$ takes on very large values, and subsequent calculations involving the hyperbolic functions of $\alpha_2 d$ and $\beta_2 d$ exceed the capacity of the computer. Therefore, a test was inserted in the program, and, if tan U exceeds a value of 200, it branches to a later point in the program, where an approximate value for the dielectric constant is calculated using Eq. 9-25 and the value of $\beta_2 d$ arrived at by the FUNCTION FINDX subroutine to be described later. A statement then appears in the printout, "Bad sample length for this frequency, nearly an odd multiple quarter-wavelength," and zeros are printed out for the loss tangent, loss factor, and conductivity.

In the usual case where tan U does not exceed a value of 200, the estimate of $\beta_2 d$ is then improved by adjusting it to satisfy (tan $\beta_2 d)/\beta_2 d$ = C in the subroutine, FUNCTION FINDX. This value of $\beta_2 d$ and a value for $\alpha_2 d$, calculated from Eq. 9-24 using this improved estimate of $\beta_2 d$, then comprise the first estimate for $\gamma_2 d$. These unadjusted values for $\alpha_2 d$ and $\beta_2 d$ are printed out as diagnostics immediately following the first estimate of $\beta_2 d$. The components $\alpha_2 d$ and $\beta_2 d$ are then adjusted in a subroutine called ADJUST, to be explained later, until Eq. 9-44 is satisfied to within a desired limit. The adjusted values of $\alpha_2 d$ and $\beta_2 d$ are also printed out along with the unadjusted values.

Since $(\tan \beta_2 d)/\beta_2 d$ and $(\tanh \gamma_2 d)/\gamma_2 d$ are multivalued functions and each solution to Eqs. 9-10 and 9-23 results in a different set of values for ε'_r and ε''_r, the program finds three sets of $\alpha_2 d$ and $\beta_2 d$ satisfying Eq. 9-10 from which to proceed with the calculations. The relative permittivity or dielectric constant and the relative dielectric loss factor of the sample are then calculated from an expansion of Eq. 9-17, $\varepsilon'_r - j\varepsilon''_r =$

$$P - \left[\frac{(\alpha_2 d + j\beta_2 d)\,\lambda_o}{2\pi d}\right]^2 = P - S^2[(\alpha_2 d)^2 - (\beta_2 d)^2] + j\,S^2\,2\,\alpha_2 d\,\beta_2 d, \text{ where}$$

$P = (\lambda_o/\lambda_c)^2$ and $S = \lambda_o/2\pi d$. The associated loss tangent for each of the three sets of values for ε'_r and ε''_r is calculated $(\tan \delta = \varepsilon''_r/\varepsilon'_r)$. The correction for wall losses with the sample present in the guide, $\tan \delta_{ws}$, is then calculated using Eq. 9-42, after getting $\tan \delta_w$ using Eq. 9-29, and $\tan \delta_{ws}$ is subtracted from $\tan \delta$ to give the corrected value for $\tan \delta$. Using this corrected value, a corrected ε''_r is found as the product of ε'_r and the corrected $\tan \delta$. The three sets of dielectric properties are printed out along with important input data and a few diagnostics, unless this printout is suppressed by instructions on the parameter card, i.e., nothing punched in columns 68 to 73. The program selects the probable value of ε'_r, that which is closest to the estimated value for ε'_r from the input data, and, at the end of the calculations for a given data set, prints out a summary table including description, date, moisture content, temperature, sample identification, frequency, and values for ε'_r, ε''_r, $\tan \delta$, and conductivity, calculated as $\sigma = \omega \varepsilon_o \varepsilon''_r = 0.55668f \varepsilon''_r$ for σ in millimhos - cm^{-1}. Examples of the input card data and printout for rectangular and cylindrical waveguide and coaxial line cases are shown in Figs. 9-6, 9-7, and 9-8. The summary table printout is shown in Fig. 9-9.

It should be noted that the relationship of Eq. 9-38 based on twice-minimum-power or 3-dB points is utilized in the derivation of Eqs. 9-26 and 9-29. Therefore, in this program, the wall loss correction for the sample-filled portion of the waveguide tan δ_{ws} of Eq. 9-42 is also based on the assumption of a 3-dB air-node measurement. Since the program automatically converts the dB level for the air-node measurement to that employed for the sample-node measurement, sample-node measurements on very low-loss materials, where the wall loss correction is important, should probably be performed using the 3-dB level. In practice, the need for less than 3-dB sample-node measurements was encountered only with high-loss materials where the wall loss correction was insignificantly small anyway. Therefore, the 3-dB level requirement for sample-node measurements is only necessary when working with very low-loss materials.

```
3-3     7/30/71 10.5    76   8388     13542  13833   19130   25430   348       6    3 27

  000000000  0    0000   0000000000000000000000000000000000  000000  0000000000000000000000
  1 2 3 4 5 6 7 8 9 10 11 12 13 14 15 16 17 18 19 20 21 22 23 24 25 26 27 28 29 30 31 32 33 34 35 36 37 38 39 40 41 42 43 44 45 46 47 48 49 50 51 52 53 54 55 56 57 58 59 60 61 62 63 64 65 66 67 68 69 70 71 72 73 74 75 76 77 78 79 80
```

```
  1 1970 SCOUT 66 HRW WHEAT, X-BAND                  2286  1016 130                    1

  0000000  0  00   000000  0  000    0  0000000000000000000000000  00000  0000000000000000000000
  1 2 3 4 5 6 7 8 9 10 11 12 13 14 15 16 17 18 19 20 21 22 23 24 25 26 27 28 29 30 31 32 33 34 35 36 37 38 39 40 41 42 43 44 45 46 47 48 49 50 51 52 53 54 55 56 57 58 59 60 61 62 63 64 65 66 67 68 69 70 71 72 73 74 75 76 77 78 79 80
```

DIELECTRIC PROPERTIES FOR   1970 SCCUT 66 HRW WHEAT, X-BAND

RUN   1   7/30/71

```
MOISTURE CONTENT                                      10.5
TEMPERATURE (CEGREES FAHRENHEIT)                      76
FREQUENCY (GIGAHERTZ)                                  8.3880
WAVEGUIDE HORIZONTAL DIMENSION (MM)                   22.8600
WAVEGUIDE VERTICAL DIMENSION (MM)                     10.1600
SAMPLE LENGTH (MM)                                    34.8000
AIR NODE POSITICN (MM)                                13.6875
SAMPLE NODE POSITION (MM)                             22.2800
AIR NODE WIDTH (MM)           6.0 CB                   0.2910
SAMPLE NODE WIDTH (MM)        3.0 CB                   6.3000
         REFERENCE DIMENSION (MM)                    130.0000
ESTIMATED DIELECTRIC CONSTANT                          2.7000
FIRST ESTIMATE OF B2D (ESTX)                           5.7042


UNADJUSTED A2D, B2C            0.33920               5.73540
ADJUSTED A2D, B2D              0.42670               5.82789
```

SAMPLE   3-3   RESULTS

```
DIELECTRIC CONSTANT          1.512730      2.624163      4.204988
LOSS TANGENT                 0.087389      0.091700      0.075326
LOSS FACTOR                  0.132196      0.240635      0.316744
CONDUCTIVITY                 0.617282      1.123630      1.479012
```

DIELECTRIC PROPERTIES FOR   1970 SCOUT 66 HRW WHEAT, X-BAND

SUMMARY TABLE

DATE	MOIST CONT. (F.)	TEMP	SAMPLE IDENT.	FREQ. (GHZ)	DIELECTRIC CONSTANT	LOSS FACTOR	LOSS TANGENT	CONDUCTIVITY MILLIMHOS/CM
7/30/71	10.5	76	3-3	8.388	2.6242	0.2406	0.0917	1.1236

Fig. 9-6.   Parameter card and sample data card input with printout for
           a rectangular waveguide measurement

```
3-1      8/3/71 10.5   76          61123  61212  75300  84620  46                      27
```

```
0000000000 0 0000 0000000000000000000000000000000000000   000000  0000000000000000000000
1 2 3 4 5 6 7 8 9 10 11 12 13 14 15 16 17 18 19 20 21 22 23 24 25 26 27 28 29 30 31 32 33 34 35 36 37 38 39 40 41 42 43 44 45 46 47 48 49 50 51 52 53 54 55 56 57 58 59 60 61 62 63 64 65 66 67 68 69 70 71 72 73 74 75 76 77 78 79 80
```

```
                                             61123  61212  91182  91277
```

```
000000000000000000000000000000000000000000000000000000000000000000000000000000000000000000
1 2 3 4 5 6 7 8 9 10 11 12 13 14 15 16 17 18 19 20 21 22 23 24 25 26 27 28 29 30 31 32 33 34 35 36 37 38 39 40 41 42 43 44 45 46 47 48 49 50 51 52 53 54 55 56 57 58 59 60 61 62 63 64 65 66 67 68 69 70 71 72 73 74 75 76 77 78 79 80
```

```
 1 1970 SCOUT 66 HRW WHEAT, CRL DIELECTR.     2545           300               1
```

```
0000000 0 00  000000 0 000  00000000000 00000000000000000  000000000000000000000000
1 2 3 4 5 6 7 8 9 10 11 12 13 14 15 16 17 18 19 20 21 22 23 24 25 26 27 28 29 30 31 32 33 34 35 36 37 38 39 40 41 42 43 44 45 46 47 48 49 50 51 52 53 54 55 56 57 58 59 60 61 62 63 64 65 66 67 68 69 70 71 72 73 74 75 76 77 78 79 80
```

DIELECTRIC PROPERTIES FOR 1970 SCOUT 66 HRW WHEAT, CRL DIELECTR.

RUN   1   8/3/71

MOISTURE CONTENT	10.5
TEMPERATURE (DEGREES FAHRENHEIT)	76
FREQUENCY (GIGAHERTZ)	8.5144
WAVEGUIDE HORIZONTAL DIMENSION (MM)	25.4500
WAVEGUIDE VERTICAL DIMENSION (MM)	0.0
SAMPLE LENGTH (MM)	46.0000
AIR NODE POSITION (MM)	61.1675
SAMPLE NODE POSITION (MM)	79.9600
AIR NODE WIDTH (MM) 3.0 DB	0.0890
SAMPLE NODE WIDTH (MM) 3.0 DB	9.3200
REFERENCE DIMENSION (MM)	300.0000
ESTIMATED DIELECTRIC CONSTANT	2.7000
FIRST ESTIMATE OF E2D (ESTX)	8.5951

UNADJUSTED A2D, B2D	0.42110	8.67469
ADJUSTED A2D, B2D	0.61110	8.69968

SAMPLE 3-1   RESULTS

DIELECTRIC CONSTANT	1.773952	2.641019	3.794526
LOSS TANGENT	0.088833	0.077709	0.059573
LOSS FACTOR	0.157586	0.205232	0.226052
CONDUCTIVITY	0.746929	0.972763	1.071445

DIELECTRIC PROPERTIES FOR 1970 SCOUT 66 HRW WHEAT, CRL DIELECTR.

SUMMARY TABLE

DATE	MOIST CONT. (F.)	TEMP	SAMPLE IDENT.	FREQ. (GHZ)	DIELECTRIC CONSTANT	LOSS FACTOR	LOSS TANGENT	CONDUCTIVITY MILLIMHOS/CM
8/3/71	10.5	76	3-1	8.514	2.6410	0.2052	0.0777	0.9728

Fig. 9-7. Parameter card and sample data card input with printout for a cylindrical waveguide measurement, using guide wavelength data for the frequency input

```
3-2      8/3/71 10.5   76        94700 94800 69100 72920 383              3
```

```
0000000000 0 0000 00000000000000000000  00000   00000   000000 0000000000000000000000
1 2 3 4 5 6 7 8 9 10 11 12 13 14 15 16 17 18 19 20 21 22 23 24 25 26 27 28 29 30 31 32 33 34 35 36 37 38 39 40 41 42 43 44 45 46 47 48 49 50 51 52 53 54 55 56 57 58 59 60 61 62 63 64 65 66 67 68 69 70 71 72 73 74 75 76 77 78 79 80
```

```
                                60230 60150 121650 121780
```

```
0000000000000000000000000000000000000000000 00 000 00 000000 000000 0000000000000000000000
1 2 3 4 5 6 7 8 9 10 11 12 13 14 15 16 17 18 19 20 21 22 23 24 25 26 27 28 29 30 31 32 33 34 35 36 37 38 39 40 41 42 43 44 45 46 47 48 49 50 51 52 53 54 55 56 57 58 59 60 61 62 63 64 65 66 67 68 69 70 71 72 73 74 75 76 77 78 79 80
```

```
1 1970 SCOUT 66 HRW WHEAT, R&S SLRC-LMC                       150              1
```

```
0000000 0 00  000000 0 000   000 0 000000000000000000000000000 000000000000000000000000
1 2 3 4 5 6 7 8 9 10 11 12 13 14 15 16 17 18 19 20 21 22 23 24 25 26 27 28 29 30 31 32 33 34 35 36 37 38 39 40 41 42 43 44 45 46 47 48 49 50 51 52 53 54 55 56 57 58 59 60 61 62 63 64 65 66 67 68 69 70 71 72 73 74 75 76 77 78 79 80
```

DIELECTRIC PROPERTIES FOR 1970 SCOUT 66 HRW WHEAT, R&S SLRC-LMC

RUN   1   8/3/71

```
MOISTURE CONTENT                                  10.5
TEMPERATURE (DEGREES FAHRENHEIT)                  76
FREQUENCY (GIGAHERTZ)                             2.4356
WAVEGUIDE HORIZONTAL DIMENSION (MM)               0.0
WAVEGUIDE VERTICAL DIMENSION (MM)                 0.0
SAMPLE LENGTH (MM)                               38.3000
AIR NODE POSITION (MM)                           94.7500
SAMPLE NODE POSITION (MM)                        71.0100
AIR NODE WIDTH (MM)          3.0 DB              0.1000
SAMPLE NODE WIDTH (MM)       3.0 DB              3.8200
        REFERENCE DIMENSION (MM)               150.0000
ESTIMATED DIELECTRIC CONSTANT                    3.0000
FIRST ESTIMATE OF B2D (ESTX)                     3.3873

UNADJUSTED A2D, B2D              0.16494              3.30719
ADJUSTED A2D, B2D               0.15744              3.17719
```

SAMPLE 3-2   RESULTS

DIELECTRIC CONSTANT	2.632839	10.549779	23.807678
LOSS TANGENT	0.098944	0.101583	0.105471
LOSS FACTOR	0.260504	1.071676	2.511011
CONDUCTIVITY	0.353200	1.453012	3.404506

DIELECTRIC PROPERTIES FOR 1970 SCOUT 66 HRW WHEAT, R&S SLRC-LMC

SUMMARY TABLE

DATE	MOIST CONT. (F.)	TEMP (F.)	SAMPLE IDENT.	FREQ. (GHZ)	DIELECTRIC CONSTANT	LOSS FACTOR	LOSS TANGENT	CONDUCTIVITY MILLIMHOS/CM
8/3/71	10.5	76	3-2	2.436	2.6328	0.2605	0.0989	0.3532

Fig. 9-8.   Parameter card and sample data card input with printout for
a coaxial line measurement, using guide wavelength data for
the frequency input

```
3-3     7/30/71 10.5   76 12228   15684  15599  14710  25520  364    6   2
```

```
000000000 0  0000 0000000000000000000000000000000000  000000 00000000000000000000000
1 2 3 4 5 6 7 8 9 10 11 12 13 14 15 16 17 18 19 20 21 22 23 24 25 26 27 28 29 30 31 32 33 34 35 36 37 38 39 40 41 42 43 44 45 46 47 48 49 50 51 52 53 54 55 56 57 58 59 60 61 62 63 64 65 66 67 68 69 70 71 72 73 74 75 76 77 78 79 80
```

```
3-3     7/30/71 10.5   76 11030   22491  22562  22140  26820  35     6   3
```

```
000000000 0  0000 0000000000 0  000000000000000000000000  000000 00000000000000000000000
1 2 3 4 5 6 7 8 9 10 11 12 13 14 15 16 17 18 19 20 21 22 23 24 25 26 27 28 29 30 31 32 33 34 35 36 37 38 39 40 41 42 43 44 45 46 47 48 49 50 51 52 53 54 55 56 57 58 59 60 61 62 63 64 65 66 67 68 69 70 71 72 73 74 75 76 77 78 79 80
```

```
3-3     7/30/71 10.5   76 10186    4896   4967  14910  28170  35     6  0.8
```

```
000000000 0  0000 000000000 0000000000000000000000000000  000000 000000000000 0000000
1 2 3 4 5 6 7 8 9 10 11 12 13 14 15 16 17 18 19 20 21 22 23 24 25 26 27 28 29 30 31 32 33 34 35 36 37 38 39 40 41 42 43 44 45 46 47 48 49 50 51 52 53 54 55 56 57 58 59 60 61 62 63 64 65 66 67 68 69 70 71 72 73 74 75 76 77 78 79 80
```

```
3-3     7/30/71 10.5   76  8388   13542  13833  19130  25430  348    6   3  27
```

```
000000000 0  0000 0000000000000000000000000000000000  000000 00000000000000000000000
1 2 3 4 5 6 7 8 9 10 11 12 13 14 15 16 17 18 19 20 21 22 23 24 25 26 27 28 29 30 31 32 33 34 35 36 37 38 39 40 41 42 43 44 45 46 47 48 49 50 51 52 53 54 55 56 57 58 59 60 61 62 63 64 65 66 67 68 69 70 71 72 73 74 75 76 77 78 79 80
```

```
4 1970 SCOUT 66 HRW WHEAT, X-BAND          2286  1016 130
```

```
0000000 0 00  000000 0 000  0 0000000000000000000000000  00000 00000000000000000000000
1 2 3 4 5 6 7 8 9 10 11 12 13 14 15 16 17 18 19 20 21 22 23 24 25 26 27 28 29 30 31 32 33 34 35 36 37 38 39 40 41 42 43 44 45 46 47 48 49 50 51 52 53 54 55 56 57 58 59 60 61 62 63 64 65 66 67 68 69 70 71 72 73 74 75 76 77 78 79 80
```

DIELECTRIC PROPERTIES FOR 1970 SCOUT 66 HRW WHEAT, X-BAND

SUMMARY TABLE

DATE	MOIST CONT.	TEMP (F.)	SAMPLE I CENT.	FREQ. (GHZ)	DIELECTRIC CONSTANT	LOSS FACTOR	LOSS TANGENT	CONDUCTIVITY MILLIMHOS/CM
7/30/71	10.5	76	3-3	8.388	2.6242	0.2406	0.0917	1.1236
7/30/71	10.5	76	3-3	10.186	2.6005	0.2582	0.0993	1.4643
7/30/71	10.5	76	3-3	11.030	2.5864	0.2784	0.1076	1.7095
7/30/71	10.5	76	3-3	12.228	2.5174	0.2143	0.0851	1.4590

Fig. 9-9. Parameter card and sample data card input with summary printout only for series of rectangular waveguide measurements

2. Program subroutines

a. __FUNCTION FINDX__   In the main program, an estimate for $\beta_2 d$ is obtained using Eq. 9-25 for cylindrical or rectangular waveguide, or Eq. 9-27 for the coaxial case. The FORTRAN FUNCTION FINDX is used to solve $(\tan \beta_2 d)/(\beta_2 d) = C$ for $\beta_2 d$ when C is known from measurements data. In the program, X is used to represent $\beta_2 d$. Because of the nature of the $(\tan X)/X$ function, some care must be exercised to obtain desired solutions by iterative techniques. A plot of this function is shown in Fig. 9-10 for the range $0 \leq X \leq 3\pi$. For $(\tan X)/X = C$, it is obvious that no
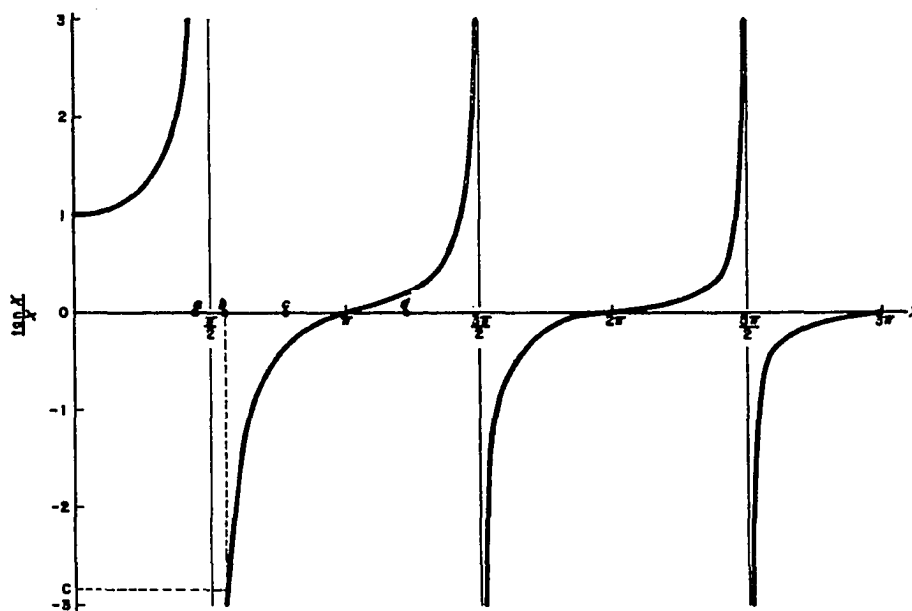
Fig. 9-10. Graph of the function $(\tan X)/X$

solutions can exist in the first quadrant for $C < 1$. For a given value of C, there are many values of X which will satisfy the equation.

The program calculates and prints out dielectric properties corresponding to three different values for X, or $\beta_2 d$, one nearest the value

derived from the estimated dielectric constant of the input data, and one
on either side of this value if possible. If the estimated value of X
obtained from Eq. 9-25 is greater than π, π is subtracted from this value
to obtain the estimated X value on the lower side of the original X esti-
mate. If this results in a value for X in the first quadrant, the pro-
gram checks to see whether $C \leq 1$, and, if it is, π is added back on to
take the estimated X into the third quadrant where a possible solution
exists. If the estimated X does not lie in the first quadrant, or, if it
does, but $C > 1$, this value is taken for the first set of calculations and
stored for printout as the estimated $\beta_2 d$ diagnostic immediately following
the printout of input data. The program then sets $\beta_2 d$ = FINDX which is a
function of C with proper sign and the estimated value of X.

The FUNCTION FINDX subroutine finds the value of X satisfying
$(\tan X)/X = C$ in the following way. First, the quadrant containing the
estimated X is identified and appropriate limits are established within
which the search for the proper value of X will be carried out. A test is
also made to determine whether C and $(\tan X)/X$ have the same sign. If
they do not, and the value of X lies near an asymptote (ascertained by
$|C| > 2$), the estimated X is shifted to the other side of the asymptote a
distance equal to its distance from the asymptote (points a and b, Fig.
9-10). This will change the sign of X thereby giving C and $(\tan X)/X$ the
same sign so that a solution will be possible. New limits for the search
are also then established ($\pi/2$ and $3\pi/2$ for point b, for example). If the
sign of C and that of $(\tan X)/X$ do not agree and the estimated X is not
near an asymptote ($|C| \leq 2$), the estimated X is shifted to the other side

of $n\pi$, in which quadrant a solution can be found (points c and d, for example).

An iterative technique employing Newton's successive approximation method, Eq. 9-43, is then used to find the proper value of X satisfying $(\tan X)/X = C$. Here $f(x) = (\tan X - CX)/X$ and $f'(x) = (X \sec^2 X - \tan X)/X^2$ so that $f(x)/f'(x) = X(\tan X - CX)/(X \sec^2 X - \tan X)$. It may happen that the value of X_2 obtained using the estimated X value for X_1 in Eq. 9-43 will fall outside the prescribed limits. For example, a solution is needed between $A = \pi/2$ and $B = 3\pi/2$ in Fig. 9-11 and the
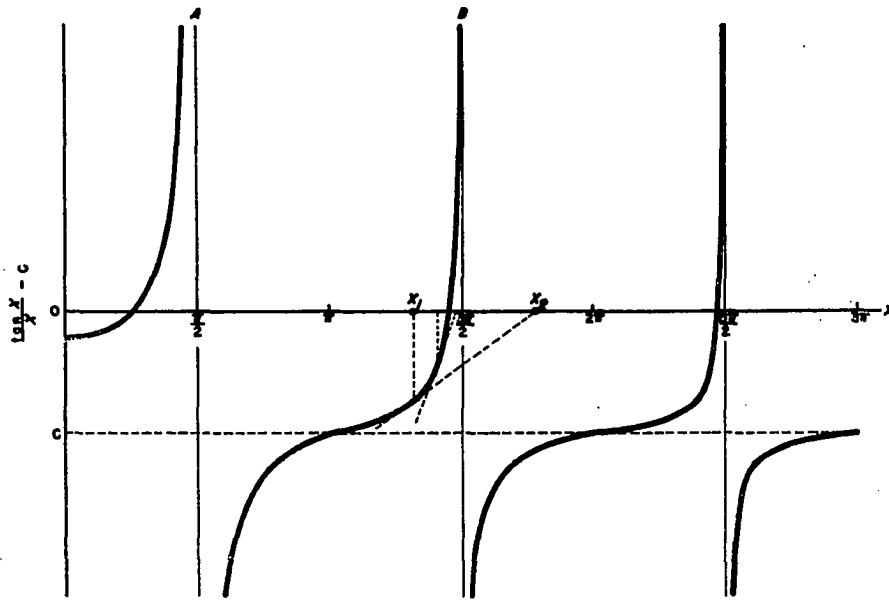
Fig. 9-11. Graph of the function $(\tan X)/X - C$ showing limits for successive approximation solution

first value obtained for $X_2 > 3\pi/2$. The program, therefore, rejects X_2 outside the prescribed region and sets the new estimate of X equal to $(X_1 + 3\pi/2)/2$ and proceeds until X_2 falls within the prescribed limits.

Successive approximations then proceed until the difference between two successive approximations of X is less than 0.0001 and the program then sets the last value for X = FINDX.

b. <u>ADJUST</u>   Following the use of the FUNCTION FINDX subroutine to improve the estimate of $\beta_2 d$ and the subsequent calculation of an estimate for $\alpha_2 d$, the ADJUST subroutine is employed to adjust the values of the components of $\gamma_2 d = \alpha_2 d + j\beta_2 d$ to satisfy Eq. 9-44.   Here U_o and V_o represent the real and imaginary parts of the right-hand side of Eq. 9-44, and their values are determined by measurement data.   The subroutine ACOMP provides values for $(\tanh \gamma_2 d)/\gamma_2 d = U_a + V_a$ from the initial $\alpha_2 d$ and $\beta_2 d$ values calculated.   The ADJUST subroutine alternately adjusts values of $\alpha_2 d$ and $\beta_2 d$ by an increment, delta, and tests to see whether the resulting $U_a + jV_a$ is approaching the desired value of $U_o + jV_o$.   This is done by calculating the difference in the two-space vectors, $U_o + jV_o$ and $U_a + jV_a$, $\sqrt{(U_o - U_a)^2 + (V_o - V_a)^2}$, and requiring that this value decrease as adjustments are made.   When no further improvement can be found by either positive or negative additions of delta to $\alpha_2 d$ and $\beta_2 d$, the value of delta is halved, and the adjusting procedure repeated.   This reduction of delta and adjusting of $\alpha_2 d$ and $\beta_2 d$ values continues in accordance with the flow chart of Fig. 9-12 until the magnitude of the vector difference is less than 0.0002, or until the delta value has been halved 12 times, when it returns to the main program.   If the vector difference is not reduced to a value less than 0.0002, the value of the difference, called DIFF1 in the program, is printed out and identified with one of the three dielectric-constant determinations to which it applies.
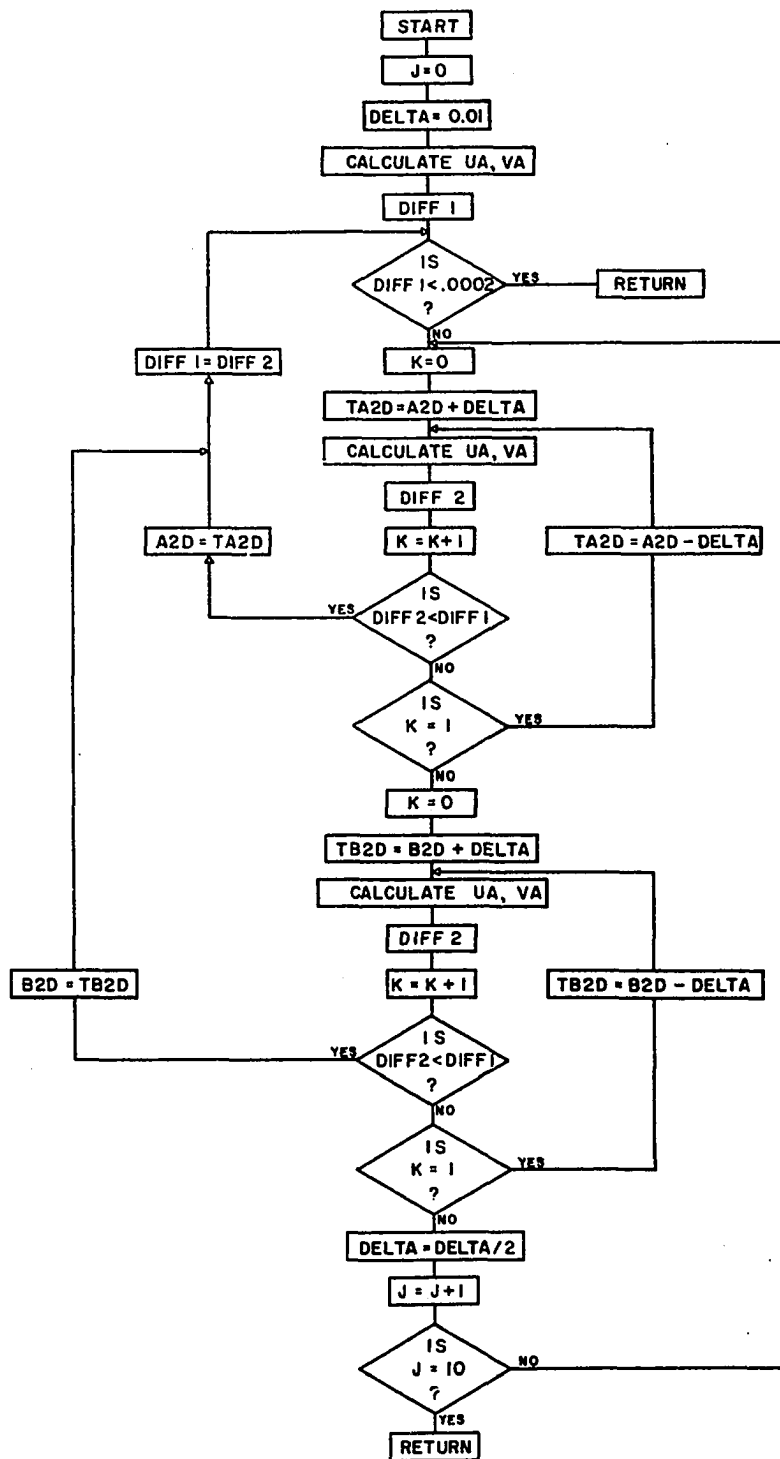
Fig. 9-12. Flow chart for the ADJUST subroutine

E. Computer Program Listing

FORTRAN IV G LEVEL 19   MAIN   DATE = 72004

```
      C     LATEST REVISION MADE AUGUST 10, 1971.  SHORTLIN
      C  MAIN PROGRAM FOR CALCULATING DIELECTRIC PROPERTIES FROM
      C  SHORT-CIRCUITED COAXIAL-LINE OR WAVEGUIDE MEASUREMENTS
      C  INPUT DATA DESCRIPTION
      C        LL          NUMBER OF SETS OF DATA
      C        JJ          NUMBER OF READINGS PER SET
      C        SAMPL       DESCRIPTION OF THE DATA SET, 40 SPACES
      C        HDIMW       HORIZONTAL DIMENSION OF THE WAVEGUIDE IF RECTANGULAR
      C                    DIAMETER OF THE WAVEGUIDE IF CIRCULAR
      C                    ZERO FOR COAXIAL WAVEGUIDE
      C        VDIMW       VERTICAL DIMENSION OF THE WAVEGUIDE IF RECTANGULAR
      C                    ZERO OTHERWISE
      C        RDIMW       WAVEGUIDE REFERENCE DIMENSION, MEASURED FROM THE
      C                    SHORT TO THE 0 MM. REFERENCE POINT OF THE PROBE.
      C        SLOT        WIDTH OF SLOT IN SLOTTED SECTION
      C        ALCALC      ANY POSITIVE NUMBER IF COMPLETE RESULTS ARE TO BE
      C                    PRINTED
      C                    ZERO IF SUMMARY TABLE ONLY IS DESIRED
      C        SAMID       INDIVIDUAL SAMPLE DESCRIPTION, 8 SPACES
      C        DATE        E.G. 12-25-70
      C        MC          MOISTURE CONTENT OF SAMPLE, 4 SPACES
      C        TEMPF       SAMPLE TEMPERATURE IN DEG. FAHRENHEIT, 4 SPACES
      C        FREQ        FREQUENCY IN GIGAHERTZ
      C        ANODP       AIR NODE PLUS HALF NODE WIDTH
      C        ANODM       AIR NODE MINUS HALF NODE WIDTH
      C        SNODP       SAMPLE NODE PLUS HALF NODE WIDTH
      C        SNODM       SAMPLE NODE MINUS HALF NODE WIDTH
      C        DDIMS       DEPTH OF THE SAMPLE
      C        ADB         DB LEVEL FOR AIR-NODE MEASUREMENT
      C        SDB         DB LEVEL FOR SAMPLE-NODE MEASUREMENT
      C        ESTDC       ESTIMATED DIELECTRIC CONSTANT
      C        WL          WAVELENGTH IN FREE SPACE
      C        WLC         CUTOFF WAVELENGTH
      C        WLG         WAVELENGTH IN THE WAVEGUIDE
      C  ALL MEASUREMENTS ARE IN MILLIMETERS
      C
0001        REAL MC,LTW,LTWS
0002        DIMENSION ALPHA(3),BETA(3),DC(3),ALT(3),FACTOR(3),SDC(50),SLT(50),
           * SFACT(50),SCOND(50),SF(50),STF(50),SAMPL(10),SAMID(2),  DATE(2),
           *SDAY(50,2),SSMP(50,2),SMC(50),DIFF(3),COND(3)
0003        IREAD=5
0004        IRITE=6
0005        TNU=0
0006        ESTEPM=2.5
      C
0007        PI=3.141592654
0008        READ(IREAD,300) LL
0009    300 FORMAT(I5)
0010        DO 500 L=1,LL
0011        WRITE(IRITE,1200)
0012   1200 FORMAT(1H1)
0013        READ(IREAD,305) JJ,SAMPL,HDIMW,VDIMW,RDIMW,SLOT,ALCALC
0014    305 FORMAT(I3,10A4,5F6.2)
0015        SLOTC=1
0016        IF (SLOT.EQ.0.AND.HDIMW.GT.0.AND.VDIMW.GT.0) SLOT=3.20
0017        IF (SLOT.EQ.0.AND.HDIMW.GT.0.AND.VDIMW.EQ.0) SLOT=1.24
0018        IF (HDIMW.GT.0.AND.VDIMW.GT.0) WLC=HDIMW*2
0019        IF (HDIMW.GT.0.AND.VDIMW.EQ.0) WLC=HDIMW*1.706293
```

```fortran
      DO 400 J=1,JJ
      DATA=0
   22 READ(IREAD,311)SAMID,DATE,MC,TEMPF,FREQ,ANODP,ANODM,SNCDP,SNCDM,DD
     *IMS,ADB,SCB,ESTDC
  311 FORMAT(2A4,2A4,A4,1X,A4,F7.4,5F7.3,2F4.0,F3.1)
      TF=TEMPF
      IF (FREQ.GT.0.AND.DDIMS.GT.0) GO TO 56
      IF (FREQ.EQ.0.AND.DDIMS.GT.0) GO TO 54
C
   50 WLG=ABS(ANODP+ANODM-SNODP-SNODM)
      IF (HDIMW.EQ.0) GO TO 53
      IF (VDIMW.EQ.0) GO TO 43
      WLGN=WLG
   51 CUBIC=SLOT**2*WLGN**3+8*PI*VDIMW*HDIMW***3*(WLGN-WLG)
      CUBPM=3*SLOT**2*WLGN**2+8*PI*VDIMW*HDIMW**3
      GO TO 45
   43 WLGN=WLG
      FOFAW=1.41842*SLOT**2/(8*(PI*HDIMW/2)**4)
   44 CUBIC=FOFAW*WLGN**3+WLGN-WLG
      CUBPM=3*FOFAW*WLGN**2+1
   45 WLGN1=WLGN-CUBIC/CUBPM
      IF (ABS(WLGN1-WLGN).LE.0.0001) GO TO 52
      WLGN=WLGN1
      IF (VDIMW.EQ.0) GO TO 44
      GO TO 51
   52 WLG=WLGN1
   53 IF (HDIMW.GT.0) WLG=WLG*WLC/SQRT(WLG**2+WLC**2)
      F=299.6966/WLG
      GO TO 22
   54 FREQ=F
   56 F=FREQ
      IF (FREQ.GT.0.1.AND.FREQ.LT.13) GO TO 58
  315 DATA=1
      GO TO 350
   58 WL = 299.6966/FREQ
      IF (HDIMW.EQ.0.AND.VDIMW.EQ.0) WLG=WL
      IF (HDIMW.GT.0) WLG=WL/SQRT(1-(WL/WLC)**2)
      IF (HDIMW.EQ.0) GO TO 86
      IF (VDIMW.EQ.0) GO TO 59
      SLOTC=1+(SLOT*WLG)**2/(8*PI*VDIMW*HDIMW**3)
      GO TO 86
   59 CON=1.84118
      SLOTC=1+(SLOT*WLG*CON)**2/(8*(PI*HDIMW/2)**4*(CON**2-1))
      GO TO 86
   86 PRNT1=ABS(ANODP-ANODM)
      PRNT2=ABS(SNODP-SNODM)
      ZANODE=(ANODP+ANODM)/2
      ZSNCDE=(SNODP+SNODM)/2
      DLTZA=ABS(ANODP-ANODM)/SLOTC
      DLTZS=ABS(SNODP-SNODM)/SLOTC
   87 SHIFT=(ZANODE-ZSNODE)/SLOTC
      DE=ZANODE+RDIMW
      DET=0
   88 DET=DET+WLG/2
      IF (ABS(DE-DET).GE.WLG/4) GO TO 85
      DE=DET
      IF (ACB.EQ.0) ADB=3
      ARG=0.2302585*ADB
```

```
0020
0021
0022
0023
0024
0025
0026
0027
0028
0029
0030
0031
0032
0033
0034
0035
0036
0037
0038
0039
0040
0041
0042
0043
0044
0045
0046
0047
0048
0049
0050
0051
0052
0053
0054
0055
0056
0057
0058
0059
0060
0061
0062
0063
0064
0065
0066
0067
0068
0069
0070
0071
0072
0073
0074
0075
```

```
0076              POWER=EXP(ARG)
0077              VSWR=SQRT(POWER-COS(PI*DLTZA/WLG)**2)/SIN(PI*DLTZA/WLG)
0078              IF (SDB.EQ.0) SDB=3
0079              ARG=0.2302585*SDB
0080              POWER=EXP(ARG)
0081              ARG=SQRT((POWER-1)/(VSWR**2-1))
0082              DLTZA=WLG*ARSIN(ARG)/PI
0083              RATIO=(DE-DDIMS-SHIFT)/DE
0084         95 PHIPR=PI*(DLTZS-RATIO*DLTZA)/WLG
0085              VSWR=SQRT(POWER-COS(PHIPR)**2)/SIN(PHIPR)
0086              PHI=1/VSWR
0087        100 ZO=-(SHIFT+DDIMS)
0088              IF (ZO.GE.0) GO TO 102
0089        101 ZO=ZO+WLG/2
        C  I.E.   ADD HALF-WAVELENGTHS UNTIL ZO BECOMES POSITIVE.
0090              IF (ZO) 101,102,102
0091        102 U=2*PI*ZC/WLG
0092              TNU=TAN(U)
0093              IF (HDIMW.GT.0) P=(WL/WLC)**2
0094              IF (HDIMW.EQ.0) P=0
0095              Q=WLG/(2*PI*DDIMS)
0096              S = WL/(2*PI*DDIMS)
0097              DEN= Q/(1+(PHI*TNU)**2)
0098              A=TNU*(PHI**2-1)
0099              B=PHI*(1+TNU**2)
0100              C = SQRT(A*A+B*B)*DEN
0101              C1=C*SIGN(1.0,A)
0102              UO=A*DEN
0103              VO=-B*DEN
        C  ESTX IS THE FIRST ESTIMATE OF B2D, COMPUTED FROM E' FOR THE
        C     APPROPRIATE GUIDE WITH A2D=0.
0104              IF (ESTDC.EQ.0) ESTDC=ESTEPM
0105              ESTX = SQRT(ESTDC-P)/S
        C
        C  KWAD CORRESPONDS TO THE QUADRANT INTO WHICH ESTX (IN RADIANS) FALLS.
0106        104 KWAD= 1
0107              IF (ESTX.GT.PI) ESTX = ESTX-PI
0108          2 IF (ESTX.LT.KWAD*PI/2) GO TO 5
0109              KWAC=KWAD+1
0110              GO TO 2
        C  SOLUTICNS DO NOT EXIST IN THE FIRST QUADRANT IF C.LT.1.
0111          5 IF (KWAD-1) 6,6,40
0112          6 IF (C1.LE.1) ESTX=ESTX+PI
        C
        C  FIND THREE VALUES OF B2D AND A2D.
0113         40 ESTXO=ESTX
0114              DO 42 I=1,3
0115         42 DIFF(I)=0
0116              IF (ABS(TNU).GT.200) GO TO 230
0117              DO 110 I=1,3
0118              B2D=FINDX(C1,ESTX)
0119              ESTX=B2D+PI
0120        105 A2D=(Q*B2D*PHI*(1+TNU**2))/((1+TAN(B2D)**2)-TAN(B2D)/B2D)
0121              IF (I-1) 106,106,107
0122        106 TB2C=B2D
0123              TA2C=A2D
0124        107 CALL ADJUST (A2D,B2D,UO,VO,I,DIF)
0125              IF (DIF.LT.0.0002) GO TO 108
```

```
0126              DIFF(I)=DIF
0127          108 ALPHA(I)=A2D
0128              BETA(I)=B2D
0129          110 CONTINUE
0130          116 IF (HDIMW.EQ.0) GO TO 200
     C
     C  CALCULATE 3 DIELECTRIC CONSTANTS, LOSS FACTORS, AND LOSS TANGENTS
     C      FOR CIRCULAR OR RECTANGULAR WAVEGUIDES.
0131              DO 140 I=1,3
0132              DC(I) = P-S**2*(ALPHA(I)**2-BETA(I)**2)
0133              FACTOR(I) = S**2*2*ALPHA(I)*BETA(I)
0134              ALT(I)=FACTOR(I)/DC(I)
0135              LTW=(1-P)*CLTZA/OE
0136              IF (VDIMW.EQ.0) GO TO 132
0137              LTWS=LTW*(HDIMW/(2*VDIMW)+P/DC(I))/(HDIMW/(2*VDIMW)+P)
0138              GO TO 135
0139          132 LTWS=LTW*(0.42+P/DC(I))/(0.42+P)
0140          135 ALT(I)=ALT(I)-LTWS
0141              FACTOR(I)=ALT(I)*DC(I)
0142          140 COND(I) = .55668*FACTOR(I)*FREQ
0143              GO TO 350
     C
     C  CALCULATE 3 DIELECTRIC CONSTANTS, LOSS FACTORS, AND LOSS TANGENTS FOR
     C      COAXIAL LINES.
0144          200 DO 220 I=1,3
0145              DC(I)=S**2*(BETA(I)**2-ALPHA(I)**2)
0146              FACTOR(I)=S**2*2*ALPHA(I)*BETA(I)
0147              ALT(I)=FACTOR(I)/DC(I)
0148              LTWS=DLTZA/OE
0149              ALT(I)=ALT(I)-LTWS
0150              FACTOR(I)=ALT(I)*DC(I)
0151          220 COND(I) = .55668*FACTOR(I)*FREQ
0152              GO TO 350
0153          230 DATA=1
0154              DO 231 I=1,3
0155              B2D=FINDX(C1,ESTX)
0156              DC(I)=P+(WL*B2D/(2*PI*DDIMS))**2
0157          231 ESTX=B2D+PI
0158              DO 232 I=1,3
0159              ALT(I)=0
C160          232 FACTOR(I)=0
     C
     C  PRINT COMPLETE RESULTS IF ALCALC IS OTHER THAN ZERO.
0161          350 IF (ALCALC.EQ.0) GO TO 380
0162              WRITE(IRITE,375) SAMPL,J,DATE,MC
0163          375 FORMAT(1H0,'  DIELECTRIC PROPERTIES FOR ',10A4,//3X,'RUN',I4,5X,2A
             *4///,' MOISTURE CONTENT',31X,A4)
0164              WRITE(IRITE,376) TF,F,HDIMW,VDIMW,DDIMS,ZANODE,ZSNODE, ACB,PRNT1,
             * SDB,PRNT2,RDIMW,ESTDC
0165          376 FORMAT(1H ,'TEMPERATURE (DEGREES FAHRENHEIT)',12X,A5/' FREQUENCY (
             *GIGAHERTZ)',F33.4,/' WAVEGUIDE HORIZONTAL DIMENSION (MM)',F19.4,/'
             * WAVEGUIDE VERTICAL DIMENSION (MM)',F21.4,/' SAMPLE LENGTH (MM)',F
             *36.4,/' AIR NODE POSITION (MM)     ',F28.4,/' SAMPLE NODE POSITION
             *(MM)',F29.4/' AIR NODE WIDTH (MM)',F11.1,  ' DB ',F19.4,  /' SAMP
             *LE NODE WIDTH (MM)',F 8.1,' DB',F21.4,/'            REFERENCE DIMEN
             *SION (MM)',F20.4,/' ESTIMATED DIELECTRIC CONSTANT',F25.4)
0166              IF (DATA.EQ.0.0) GO TO 373
0167              SDC(J)=0
```

```
0168               SLT(J)=0
0169               SFACT(J)=0
0170               SCOND(J)=0
0171               ESTEPM=ESTDC
0172               WRITE(IRITE,371) TNU
0173           371 FORMAT(1H0,'BAD SAMPLE LENGTH FOR THIS FREQUENCY, NEARLY AN ODD MU
                  *LTIPLE QUARTER WAVELENGTH.',/,' TANGENT((2*PI*ZO)/WLG) =',F10.3)
0174               WRITE(IRITE,372) (DC(I),I=1,3)
0175           372 FORMAT(1H ,'DIELECTRIC CONSTANT',3F15.6,1H1)
0176               GO TO 380
0177           373 WRITE(IRITE,374) ESTXO
0178           374 FORMAT(1H ,'FIRST ESTIMATE OF B2D (ESTX)',F26.4/)
0179               WRITE(IRITE,382) TA2D, TB2D
0180               WRITE(IRITE,383) ALPHA(1), BETA(1)
0181           382 FORMAT(1H ,'UNADJUSTED A2D, B2D ',2F20.5)
0182           383 FORMAT(1H ,'ADJUSTED A2D, B2D   ',2F20.5//)
0183               WRITE(IRITE,377)SAMID
0184           377 FORMAT(18X,'  SAMPLE ',2A4,' RESULTS  '/)
0185               WRITE(IRITE,378) (DC(I),I=1,3),(ALT(I),I=1,3),(FACTOR(I),I=1,3), (
                  *COND(I),I=1,3)
0186           378 FORMAT(' DIELECTRIC CONSTANT',5X,3F15.6,/' LOSS TANGENT',12X,   3F1
                  *5.6,/' LOSS FACTOR ',12X,3F15.6,/' CONDUCTIVITY',12X,3F15.6)
0187               DO 379 I=1,3
0188               IF (DIFF(I).EQ.0) GO TO 379
0189               WRITE(IRITE,1100) DIFF(I),I
0190          1100 FORMAT(1H0,'DIFF1=',F10.6,' FOR ESTIMATE NO.',I3/)
0191           379 CONTINUE
0192               WRITE(IRITE,1200)
      C    ADD TO SUMMARY TABLE PROBABLE DC AND LOSS-TAN VALUES
0193           380 KOUNTR=1
0194               DELTA=ABS(DC(1)-ESTDC)
0195               DO 320 I=2,3
0196               GUESS=ABS(DC(I)-ESTDC)
0197               IF (GUESS-DELTA) 360,360,320
0198           360 KOUNTR=I
0199               DELTA=GUESS
0200           320 CONTINUE
0201               ESTEPM= DC(KOUNTR)
0202           321 SDC(J)=DC(KOUNTR)
0203               SLT(J) = ALT(KOUNTR)
0204               SFACT(J) = FACTOR(KOUNTR)
0205               SCOND(J) = .55668*FACTOR(KOUNTR)*F
0206           322 SF(J) = F
0207               SMC(J)=MC
0208               STF(J) = TF
0209               DO 400 N=1,2
0210               SDAY(J,N) =DATE(N)
0211           400 SSMP(J,N) = SAMID(N)
      C    WRITE SUMMARY TABLE
0212           405 WRITE(IRITE,410) SAMPL
0213           410 FORMAT(1H0,'DIELECTRIC PROPERTIES FOR ',10A4///)
0214               WRITE(IRITE,412)
0215           412 FORMAT(34X,'SUMMARY TABLE'//'   DATE    MOIST TEMP   SAMPLE    FREQ
                  *. DIELECTRIC  LOSS    LOSS    CONDUCTIVITY'/11X,'CONT. (F.)    IDENT.
                  *   (GHZ) CONSTANT  FACTOR TANGENT MILLIMHOS/CM'/)
0216               DO 414 J=1,JJ
0217           414 WRITE(IRITE,415) (SDAY(J,N),N=1,2),SMC(J),STF(J),(SSMP(J,N),N=1,2)
                  *,SF(J),SDC(J),SFACT(J),SLT(J),SCOND(J)
```

```
0218      415 FORMAT(1H ,2A4,3(2X,A4),A4,F7.3,F9.4,2F8.4,F12.4)
0219      500 CONTINUE
0220          CALL EXIT
0221          END
```

FORTRAN IV G LEVEL   19   ADJUST

```
0001          SUBROUTINE ADJUST(A2D,B2D,UO,VO,I,DIFF1)
0002          J=0
0003          DELTA=0.01
0004          CALL ACOMP(UA,VA,A2D,B2D)
0005          DIFF1=SQRT((UO-UA)**2+(VO-VA)**2)
0006        5 IF (DIFF1.LT.0.0002) RETURN
0007       10 K=0
0008          TA2C=A2D+DELTA
0009       15 CALL ACOMP(UA,VA,TA2D,B2D)
0010          DIFF2=SQRT((UO-UA)**2+(VO-VA)**2)
0011          K=K+1
0012          IF (DIFF2-DIFF1) 20,25,25
0013       20 A2D=TA2D
0014       22 DIFF1=DIFF2
0015          GO TO 5
0016       25 IF (K-1) 30,30,40
0017       30 TA2C=A2D-DELTA
0018          GO TO 15
0019       40 K=0
0020          TB2D=B2D+DELTA
0021       45 CALL ACOMP(UA,VA,A2D,TB2D)
0022          DIFF2=SQRT((UO-UA)**2+(VO-VA)**2)
0023          K=K+1
0024          IF (DIFF2-DIFF1) 50,55,55
0025       50 B2D=TB2D
0026          GO TO 22
0027       55 IF (K-1) 60,60,80
0028       60 TB2D=B2D-DELTA
0029          GO TO 45
0030       80 DELTA=DELTA/2
0031          J=J+1
0032          IF (J-13) 10,90,10
0033       90 RETURN
0034          END
```

FORTRAN IV G LEVEL   19   ACOMP

```
0001          SUBROUTINE ACOMP (UA,VA,A2D,B2D)
0002          X=A2D*2
0003          Y=B2D*2
0004          V1=A2D*SINH(X)+B2D*SIN(Y)
0005          V2=A2D*SIN(Y)-B2D*SINH(X)
0006          BOT=(A2D**2+B2D**2)*(COSH(X)+COS(Y))
0007          UA=V1/BOT
0008          VA=V2/BOT
0009          RETURN
0010          END
```

FORTRAN IV G LEVEL 19   FINDX

```
0001            FUNCTION FINDX (C,ESTX)
0002            K=1
0003            PI=3.141592654
0004            XO=ESTX
0005            NSTOP=0
0006         10 IF (ESTX.LT.K*PI/2) GO TO 20
0007            K=K+1
0008            GO TO 10
0009         20 TEST=TAN(ESTX)/ESTX
0010            IF (C*TEST.GT.0.0) GO TO 21
0011            IF (ABS(C).GT.2.0) GO TO 30
0012         21 DO 26 N=1,10
0013            IF (K-(2*N-1)) 25,22,26
0014         22 IF (K-1) 23,23,24
0015         23 A=0
0016            B=PI/2
0017            GO TO 40
0018         24 B=K*PI/2
0019            A=B-PI
0020            GO TO 40
0021         25 A=(K-1)*PI/2
0022            B=A+PI
0023            GO TO 40
0024         26 CONTINUE
0025         30 IF (C) 31,32,32
0026         31 ESTX=K*PI-ESTX
0027            A=K*PI/2
0028            B=A+PI
0029            GO TO 40
0030         32 ESTX=(K-1)*PI-ESTX
0031            B=(K-1)*PI/2
0032            IF (K-2) 33,33,34
0033         33 A=0
0034            GO TO 40
0035         34 A=B-PI
0036         40 X1=ESTX
0037         50 DELTA=X1*(TAN(X1)-C*X1)/(X1/COS(X1)**2-TAN(X1))
0038            X2=X1-DELTA
0039            NSTOP=NSTOP+1
0040            IF (X2.LT.A) GO TO 60
0041            IF (X2.GE.B) GO TO 60
0042            IF (ABS(DELTA).LE.0.0001) GO TO 80
0043            X1=X2
0044            GO TO 70
0045         60 IF (C.GT.0) ESTX=(ESTX+B)/2
0046            IF (C.LE.0) ESTX=(ESTX+A)/2
0047            X1=ESTX
0048         70 IF (NSTOP.EQ.75) GO TO 90
0049            GO TO 50
0050         80 FINDX=X2
0051            RETURN
0052         90 FINDX=XO
0053            WRITE(6,102)
0054        102 FORMAT(1H ,'FINDX=XO'/)
0055            RETURN
0056            END
```

X. APPENDIX B: ELECTRICAL MEASUREMENT DATA SHEETS

IMPEDANCE BRIDGE MEASUREMENTS FOR DIELECTRIC PROPERTIES COMPUTATION

Sample description _1970 Scout 66 HRW Wheat_
Date _8/2/71_ Moisture content _10.5_ % Temperature _76_ ° F Sample weight _806_ g
Measurements _RDN_ Calculations _RDN_ Sample holder cross-sectional area: 64.755 cm²

Sample ident.	Freq. kHz	D_B	C_y pf	D_p	C_p pf	Sample height	ϵ'_r	ϵ''_r	tan δ	σ nmhos	ρ
	0.25	0	0	0.064	284.4	6.00	7.731	2.402	0.311	0.338	0.817
	1.0	0.20	241.1	0.202	232.0	6.00	6.218	1.598	0.257	0.889	0.817
	5.0	0.0226	204.0	0.57	201.5	6.00	5.344	0.810	0.152	2.250	0.817
	20.0	0.078	221.3	0.328	215.8	6.00	5.756	1.202	0.209	1.339	0.817

RX METER MEASUREMENTS FOR DIELECTRIC PROPERTIES COMPUTATION

Sample description _1970 Scout 66 HRW Wheat_
Date _8/2/71_ Moisture content _10.5_ % Temperature _76_ ° F Sample weight _21 6548_ g
Measurements _RDN_ Calculations _RDN_ Sample holder volume: 116.485 ml Cross-section: 18.374 cm²
_95.8375_

Sample ident.	Central conductor	Frequency MHz	Capacitance C_p	Resistance R_p	Sample height	ϵ'_r	ϵ''_r	tan δ	σ μmhos	ρ
Natural	LF	50	10.63	14.4		3.467	0.333	0.096	9.26	0.787
		100	11.23	5.7		3.376	0.334	0.102	19.14	0.787
Silky		50	10.77	13.5		3.681	0.374	0.102	10.34	0.823
		100	11.33	5.5		3.500	0.366	0.105	20.40	0.823

ADMITTANCE METER MEASUREMENTS FOR DIELECTRIC PROPERTIES COMPUTATION

Sample description _1970 Scout 66 HRW Wheat_
Date _8/3/71_ Moisture content _10.5_ % Temperature _76_ ° F. Sample weight _38 846_ g
Measurements _RDN_ Calculations _RDN_ Sample holder volume: 50.249 ml

Sample ident. G correct.	Frequency MHz	Admittance (millimhos) Conductance G	Susceptance jB	Multiplier	ϵ'_r	ϵ''_r	tan δ	σ μmhos	ρ
0	200	1.0	15.2	1	3.036	0.287	0.095	32.21	0.773
0.1	300	1.6	17.2	1.5					
		2.3	25.8		3.00	0.303	0.100	50.53	0.773
0.3	440	3.6	18.2	3					
		10.5	54.6		3.037	0.384	0.126	74.09	0.773

Fig. 10-1.   Data forms for impedance bridge, RX-Meter, and Admittance-Meter measurements with examples of data recorded

Q-METER MEASUREMENTS FOR DIELECTRIC PROPERTIES COMPUTATION

Sample description *1970 Scout 66 HRW Wheat*
Date *8/2/71* Moisture content *10.5* % Temperature *76* °F Sample weight *79.5668* g
Measurements *JDN* Calculations *JDN* Sample holder cross-sectional area: 38.657 cm²

Sample ident.	Freq. MHz	Sample				C_x Scale	Air				h(cm) or v	ϵ'_r	ϵ''_r	tan δ	σ μmhos	ρ
		V_m	V	+C	-C		V_m	V	+C	-C						
	0.050	1.7	1.5	2.62	2.43	29.75	1.8	1.6	2.23	2.49	2.60	4.623	0.183	0.040	0.01	0.792
	0.20	2.7	1.4	1.32	1.47	28.0	3.6	1.4	1.42	1.64	2.54	4.439	0.244	0.055	0.03	0.810
	1.0	2.1	1.4	0.67	0.78	26.75	3.1	1.4	0.78	0.95	2.54	4.246	0.260	0.061	0.14	0.810
	5.0	2.3	1.4	0.77	0.83	26.0	4.4	1.4	0.93	1.11	2.54	4.131	0.338	0.082	0.94	0.810
	20.0	2.4	1.4	0.72	0.78	24.5	5.0	1.4	0.68	0.78	2.54	3.899	0.414	0.106	4.60	0.810
	50.0	2.2	1.4	0.87	0.79	23.75	5.0	1.4	0.96	1.01	2.54	3.784	0.510	0.135	14.19	0.810
	50.0	2.2	1.4	0.83	0.87	23.75	5.0	1.4	0.88	1.08	2.60	3.719	0.524	0.141	14.58	0.792

Fig. 10-2. Data form for Q-Meter measurements with examples of data recorded

SHORT-CIRCUITED LINE OR WAVEGUIDE MEASUREMENTS FOR DIELECTRIC PROPERTIES COMPUTATION

Sample description (40)	Equipment	Waveguide dim.	Ref. dim.	λ_c	Slot width	Sample holder constants
1970 Scout 66 HRW Wheat	X-Band	22.86 10.16	(130) 120	45.720	3.2 mm	60.03 mm, 2.323 cm², 4.306 mm/ml
	CRL Cylindr.	25.45	0, 150, (300)	43.425	1.24	5.087 1.966
Date Moist. cont. Temp.	Coaxial		0, 150, 300	0	$\bar{r} = 299.6966/\lambda_0$	4.379 2.284
7/30/71 10.5 % 76°F	R&S Coaxial		150	0	$1/\lambda_0{}^2 = 1/\lambda_g{}^2 + 1/\lambda_c{}^2$	2.810 3.559

Sample ident. (8)	Frequency GHz	Air node readings mm		Sample node readings mm		Sample length mm	dB level Air	dB level Samp.	Est. ϵ_r'	Remarks	ϵ_r'	ϵ_r''	tan δ	σ mmhos	ρ
3-3	8.388	13.542	13.833	19.13	25.43	34.8	6	3	2.7		2.624	0.241	0.092	1.12	0.800
3-3	10.186	4.896	4.967	14.91	28.17	35.0	6	0.8	2.7		2.600	0.258	0.099	1.46	0.795
3-3	11.030	22.491	22.562	22.4	26.82	35.0	6	3	2.7		2.586	0.278	0.108	1.71	0.795
3-3	12.228	15.684	15.699	14.71	25.52	36.4	6	2	2.7		2.517	0.214	0.085	1.46	0.764
freq.		61.123	61.212	91.182	91.277					*f= 8.5144*					
3-1		61.123	61.212	75.30	84.62	46.0	3	3	2.7		2.642	0.205	0.078	0.97	0.799
freq.		60.23	60.15	121.65	121.78										
3-2		94.70	94.80	69.10	72.92	38.3	3	3	2.7	*f= 2.4356*	2.633	0.261	0.099	0.35	0.796

Fig. 10-3.   Data form for short-circuited waveguide measurements with examples of data recorded for rectangular, cylindrical, and coaxial waveguide measurements corresponding to data for Figs. 9-6 through 9-9